SYNTHESIS AND CHARACTERIZATION OF A BIOCOMPOSITE DERIVED FROM BANANA PLANTS (*MUSA CAVENDISH)*

Submitted in fulfillment of the requirements of the degree of Doctor of Philosophy in Chemistry in the Faculty of Applied Sciences at the Durban University of Technology

Vimla Paul

2015

DECLARATION

This thesis is being submitted to the Durban University of Technology for the degree of Doctor of Philosophy in Chemistry. I declare that this work is my own and has not been submitted before for any degree or examination to this or any other university or institution for this or any other degree or award.

_____

Vimla Paul

Student Number: 18551350

I hereby approve the final submission of the thesis.

Supervisor: _____ Date:_____

Professor K Kanny

Co- supervisor:_____ Date:_____

Professor GG Redhi

ABSTRACT

Over decades synthetic composites have become an indispensable part of our lives with their various applications such as packaging, sporting equipment, agriculture, consumer products, medical applications, building materials, automotive industry, and aerospace materials among others. Although these polymers have the desired properties for the above applications, they are invariably costly. Furthermore, they cannot be easily disposed of at the end of their useful lives and simply pile up and cause significant damage to the environment. However, the dwindling supply of fossil fuel, increased oil prices, together with the growing public concern of greenhouse gas emissions and global warming, has forced scientists to search for new development of sustainable materials from renewable resources. Hence in recent years, there is an increased interest in biocomposite manufacturing with natural resources as environmental issues are addressed.

The research work presented in this dissertation is to the best of the author's knowledge a world-first overall investigation pertaining to the concept of synthesizing a banana sap based bio-resin (BSM) reinforced with banana fibres. In this work the chemical composition of banana sap was determined to investigate the chemical reactions taking place in the resin formulation.

BSM was synthesized, characterized and proposed as a potential bio-resin to be used in the biocomposite manufacture for non-functional motor vehicle components. BSM, a hybrid bio-resin was synthesized with equimolar quantities of maleic anhydride and propylene glycol and 50% banana sap. A control resin without the banana sap was also synthesized for comparison purposes. It was proposed that the presence of sugars, esters and pthalates from the sap, determined by HPLC and GC-MS, contributed to the cross-linking of the polymer chain. The acid value and viscosity of BSM were determined and found to be within specification of an industry resin. The molecular weights of the BSM and control resins were 2179 and 2114 units respectively. These were within the required molecular weight of

unsaturated polyester resins. The gel and cures times of the BSM were 60% lower than the control resin suggesting that the banana sap behaved as an accelerator for the curing process. The lower cure time meant that using the banana sap in the formulation was cost effective and time saving. The thermal properties of BSM showed improved degradation temperatures and degree of crystallinity compared to the control resin. A parametric study showed that increasing banana sap concentration in the resin formulation led to increased tensile and flexural properties with 50% being the optimum amount of sap to be added to the formulation.

The synthesized bio-resin and control resin were applied to biocomposites and characterized in terms of physical, thermal, mechanical, morphological, chemical and biodegradable properties. Mechanical tests indicated a 15 % increase in tensile strength, 12 % improvement in tensile modulus and a 25 % improvement in the flexural modulus, when compared to structures produced without banana sap. Natural fibres present the challenge of poor adhesion to the matrix. Chemical treatment of the banana fibre was done to improve on the compatibility of resin to fibre. Fibre pull-out showed that treated fibres had a better bond than the untreated fibre.

Parametric studies were also done to evaluate the effect of fortifying the BSM resin with nanoclay. A 5% clay loading resulted in a 24% increase in tensile strength and 28% increase in flexural properties.
Finally biodegradation studies of the BSM bio-resin, BSM biocomposite, control resin and control composite were investigated and compared to a positive reference, cellulose. Results showed that over a period of 55 days the BSM biocomposite showed 17.6% biodegradation compared to 8% with the control composite. No difference in biodegradation between the BSM bio-resin and the control resin was recorded. BSM biocomposite was proposed as a potential replacement to synthetic composites that contribute to the environmental landfill problems.

The main contribution of this research is the use of the reinforcement and matrix from the same natural source. An enriched understanding of the synthesis,

characterization and performance of the banana sap based bio-resin and biocomposite for the use of non-functional motor vehicle components is the key outcome of this investigation.

PLAGIARISM

I declare that this thesis is my own work. I have appropriately referenced the work of other people that I have used. I have not and will not allow anyone to copy my work with the intentions of passing it as his or her own work.

_____

Vimla Paul

Student Number: 18551350

DEDICATION

To my parents…… you raised me up

ACKNOWLEDGEMENTS

I would like to thank my Lord and Saviour Jesus Christ for giving me the wisdom and knowledge from above to complete this thesis. You have made all things possible for me.

My heartfelt appreciation and gratitude goes to Prof. K Kanny for introducing me to the fascinating world of biocomposites. His continuous support and guidance is highly appreciated.

I would like to thank my co-supervisor, Prof. G Redhi for his assistance.

My heartfelt gratitude goes to Dr Shalini Singh for her continued assistance in her thorough editing of the thesis.

Sincere thanks goes to Dr Ajay Bissessur for all his guidance and editing of the analytical aspect of this research.

My appreciation goes to the staff in the Department of Chemistry, Mechanical Engineering, Biotechnology, Mathematics and Physics and the Institute of water research who assisted me in so many ways.

I would like to place on record my sincere thanks to Dr Mohan, Dr Mithilkumar, Avinash Ramsaroop, Avy Naicker, Jimmy Chetty and Ugan Padayachee for their constant advice and assistance.

I would also like to thank Paul Moonsamy and Kreson Moodley from NCS resin for their invaluable contribution to this research.

My appreciation goes to Dr Maya Jacob and Dr Sudhakar Muniyasamy from CSIR, Port Elizabeth.

I acknowledge the financial support received from National Research Foundation (NRF), DUT Research Department and Kentron Student Support.

Last but most important, thanks to my husband, Noah and my two daughters, Kirvania and Gabrielle for their constant encouragement, ceaseless moral support and continuous prayers throughout the course of my study.

ABBREVIATIONS

BS	- Banana sap
MA	- Maleic anhydride
PG	- Propylene glycol
BSM	- Banana sap maleate bio-resin
HPLC	- High performance liquid chromatography
GC–MS	- Gas chromatography–mass spectroscopy
TA	-Thermal analysis
DSC	- Differential scanning calorimetry
TG	- Thermogravimetry
DMA	- Dynamic mechanical analysis
UV/VIS	- Ultra violet/visible spectroscopy
nm	- nanometre
FT-IR	- Fourier transform infra-red
DCM	- Dichloromethane
ASTM	- American Society for Testing and Materials
XRD	- X-Ray diffraction
SEM	- Scanning electron microscope
ICP-AES	- Inductively coupled plasma-atomic emission spectroscopy
UPR	- Unsaturated polyester resin
HDT	- Heat deflection temperature
MEKP	- Methyl Ethyl Ketone Peroxide
UPR	- Unsaturated polyester resin
SENB	- Single edge notch beam
BSMF	- Banana sap bio-resin + fibre
CRF	- Control resin + fibre
CR	- Control resin
LCA	- Life cycle analysis
AFM	- Atomic force microscopy

LIST OF FIGURES

LIST OF TABLES

TABLE OF CONTENTS

CHAPTER 1- INTRODUCTION

"Persistence of plastics in the environment, the shortage of landfill space, the depletion of petroleum resources, concerns over emissions during incineration, and the entrapment by and ingestion of packaging plastics by fish, fowl and animals have spurred efforts to develop biodegradable/bio-based plastics."[1]

This thesis is concerned with the study involving the formulation of a bio-composite with a banana sap based bio-resin (referred to as BSM) as the matrix and banana fibres as the reinforcement to replace traditional composites. The thesis gives a brief overview to bio-based composites. It is followed by the introduction of the context of the work, the overall objectives of the study, the delimitations, scope and finally the structure of the thesis.

1.1 Overview

Over decades synthetic composites have become an indispensable part of our lives with their various applications such as packaging, sporting equipment, agriculture, consumer products, medical applications, building materials, auto-industry and aerospace materials among others. Although petroleum derived polymers (namely, vinyl ester, polyester and epoxy) have the desired properties for the above applications, they are invariably costly. These traditional synthetic resins are also unsustainable as petroleum resources are being depleted [1, 2]. Furthermore, they cannot be easily disposed of at the end of their useful lives and simply accumulate causing significant damage to the environment. The occurrence of plastics in the environment, the lack of landfill space, CO_2 emission during incineration of the plastics and the ingestion and entrapment hazards has created an enormous environmental impact [1]. There is therefore an increasing urgency to develop bio-based products that can ease the widespread dependence on fossil fuels. The use of natural fibres and natural bio-based resin systems for the production of bio-composites has been pursued by researchers worldwide as they address environmental concerns [3, 4]. These new bio-based materials are used for

construction, furniture, packaging and automotive components [5]. Furthermore, according to the European Union's directive on end-of-life vehicles, from 2015 onwards, all new vehicles should be 85% reusable and recyclable by weight, 10% can be used for energy recovery and only 5% can be used in landfills [6]. Japan has stipulated similar stringent legislation requiring 88% of a vehicle to be recovered in 2005 and 95% by 2015 [7]. These concerns and new legislations have forced the development of environmentally friendly bio-based and biodegradable polymers and their composites in recent years [8]. The composite manufacturing industry is thus searching for an alternative plant based natural fibre reinforcement source which could be derived from flax, hemp, kenaf, jute, sisal, pineapple and banana fibre that will not burden the environment [9]. These materials ought to perform their function sufficiently, and also need to decompose in the environment with time thereby addressing the landfill and CO_2 emission problems.

In order to reduce the environmental impact, synthetic resins can be replaced with more "green" alternatives. For example, they can be sourced from soybean, tung oil, corn and sugar cane and processed as natural thermosetting polymers or natural resins [10-13]. Numerous studies have been done on natural resins in combination with natural fibres to create this desired polymer [13-15]. However, no reports have been found where the bio-resins and fibres are from the same source as outlined in this study.

Over the last decade there has been a significant increase in research on the replacement of synthetic fibres with natural fibres as reinforcement in plastic composites especially in the auto-industry [1, 16-19]. The use of natural fibres has the advantages of its non-abrasive behaviour, biodegradability, low energy consumption and low cost. Furthermore, natural fibres have been extensively used as reinforcements with polymeric matrices [20].

In the quest to utilize the natural resources of South Africa to address this situation, it was found that among all the natural resources, banana fibre and plant research was relatively new and unexplored. In Kwa-Zulu Natal, South Africa, there is an abundance of banana plants that grow within 2 to 3 years and once the fruit is

harvested the plant is thereafter unused and regarded as waste. Currently there is no information available locally on how much of banana sap and fibre is left over as waste annually. However, a study in Kolkata, India estimated this to be 60-80 t/ha of biomass residue [21].

Studies by Satyanarayana and co-workers show that banana fibres can be a good choice for reinforcement in composites [22]. Banana fibres are used in many types of synthetic and bio-based polymers. Since the intention of this study is to derive the matrix and reinforcement from the same plant source, it was then decided to utilize the banana sap in the formulation of the resin, and the banana fibre as the reinforcement. It is also significant to note that this bio-composite is produced from agricultural waste. To the best of our knowledge, there have been no reports of a banana sap based bio-resin reinforced with banana fibres.

Natural fibre-reinforced composites, also known as bio-composites, could also be used in the plastic industry, auto-industry and packaging industry to reduce material costs [17]. The automobile industry applies bio-composites in a variety of interior and exterior applications such as door and instrument panels, glove-boxes, arm rests, seat backs and package trays [23]. There are some biologically derived polymers that are used in car tyres, biomedical applications, clothing fibres and packaging [24]. The significant weight saving, the ease of production, and the low cost of the reinforcement and matrix have made natural fibre reinforced composites an attractive alternate material to glass fibre reinforced composites.

1.2 Purpose of the study

The purpose of this study was to synthesize a bio-derived, bio-based resin using banana sap as a starting material; to prepare a bio-composite reinforced with non-woven banana fibres and to examine the potential mechanical, chemical and morphological properties of the bio-composite.

1.3 Aims and Objectives of the research

The aim of this research was to develop a bio-resin from banana sap, using banana fibres as the reinforcement and thus forming a bio-degradable bio-composite which can be used for non-functional components in the automotive industry and is compliant with respect to the new legislation implemented by the EU.

The following specific research objectives were targeted:

1. To identify the chemical composition of the extracted banana sap from the pseudostem of a banana plant.
2. To synthesize and characterize a natural resin system using the sap of the banana plant in the resin formulation. To study the cure behaviour of the banana sap based bio-resin.
3. To extract the banana fibre from the plant and to treat the fibre to improve adhesion in the matrix.
4. To reinforce the banana fibre with banana sap based bio-resins using vacuum infusion.
5. To use analytical techniques such as Inductively coupled plasma-atomic emission spectroscopy (ICP-AES), High performance liquid chromatography (HPLC), Gas chromatography-mass spectrometry (GC-MS), Scanning electron microscopy (SEM), Fourier transform infra-red (FT-IR), Dynamic mechanical analysis (DMA), Differential scanning calorimetry (DSC) and Thermogravimetric analysis (TGA) to characterise the sap, bio-resin and bio-composite.
6. To determine the mechanical properties of the neat bio-resin and the biocomposite. To fortify the bio-resin with nanoclays and study the mechanical and thermal properties thereof.
7. To study the biodegradable nature of the biocomposite.

1.4 Delimitations of the study

- Only banana plants collected from Durban, Kwa-Zulu Natal will be used.
- The bio-resin produced is not a 100% “green bio-resin”.
- The fibres are hydrophobic making compatibility with the bio-resin difficult. To overcome this problem, the fibre will be treated before mixing with the bio-resin.
- In this study only 30% fibre loading will used for the manufacture of the biocomposite.

1.5 Structure of the thesis

The thesis is divided into 7 chapters. This chapter provides a background to the study by detailing the replacement of traditional composites with bio-composites. It also gives the aims and objectives of the study and the delimitations.

Chapter 2 presents a comprehensive literature review outlining fibre reinforced polymer (FRP) composites followed by the use of biocomposites to address the environmental issues at hand. This chapter makes reference to the current status of natural fibre or bio-composite research with emphasis on bio-based thermosetting polymers. A review of natural fibres is also presented, in particular banana fibres: its origin and uses are reported. The chapter concludes with a review of research in the development of bio-composites and its applications.

Chapter 3 details the research design and methodology of the study. This chapter includes the detailed description on the synthesis of two resins, namely 1) the bio-resin made with banana sap and 2) control resin without the banana sap. In addition, a description of the two biocomposites that were manufactured, namely the BSM biocomposite and the control biocomposite is outlined.

Chapter 4 reports on the chemical composition of the banana sap and its function in the formulation of the bio-resin[1]. Firstly, a detailed description of the chemical and physical properties of the banana sap by various analytical techniques namely ICP, HPLC and GC-MS is presented. A parallel comparison is drawn to a control resin without the banana sap for all the analyses. A detailed description of the chemical, physical and mechanical properties of the bio-resin is presented.

Chapter 5 discusses the chemical composition of the banana fibres and addresses the hydrophilic property of the fibre by chemical treatment, and the synthesis and characterization of the bio-composite. A comparative study on the chemical, physical and thermo-mechanical properties of the biocomposite between the BSM bio-composite and the control composite[2] is given. The latter part of Chapter 5 reports on the effect of nanoclay infusion with the bio-resin and the resultant properties. The mechanical, thermal and dynamic mechanical properties of the nanoclay infused bio-resin and biocomposite is given.

Chapter 6 presents the study of the biodegradation of the bio-composites. Biodegradation tests conducted with the fungal growth of *Aspergillis Niger* on the biocomposite and soil burial test is detailed. To verify the biodegradation of the composite material, respirometric testing was conducted over a period of 55 days to measure the conversion of organic carbon into carbon dioxide.

Chapter 7 will provide conclusions based on major findings obtained in Chapters Four to Six. Recommendations and areas for future work based on this thesis are also presented.

[1] Extracts from Chapter 4 have been published as "Formulation of a novel bio-resin from banana sap", Industrial Crops and Products, 43, (2013), 496-505.

[2] Extracts from Chapter 5 have been published as "Mechanical, thermal and morphological properties of a bio-based composite derived from banana plant source", Composites Part A, 68, (2015), 90-100.

CHAPTER 2- LITERATURE REVIEW

This chapter deals with literature review of both traditional composites and biocomposites. It is structured into three main sections namely the matrix, reinforcement (natural fibres), and the bio-composite. The first section describes various sources, uses and synthesis of bio-based resins. The second section describes the different natural fibres, their classification and structure as well as various bio-resins. Finally a description of the bio-composites is given.

Introduction

Composite material have been used for centuries dating back to about 2500 years ago where the Egyptians used straw and clay in composite systems to build walls [25]. The rapid development and use of composites led to an increased production of synthetic composites dating back to 1940 [26, 27].

Over the last several decades, there has been an increased use of composite material in the auto industry, sports industry, civil engineering and construction industries and these industries exploit the advantages of the composite materials. Karbhari reasons that there are many benefits associated with using fibre reinforced polymers, such as lightweight properties, ease of construction and corrosion resistant features [28]. Matthews and Rawlings further argue that composites possess very high strength-to-weight and stiffness-to-weight ratios that has made them attractive to the aviation industry and recently in the sports and leisure industry [27].

Composites are lightweight, strong, stiff material made from two or more constituents with significantly different physical or chemical properties that when combined, produce a material with characteristics different from the individual components [29]. There are two main categories of constituent materials: matrix (polymer) and reinforcement (fibre) and the interaction of the combined constituents ensure the final composite material has superior material properties for the required

application. Figure 2.1 shows the cumulative effect of adding fibres to the matrix forming the composite.

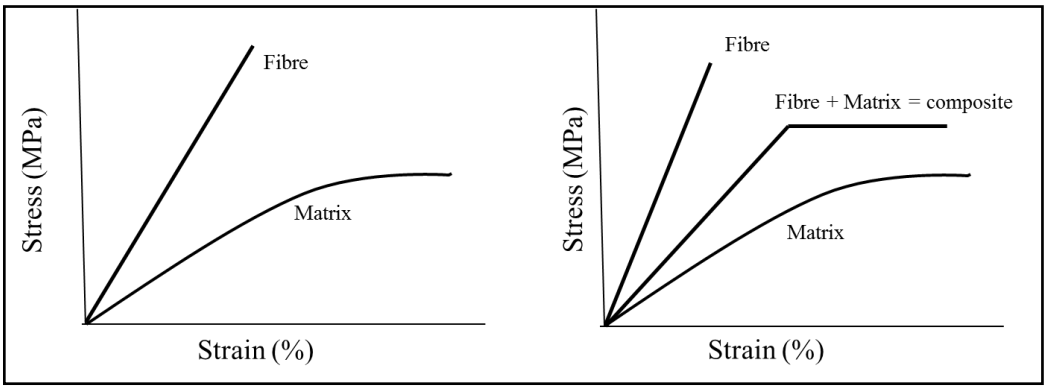

Figure 2.1: Graph showing the effect of adding fibre to the matrix

These versatile materials are used in many diverse fields, from surf boards to guitars, motor vehicle components to microlight aircrafts, and electronic components such as printed circuit boards and electrical contacts [1, 30]. Glass fibres have been the dominant fibre and are used in 95% of cases to reinforce thermoplastics and thermoset composites. The fibre-reinforced composites market (Figure 2.2) is a multibillion-dollar business [31] and 31% of this market is dominated by the automotive industry using natural fibre-based materials. Furthermore, Thomas and Pothan reported that the automotive industry were the forerunners in changing from conventional to biocomposite material which will be highlighted in the next section [32].

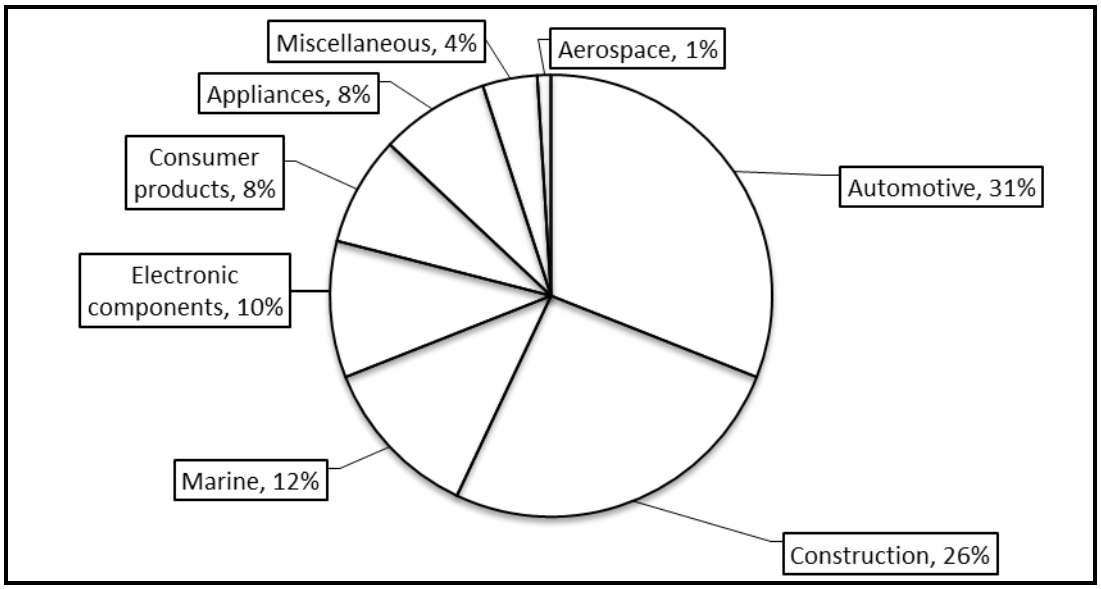

Figure 2.2: Fibre - reinforced plastic composites used in 2002 [33]

2.1 Biocomposites

Broadly defined, biocomposites as shown in Figure 2.3 are composite materials made from natural or biofibre and non-biodegradable polymers such as polypropylene (PP), polyethylene (PE) and epoxies, or with biopolymers such as polylactic acid (PLA) and polyhydroxyalkanoates (PHAs) [1, 34]. The biocomposite made in this study was classified as eco-friendly and "green" since natural fibre and a renewable resource-based polymer were used.

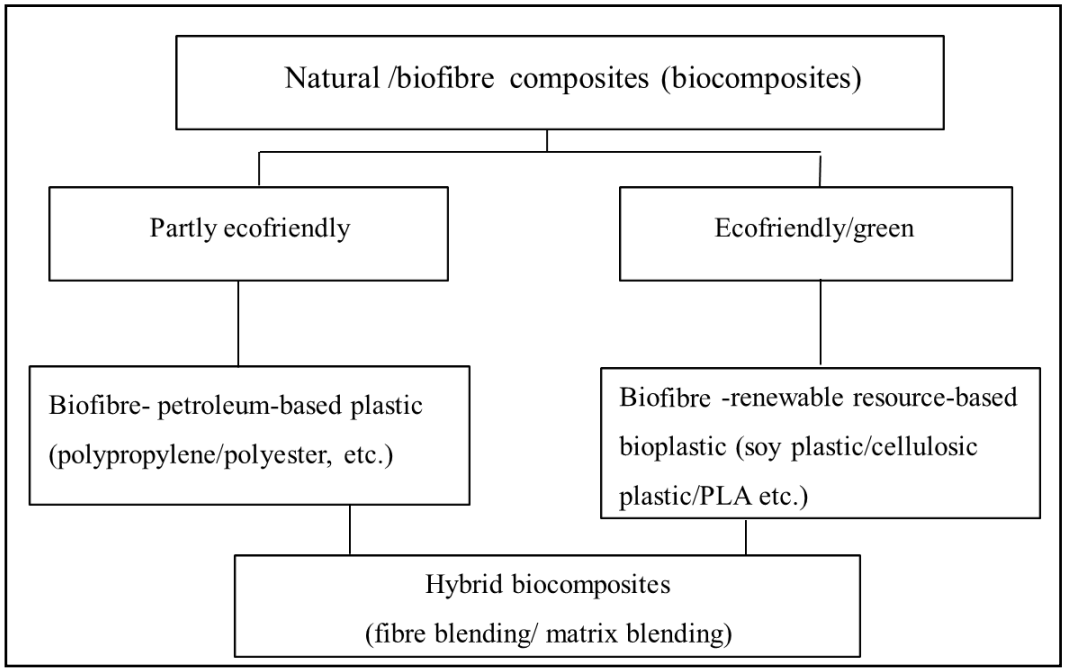

Figure 2.3: Classification of bio-based composites [1]

Several researchers have contributed to the knowledge of biocomposites. For instance, Thomas and Pothan present a book on natural fibre reinforced polymer composites. In particular, natural fibre-surface modification, nanocomposites based on natural fibres and fibre reinforced rubber composites to name a few are discussed in detail [32]. A number of high quality chapters have been included in the book. Meier *et al.* reviewed plant oil renewable resources as green alternatives with emphasis on using plant oils as raw materials for monomers and polymers [35]. Puglia *et al*. reviewed natural fibre based composites with emphasis on natural fibres with matrices ranging from thermosets, thermoplastic and biodegradable biocomposites [36]. John and Thomas reviewed various aspects of biofibres and biocomposites in their review article [37] where they classified biocomposites into green, hybrid and textile and highlighted the applications of these biocomposites. Finally, they discuss that the material revolution of this century may be provided by the green composites.

Although very little reviews have been found on banana fibre with natural-based bio-resins, research is growing with regards to banana fibre as reinforcement with

synthetic resin especially unsaturated polyester resin, which is the type of resin used in this study.

Several researchers have used banana fibres as reinforcements. Indira *et al.* found that a 30% banana fibre content reinforced in a phenol formaldehyde (PF) resin by resin transfer moulding, gave a maximum tensile strength of 24 MPa and flexural strength of 44 MPa [38]. Joseph *et al.* compared two composites (banana fibre/PF and glass/PF) and they reported that the tensile strength was 26 MPa for the banana fibre/PF at 45% fibre loading and 13 MPa for the latter at 25% fibre loading [39]. In another study, Lui *et al.* used banana fibres in a high density polyethylene/nylon-6 blend matrix and found that the tensile and flexural strengths of a 29.3% fibre loading were 25.5 MPa and 31.7 MPa respectively [40]. In addition, Singh *et al.* found that 10% banana fibre reinforced with a silica powder gave the tensile and flexural strengths of 27.6 MPa and 29.6 MPa respectively [41]. Furthermore, Pothan *et al.* reinforced banana fibres with 30% fibre loading in a polyester resin and they found that the tensile and flexural strengths were 47.6 MPa and 53.5 MPa respectively [42].

Pothan and co-workers reported on the dynamic mechanical analysis of different fibre loading of banana fibre reinforced polyester composites [3]. In addition, Savistano reported on the mechanical properties of Kraft pulp made from waste sisal and banana fibres reinforced cement composites [43]. They reported that the composites had flexural strength of 20 MPa and fracture toughness values in the range 1.0-1.5 $kJ.m^{-2}$. The afore mentioned researchers have used banana fibre in a synthetic resin system compared to a natural/hybrid resin system used in the current study and the results that they reported are similar to what was obtained in this thesis. Majhi *et al*. made a biocomposite of polylactic acid and banana fibre at 30% fibre loading and they reported that a tensile strength of 35 MPa was possible for a natural fibre/natural resin system [44].

It will be shown in Chapter 5 that the strength of the biocomposite produced in this study compares well to the work of other researchers.

2.2 Applications of biocomposites

Biocomposites have various uses such as household appliances, housing, construction, medical, aerospace, automotive among others.

The applications of natural fibre composites are greatly concentrated in the interior of passenger cars and truck cabins. They are used in door panels, cabin linings and for thermo-acoustic insulation. The natural fibre composites can be a very cost effective material for the following applications: interior of automotive vehicle, furniture, building and construction industry, toys, lampshades, suitcases, helmets, electrical devices among others [45].

Many European industries are eco-driven; especially the European automotive industry which is trying to make every component recyclable [46, 47]. Leao *et al*. reported that the tensile strength of caraua, jute, sisal and ramie with polypropylene biocomposites used in the automotive industry were 46 MPa, 16 MPa, 23 MPa and 34 MPa at 50% fibre loading respectively [48]. According to Luz *et al*. sugarcane bagasse-reinforced composites used for aesthetic covering inside a motor vehicle results in lower environmental impacts and are lighter when compared to talc-filled composites [49]. Alves and co-workers replaced glass fibres with jute fibres to produce a structural frontal bonnet of an off-road vehicle (Buggy) [5]. They showed that the jute fibre composites, being lighter in weight, reduced fuel consumption hence enhanced the environmental performance of the buggy. Shih and Huang found that the mechanical properties and thermal stability were enhanced when banana fibres were mixed by melt blending with polylactic acid (PLA) compared to the virgin PLA [50]. They concluded that the incorporation of banana fibres can reduce production cost while meeting demands of environmental protection agencies.

Due to its good compatibility and bonding with resin matrix, banana fibre is considered as an effective reinforcing constituent in both natural and synthetic resin systems [51].

Daimler- Chrysler has used flax and hemp instead of glass fibres [46]. Mercedes-Benz and Toyota have also incorporated the uses of natural fibre into composites [6]. Thomas Schuh reported that when flax/sisal fibre mat embedded in an epoxy resin matrix was used for door panels of Mercedes-Benz E-Class, a 20 % weight reduction was achieved, and the mechanical properties were improved [52]. The distribution of these composites throughout the vehicle is shown in Figure 2.4.

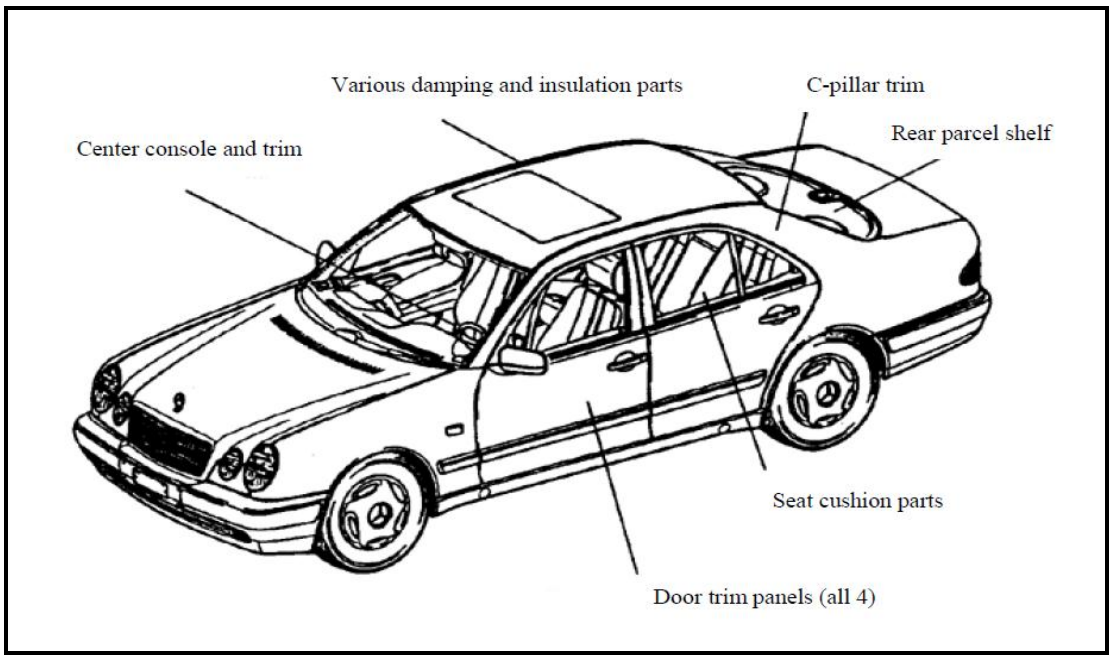

Figure 2.4: Natural fibre composites in the Mercedes Benz E-class [52]

2.3 Biodegradation of polymers

An important function of biocomposites in automotive components is that it must biodegrade after its end of life.

Biodegradability is defined as the degradation results from the action of naturally-occurring microorganisms such as bacteria, fungi and algae (according to ASTM D6400-99) [53, 54]. A compostable plastic is one that undergoes degradation by biological processes during composting to yield CO_2, water, inorganic compounds and biomass and leaves no visible, distinguishable or toxic residue. The consumption of oxygen or the formation of CO_2 is also a good indicator of polymer degradation [55, 56].

Smith classified biodegradable polymers according to their chemical composition, synthesis method, processing method, economic importance, application among others [57]. Furthermore, these polymers can be obtained from natural resources, or they can be synthesized from crude oil [53, 57]. Biodegradation of polymers can be monitored by visual observations (roughening of the surface, formation of holes or cracks, defragmentation, changes in colour or formation of biofilms on the surface. Degradation mechanism can be obtained by scanning electron microscopy (SEM) or atomic force microscopy (AFM).

Polymers are potential substrates for heterotrophic microorganisms such as bacteria and fungi. According to Muller [54], microorganisms are unable to transport polymeric material directly to the cells but must first eliminate enzymes, which depolymerize the polymers outside the cells as illustrated in Figure 2.5 to produce water, carbon dioxide and methane, together with new biomass as bi-products.
Laboratory test for biodegradation involves the use of synthetic media and inoculation with either a mixed or individual microbial strains. In such tests, the activity of the mircoorganisms is observed.

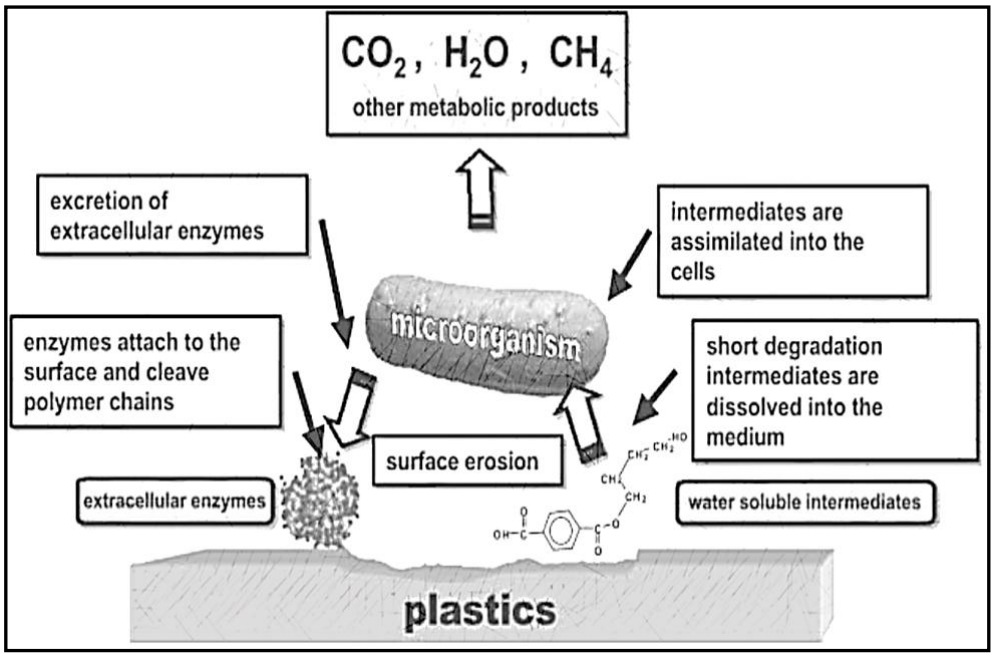

Figure 2.5: General mechanism of plastic biodegradation under aerobic conditions [54]

The objective is to design polymers that will serve its purpose and use and thereafter undergo destruction by a stimulus of the environment, such as microbial, hydrolytic, oxidative or catalytic [58]. More importantly, the breakdown products should not be toxic or persist in the environment.

Gautam identified many uses of biodegradable polymers such as packaging (food containers, wraps, nets, foams), plastic bags (super market carrier bags), catering products (cutlery, plates, cups), agriculture (mulch films, plant pots, nursery films), hygiene products and medical and dental implants [58].

It is important to note that the biodegradation of the biocomposite is caused by the natural fibres and the bio-resin system. The next sections deal with these two components.

2.4 Natural fibres

The use of natural fibres dates back to at least 5500 years ago when ancient Egyptians pressed thin stems of papyrus on which to write [59]. There are about 2000 species of fibres in various parts of the world used for various applications, classified into three major types as animal fibres, vegetable fibres and mineral fibres. A broad classification of vegetable fibres [1] is represented schematically in Figure 2.6 with banana fibres classified as a leaf fibre.

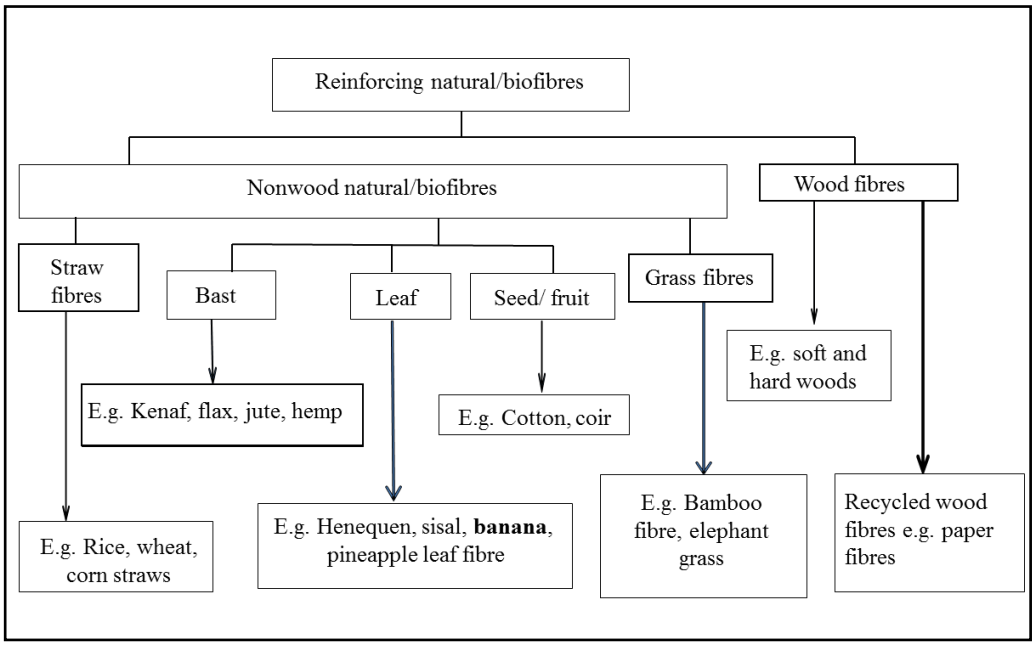

Figure 2.6: Schematic classification of reinforcing natural fibre [1]

Although natural fibres were used in composites for many years, synthetic fibres such as glass and carbon fibres were preferred due to their high strength-to-weight ratios, easy mouldability and durability [32]. The automotive industry is under tremendous pressure to utilize natural fibres for the manufacture of the components such as door panels, headliners, package trays, dashboards and trunk-liners. Lightweight parts are produced from natural fibre composites, consequently reducing fuel consumption. Furthermore, natural fibre composites aids in improved recycling possibilities, hence reducing the waste disposal predicament.

The advantages of natural fibres listed below renders it a potential replacement for synthetic fibres in composites [46, 60-62]:

- Readily available, abundant, low density, low cost and biodegradable.
- Plant fibres are obtained from renewable resources. Low energy is required during production and show carbon dioxide neutrality.
- Natural organic products. There is no dermal issue for their handling compared to glass fibres and do not pose a bio-hazard upon disposal.
- Natural fibres are non-abrasive and exhibit great formability.

- Light in weight (less than half the density of glass fibres).
- Cheap compared to glass fibres.
- Exhibit good thermal insulating and acoustic properties due to their hollow tubular structures.

However natural fibres have the disadvantages of low modulus, high moisture absorption, decomposition in alkaline environment or in biological attack, and variability in mechanical and physical properties. To overcome the high moisture absorption problem, the fibres need to be chemically treated, which will be discussed later in section 2.4.2.2.

2.4.1 Structure and composition of natural fibres

All plant fibres are composed of cellulose and are stronger and stiffer than animal fibres. Since they are more suitable for use in composite material, this study will focus on plant fibres. Biofibres are hollow cellulose fibrils held together by lignin and hemicellulose [63]. The main components of natural fibres are cellulose, hemi-cellulose, lignin, pectin and waxes [37, 47, 61, 64].

Cellulose is regarded as the most abundant polymer in nature that is found in plants, green algae and some bacteria [65]. Cellulose is a linear, high molecular weight polymer that can be described as natural, renewable and biodegradable [66]. Cellulose is a natural polymer consisting of 1,4-β-D- anhydroglucose ($C_6H_{11}O_5$) repeating units joined by 1,4-β-D-glycosidic linkages at C_1 and C_4 position, in which each single unit contains three hydroxyl groups as shown in Figure 2.7 [67, 68]. The hemicellulose is responsible for the biodegradation, moisture absorption and thermal degradation of the fibre. It is made up of polysaccharides composed of a combination of 5- and 6 carbon ring sugars.

Lignin is a complex hydrocarbon polymer with both aliphatic and aromatic constituents. Lignin, an amorphous polymer is thermally stable but is responsible for UV degradation. It is a complex three-dimensional copolymer of aliphatic and aromatic constituents of very high molecular weight [37, 67]. Pectin, whose function is to hold the fibre together, is a polysaccharide like cellulose and hemicellulose. The mechanical strength of the plant fibre is related to the distribution of lignin between

hemi-cellulose and cellulose, causing binding and stiffening of the plant fibers to occur.

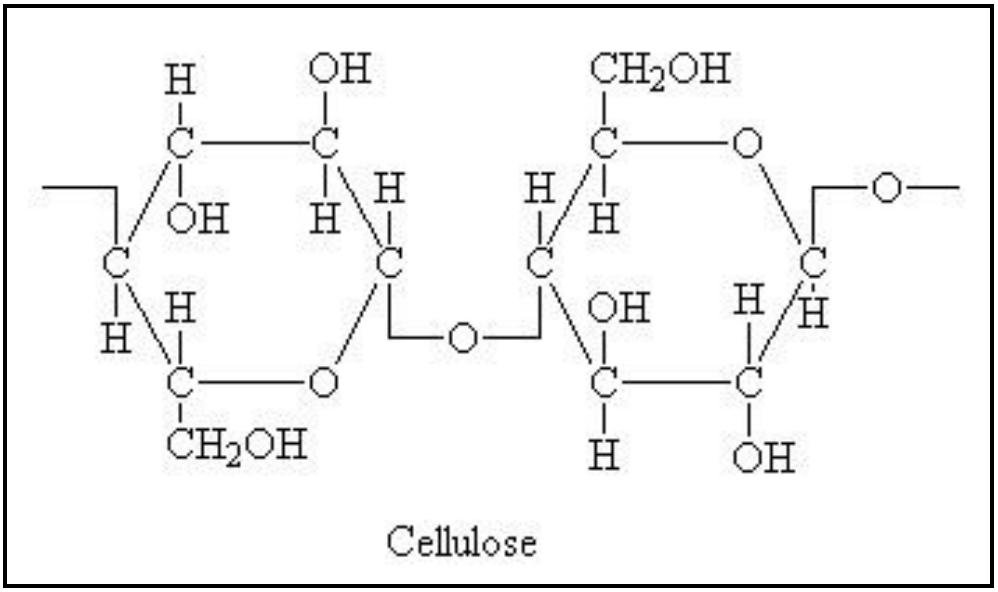

Figure 2.7: Schematic drawing of cellulose [69]

A single fibre has a diameter of approximately 10-20 μm. The microstructure of natural fibres is made up of different hierarchical structures as shown in Figure 2.8. Each fibre cell is made up of four concentric layers i.e. primary wall, outer secondary wall, middle secondary wall and inner secondary wall.

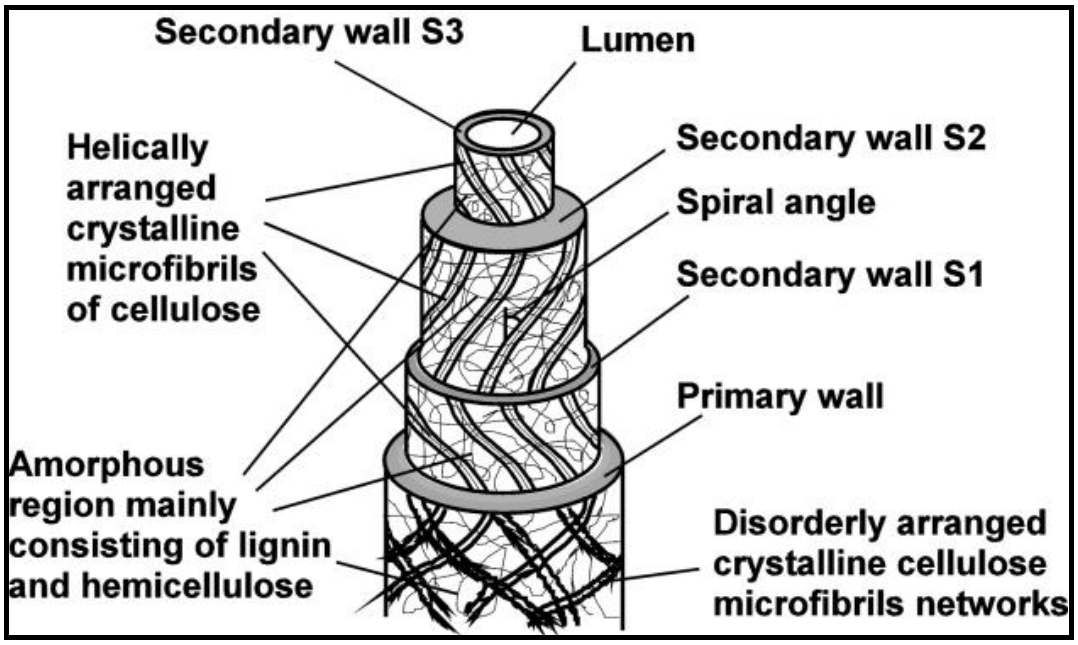

Figure 2.8: Structural constitution of a material vegetable fibre cell [70]

As mentioned earlier cellulosic fibres have the disadvantage of absorbing moisture. One way of overcoming this is to chemically treat the fibres to promote better adhesion to the matrix. Pretreatment of fibres can clean the fibre surface, reduce the moisture uptake and increase the surface roughness.

2.4.2 Factors affecting natural fibres in composite applications

Although natural fibres has some advantageous properties, they also have the drawback of forming aggregates during processing, variation in fibre quality due to the natural processes affecting growth, thermal instability and low resistance to moisture absorption [61, 71]. Although variation in fibre quality is a serious delimitation, banana fibre is an agricultural waste product which is available all year round. The banana plant (genus *Musa Cavendish),* is an annual herbaceous plant, and has been suggested as a suitable crop for bio-composite applications [72-74]. These characteristics lead to poor matrix-fibre compatibility and therefore compromise overall composite performance. In this study, these limitations have restricted the application of natural fibre biocomposite to the interior components of the motor vehicle.

2.4.2.1 Moisture absorption in fibres

The absorption of moisture by biocomposites decreases their mechanical properties [75-77]. It was found that moisture absorption of pineapple-leaf fibre reinforced low density polyethylene (LDPE) composites increased linearly with fibre loading [78]. Stark (2001) reported that wood flour-polypropylene (PP) composites with 20% wood flour reached equilibrium after 1500 hours in a water bath and absorbed only 1.4% moisture while composites with 40% loading reached equilibrium after 1200 hours and absorbed 9% moisture [76]. Factors such as fibre concentration, size and shape affect moisture absorption in composites [79].

If the reinforcement does not properly adhere to the matrix, it does not add strength to the composite. Therefore, different fibre treatment methods have been invented to (i) obtain an efficient hydrophobic barrier and (ii) minimize their interfacial energy with the non-polar polymer matrix and improve adhesion between biofibres and the

matrix [68, 77]. Several authors [62, 71, 80, 81] have suggested various chemical treatments of natural fibres to improve adhesion between the fibre and matrix.

2.4.2.2 Fibre treatment

The interaction and adhesion between the fibre and the matrix have a noteworthy effect on the mechanical and physical properties of the fibre composites. To ensure good compatibility, treatment of the fibres has been attempted. These reagents contain reactive functional groups that modify the fibre making them hydrophobic and improves interfacial adhesion between the fibre and matrix [82].

Bogoeva-Gaceva investigated various chemical treatments of fibres such as dewaxing, mercerization, bleaching, cyanoethylation, silane treatment, benzoylation, peroxide treatment, isocyanate treatment, acrylation, latex coating and steam-explosion [60]. Furthermore, Nassif used 10% NaOH to chemically treat banana fibres and reported that the dielectric strength and thermal conductivity increased by 29% and 139% respectively [83]. Li *et al.* suggested that alkaline treatment was one of the most-used classical treatments that partially removes lignin, wax and oils from the fibre cell wall [62]. Therefore this research focused only on alkali treatment of the fibres. Moreover, Herrera and George *et al.* explain that the purpose of the alkaline treatment was to increase the surface roughness and the amount of cellulose exposed on the fibre surface, resulting in better mechanical interlocking and increased number of reaction sites [68, 78]. Hydrogen bonding broken in the network structure increases the surface roughness. The fibre treatment therefore improves the bonding strength between the fibre and the matrix which is of utmost importance in the formation of composites [84]. This bonding strength is determined by measuring the force required to pull out a fibre embedded in the matrix. Single fibre test can be used to measure interfacial properties such as interfacial shear strength and frictional stress [85].

2.4.3 Properties of natural fibres

The mechanical properties of natural fibres are much lower when compared to synthetic fibres as shown in Table 2.1. However, properties such as density, stiffness

and elongation render plant fibres comparable to values of E-glass, Kevlar and carbon, making them suitable replacements in composites [1]. In particular banana fibre has comparable density and elongation to break. Plant fibres have low elongation to break compared to thermoplastics, however they have much higher tensile strength and stiffness [34]. The principal benefits of using plant fibres in composites are to reduce costs, improve tensile strength, stiffness or other mechanical properties and finally to make the composite "greener" [34].

Table 2.1: Mechanical properties of natural fibres as compared to conventional reinforcing fibres [1, 17, 62]

Fibre	**Density/ (g/cm^3)**	**Elongation/ (%)**	**Tensile strength/ (MPa)**	**Young's Modulus/ (GPa)**
Cotton	1.5-1.6	3.0-10.0	287-597	5.5-12.6
Jute	1.3-1.46	1.5-1.8	393-773	10-30
Flax	1.4-1.5	1.2-3.2	345-1500	27.6-80.0
Hemp	1.48	1.6	550-900	70
Ramie	1.5	2.0-3.8	200-938	44-128
Sisal	1.3-1.5	2.0-14	400-700	9.0-38
Coir	1.2	15.0-30.0	175-220	4.0-6.0
Oil Palm	1.4	14	248	2
Banana	1.3	2.5-3.7	540	13-26
E-glass	2.55	2.5	3400	73
Kevlar	1.44	2.5-3.7	3000	60
Carbon	1.78	1.4-1.8	4000	230-240

2.4.4 Banana fibres

Bananas are a major food crop globally and are grown and consumed in more than 100 countries throughout the tropics and sub-tropics [86]. It is the fourth most widespread fruit crop in the world [87]. Bananas are said to be native to tropical South and Southeast Asia. They are among the most important commercial

subtropical fruits grown in South Africa and are planted for sale in local markets or self-consumption [88]. Since only a fraction of all bananas are sold in the world markets, according to the Agri-food business development centre, South Africa ranks 29th in the world producing 250 000 metric tonnes of bananas [88, 89].

Bananas are mainly produced in Mpumalanga, Limpopo and both the North and South Coasts of Kwa-Zulu Natal. In Kwazulu Natal the major banana growing area is the North Coast with 15% (1 700 ha) of total area cultivated with bananas in 2010 [88]. South African records refer only to banana used for consumption and there are no records of the use of the wasted banana plant once the fruit is harvested.

The banana plant is a large herbaceous flowering plant of the genus *Musa*. Each pseudostem can only produce a single bunch of bananas. After harvesting of a single bunch of bananas, the pseudostem dies and great amounts of agricultural residues are produced, causing environmental pollution [90, 91]. Exploitation of waste banana plants will be favorable to the environment and will have profitable economic benefits [92]. Since there is no further use for the plant, the researcher decided to use this waste material to produce a biocomposite material. Figure 2.9 shows typical mature local banana plants and the banana fibres extracted from the pseudostem. The fibres have many uses such as making cloth, string, rope, cordage and paper making [93]. Applications for the banana plant residues represent an important contribution to increase the economic importance of banana plantations [90].

Figure 2.9: Mature local banana plants (left). Extracted banana fibres (right)

2.5 Matrices in biocomposites

Already mentioned biocomposites comprises of natural fibres and synthetic or natural resin systems. Synthetic resins are either thermosets or thermoplastics. This study is confined to the use of thermosets and the modification thereof.

2.5.1 Thermosetting Polymers

Thermosets are polymers made of large molecules, with repeating structural units of monomers that undergo irreversible curing. These liquids at room temperature enable easy addition of fibres or other additives before being cured. Curing of thermosets is achieved by the addition of a catalyst or hardener and an accelerator and or heat. Unlike a thermoplastic, once cured, thermosets cannot be reversed to the liquid phase. This is due to the crosslinking of the molecules whereby a rigid three dimensional network is formed through the reactive sites within the molecule [27].
Thermosetting polymers are the commonly used in the composites industry [27]. Holbery and Houston also reported that thermosets generally have low viscosity, perform at ambient temperatures and low pressures and are therefore appropriate for typical composite applications [6].

The most commonly used thermoset resins in natural-fibre composites for automotive applications are polyester, vinylester and epoxy resins [6, 94]. Mohanty

et al. have reported that polymeric resins such as vinyl ester, polyester and epoxy, used in the composites are invariably costly and unsustainable as petroleum resources are being depleted [1]. The focus of this research is on the development of a bio-resin by modifying the unsaturated polyester with banana sap to produce a hybrid polyester resin.

2.5.2 Polyester chemistry

Unsaturated polyester resins (UPR) are important matrix resins for general purpose fibre reinforced composites [27, 95, 96]. UPR consists of two polymers, namely a short chain polyester containing polymerizable double bonds and a vinyl monomer. They are rarely sold as such, because they are brittle at room temperature and difficult to handle. Instead, whenever polyester is freshly synthesized in a plant, it is mixed with the vinyl monomer in the molten state. Thus materials that are viscous at room temperature, with a styrene content of approximately 60% are sold. However, in this study 35% styrene was used for easy diffusion of the bio-resin into the fibres by vacuum infusion and to reduce the styrene emission making the biocomposite environmentally friendly. UPR are made in a two-step process: first, unsaturated and saturated acids or anhydrides are reacted with diols in a polycondenzation reaction; secondly the resulting pre-polymer is dissolved in styrene to form a syrup like resin [97, 98]. This research is based on the two-step process adopted by UPR systems.

2.5.3 Properties of polymers

Since the resin or matrix is a binding agent for the composite, it should have properties of stiffness, good strength and toughness, good thermal properties, good adhesion and chemical properties. Chemical properties such as viscosity, glass transition temperature, gel time, cure time, shelf life or stability, environmental resistance and volatile emissions during processing, are some of the parameters to be considered when processing a resin [97]. A major concern regarding the application of these resins in composite materials is the phenomenon of temperature elevation, such as the interior of a motor vehicle which can become extremely hot in summer. This study focusses on characterizing the bio-resin for the above mentioned properties.

2.6 Bio-based matrix systems

The American Society for Testing and Materials (ASTM) defines a bio-based material as ***an organic material in which carbon is derived from a renewable resource via biological processes. Bio-based materials include all plant and animal mass derived from CO_2 recently fixed via photosynthesis*** [99].

The schematic classification of bio-based polymers is represented in Figure 2.10. This study produced a renewable resource-based polymer from banana fibre and a hybrid resin using banana sap.

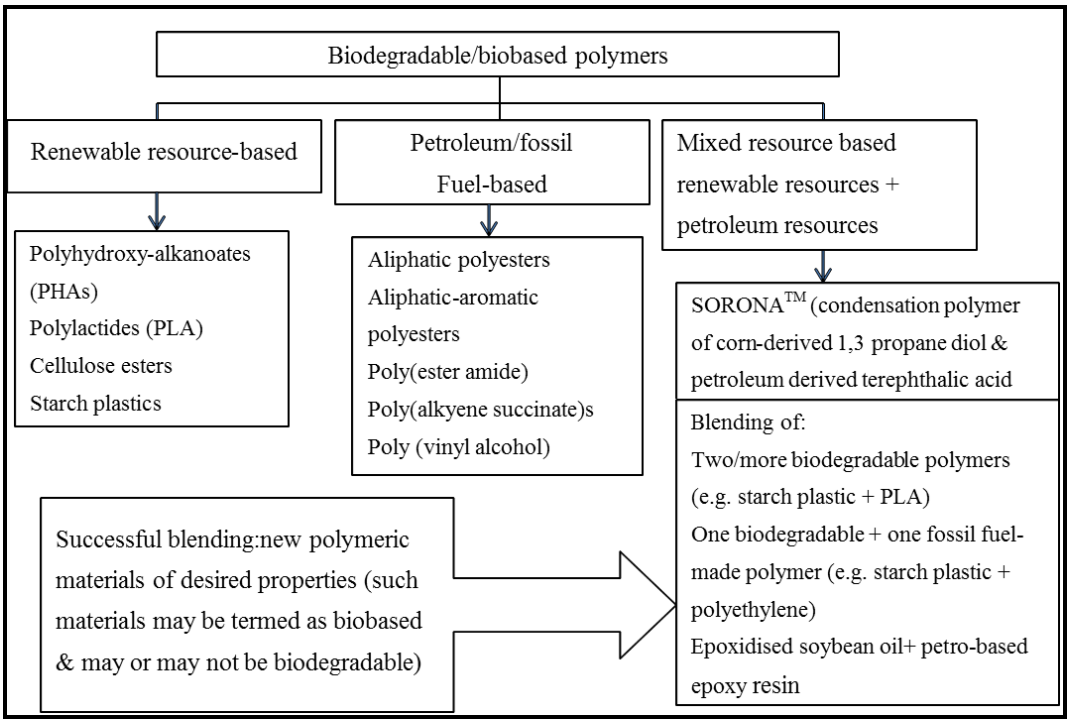

Figure 2.10: Classification of bio-based polymers [1]

The term "bio-resin" refers to a resin that is made of raw materials derived from renewable resources such as plant oils (soybean oil, pine oil castor oil), polysaccharides (starch, cellulose) and proteins [60, 77]. Rubber, tannins, lignin, soybean oil, epoxidized pine oil waste, castor oil, furfural alcohol-based resins, lactic acid, cashew nut shell liquid, carbohydrates, proteins and bio-alkyds are some of the raw materials used in the manufacturing of commercial thermosetting resins [77]. Table 2.2 shows selected bio-resins and that have been used to replace synthetic resins. It has been noted that world production giants are incorporating bio-resins

into their products [100]. For instance, in 1941 Henry Ford made a car with 70% cellulose fibers in a phenolic resin matrix extended with soybean meal. He used a sledgehammer to demonstrate the strength and impact resistance of his company's all-plastic-body car [46]. Furthermore, John Deere built tractor bodies using soy bean oil based bio-resins [46] whilst Airbus and Boeing replaced old aircraft with new bio-resin bodies [99].

Table 2.2: Selected bio-resins showing their origin and uses

Bio-resin	**Origin, properties, uses**	**Reference**
Natural rubber	Milky white fluid known as latex from a tropical rubber tree.	[101]
Tannin-based adhesives	From timber species such as wattle or mimosa bark extract and pine. Used for exterior wood bonding.	[99, 102-104]
Lignin	From woody plant glue. Lignin with hemp and flax used for car dashboard panels, computer and television frames.	[105]
Cashew nut shell liquid (CNSL)	Phenolic-based for uses such as resins, friction lining material, surface coating. CNSL with hemp fibres gave low cost, mechanically robust materials	[106-108]
Polysaccharides	Blends from starch with aliphatic polyesters, PLA, polycaprolactone, PVA or cellulose acetate. Uses: single use microwavable dishes, catering utensils, horticultural applications, mulch bags, shopping bags.	[105]
Cellulose derived biopolymers	From wood and sugar cane bagasse. Used for cellophane films, membranes for reverse osmosis, packaging.	[99]
Furfural	By-product of sugar cane bagasse, oats, wheat bran and corncobs. Used for binding glass, rockwool and carbon fibres.	[109]
Soybean and palm oil	From soy bean and oil palm trees. Used for particle boards, thermoset resins, foams, household and furniture applications	[11, 110]
Polylactic acid (PLA)	From lactic acid. Used in medical applications, packaging among others.	[111-113]
Aliphatic polymers	From polycondenzation of aliphatic glycol and aliphatic dicarboxylic acid. Used in medical application, films, compost bags, bottles among others	[114]

The review of plant based polymers from different natural sources however indicates that no research has been done using banana sap in the resin. It is therefore the focus of this research to develop a bio-resin using banana sap.

2.7 Banana sap

Banana sap is a clear liquid extracted from the pseudostem of the banana plant.

Studies on the chemical composition of the banana sap from pseudostem such as carbohydrates, fibre composition and mineral content have been reported [87, 90, 115, 116]. It is also reported that the moisture content of fresh banana pseudostem is about 96% [91]. Furthermore, Aziz and co-workers reported the presence of polyphenols and flavonoids in the sap [87]. Oxidative browning takes place when the sap is exposed to air implying the presence of phenolic compounds. However, to the best of our knowledge, there is still a gap of knowledge regarding the full characterization, especially the chemical structures of the components of the banana sap. In this study, monosaccharides (glucose and fructose) and disaccharide (sucrose) were found in the banana sap, the structures of which are shown in Figure 2.11. With reference to other research [117] on the use of saccharides in the formation of ester-carboxylic derivatives, we predict that these sugars actually attach themselves to the backbone of the maleate polymer. Hirose and coworkers dissolved glucose in ethylene glycol and added it to succinic anhydride and dimethylbenzylamine to form a saccharide polyacid and consequently the thermal stability increased [117].

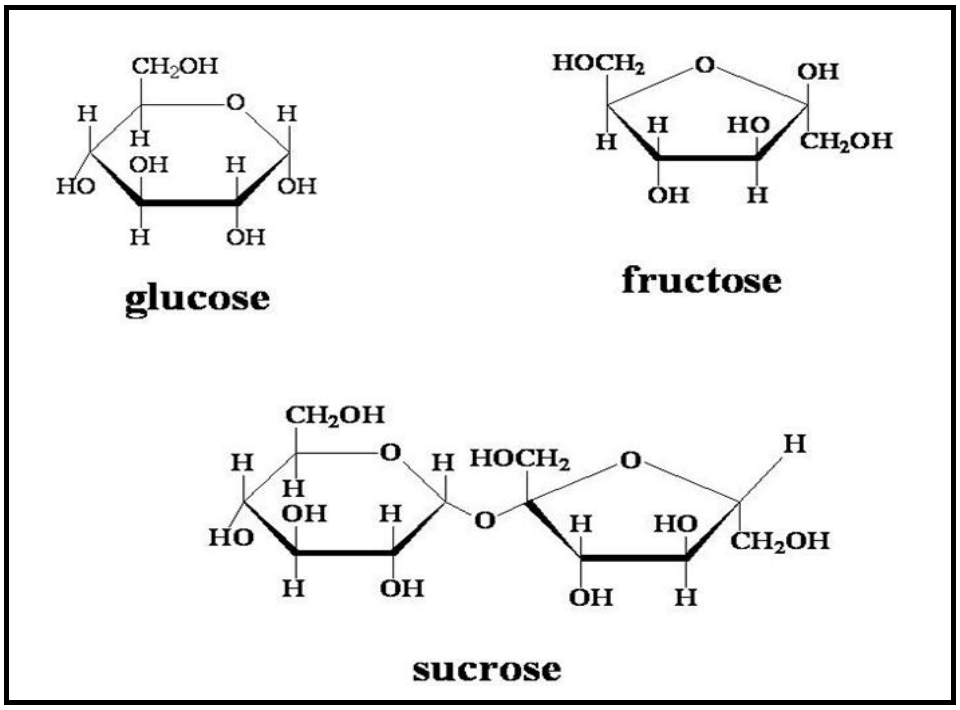

Figure 2.11: Structures of glucose, fructose and sucrose found in banana sap [118]

2.8 Summary

In this chapter the biocomposites from various sources was reviewed and it is clear that natural fibres are gaining acceptance within the auto-industry. Various researchers have used banana fibres and synthetic or in some cases natural resin systems and it was found that comparable mechanical properties such as tensile strength were obtained. However it has been found that no research has been conducted with banana sap used in resin formation. An ideal agricultural waste has been suggested in the form of banana sap. Using the fibre and sap from the same plant source led to the development of a biocomposite with similar or better mechanical properties that could be used for non-functional motor vehicle components.

The next chapter will provide the research methodology and design used in this study.

CHAPTER 3 - RESEARCH METHODOLOGY AND RESEARCH DESIGN

Introduction

In order to achieve the objectives of this research, a quantitative research approach was used, where the research was conducted by collecting numerical experimental data that was then objectively analyzed with value-free and unbiased facts. The literature review that was conducted early in the study provided the underpinning knowledge for the research that has been done and the current trends and more importantly the gaps in the knowledge in this field.

A positivist approach based on knowledge gained from "positive" verification of observation of experimentation was used in this study. A schematic diagram (Figure 3.1) outlines the design of the experiment followed by a synopsis of the experimentation.

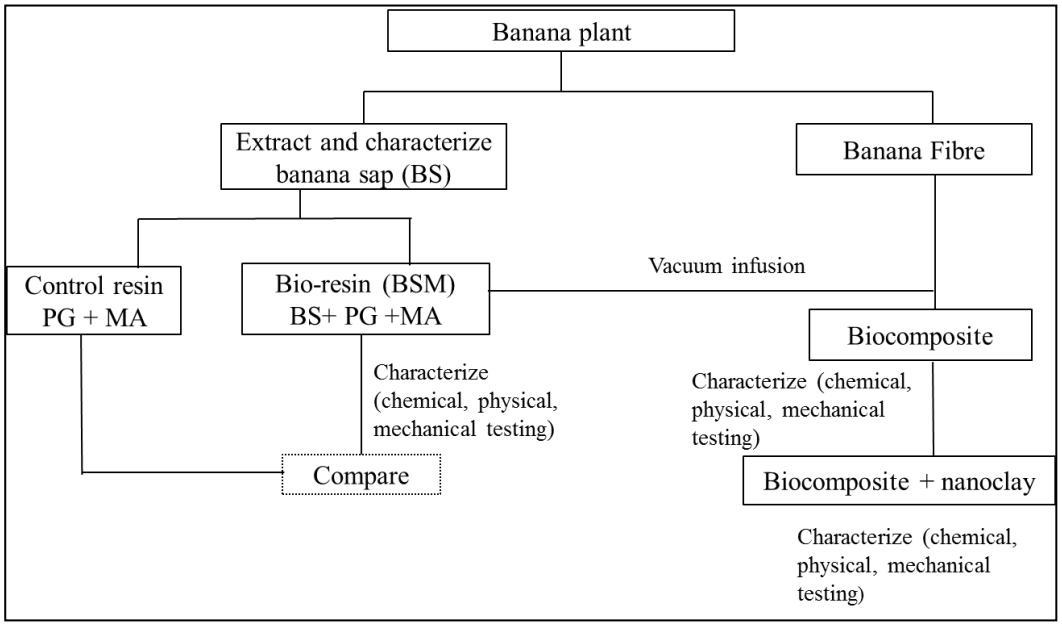

Figure 3.1: Schematic diagram of research design

The banana sap and fibres were extracted from the pseudostem of the banana plant obtained from a local plantation in Durban, Kwa-Zulu Natal. The sap was characterized by HPLC and GC-MS to determine the constituents, and the sap was

then used as is in the resin formulation. The bio-resin was constituted from banana sap, maleic anhydride and propylene glycol. This was compared to a control resin made with maleic anhydride and propylene glycol. The bio-resin and the control resin were fully characterized for their thermal, mechanical and chemical properties. The banana fibres were extracted, washed and chemically treated with alkaline solution. The fibres were infused with the bio-resin by vacuum infusion and cured. A control composite specimen was also prepared and a comparison was made between both composites. Five samples were tested for mechanical properties and triplicate analyses were performed for all other tests. To improve the strength of the resins, the resin was fortified with nanoclay and the mechanical and thermal properties were determined.

This chapter outlines the materials used in the preparation of the bio-resin and biocomposites followed by the experimental section discussing the instrumentation used. Extraction and characterization of the sap and fibres are also given.

3.1 Materials

Maleic anhydride (MA), propylene glycol (PG), cobalt napthenate (6%), styrene and methyl ketone peroxide (MEKP), *tert*- hydroquinone (THQ) and *tert*- butyl catechol (TBC) were all purchased from Sigma Aldrich, South Africa. Table 3.1 summarizes the properties of MA and PG.

Table 3.1: Chemical and physical properties of MA and PG [119]

	Maleic anhydride (MA)	**Propylene glycol (PG)**
Appearance	white solid	colourless clear liquid
Molecular weight (g/mol)	98.06	76.1
Boiling point (°C)	202	188
Melting point (°C)	52.8	-59

In this study MA was converted to maleic acid and reacted with PG to form the unsaturated polyester resin. MA is soluble in water, ether, acetate, chloroform and

dioxane at ambient temperature and is used as a chemical intermediate in the synthesis of fumaric and tartaric acid, certain agricultural chemicals, many resins, dye intermediates and pharmaceuticals. It is also used as a co-monomer for saturated polyester resins, as an ingredient in bonding agents used to manufacture plywood, a corrosion inhibitor and a preservative in oils and fats [120]. PG is one of the main reactants for UPR. It is also used as a preservative in food and tobacco products, in pharmaceuticals and personal-care products [121].

The bio-resin was fortified with the nanoclay, Cloisite® 30B which was obtained from Southern Clay Products, USA. Cloisite® 30B is a natural montmorillonite modified with a quaternary ammonium salt. The properties of the salt are shown in Table 3.2.

Table 3.2: Properties of Cloisite® 30B [122]

Specific Gravity (g/cm^3)	1.98
Bulk Density (g/cm^3)	0.2283 (loose), 0.3638 (packed)
Loss On Ignition (%)	30
Particle Size ($\leq \mu m$)	2 (10 %), 6 (50 %), 13 (90 %)
Hardness (Shore D)	83
Tensile Strength, Ultimate	101
Elongation at Break (%)	8
Modulus of Elasticity (GPa)	4.657
Flexural Modulus (GPa)	3.78
Izod Impact, Notched (J/cm)	0.27
Deflection Temperature at 0.46 MPa (°C)	96
Moisture Content (%)	< 2
Organic Modifier	methyl, tallow, bis-2-hydroxyethyl, quaternary ammonium
X-Ray Diffraction d-Spacing (001) (Å)	18.5
Modifier Concentration (meq/ 100g clay)	90.00

3.2 Experimental Design and methodology

This section explains the extraction of the banana sap and fibres. The methodology used for 1) the determination of the composition of the sap, 2) procedure for processing of bio-resin, 3) procedure for preparation of biocomposite will also be given. Finally, the instrumentation used for the characterization will be detailed.

3.2.1 Extraction of BS and BF

The stem of the banana plant was collected from a banana plantation in Durban, South Africa. The sheets of the plant were separated and crushed with a Pinette Emidecau Hydraulic Press (OB 102, France) shown in Figure 3.2. The extracted sap was collected and stored in the freezer at -18 °C for later use. The fibres were washed several times to remove the pith, air dried and then stored in plastic bags, for further use.

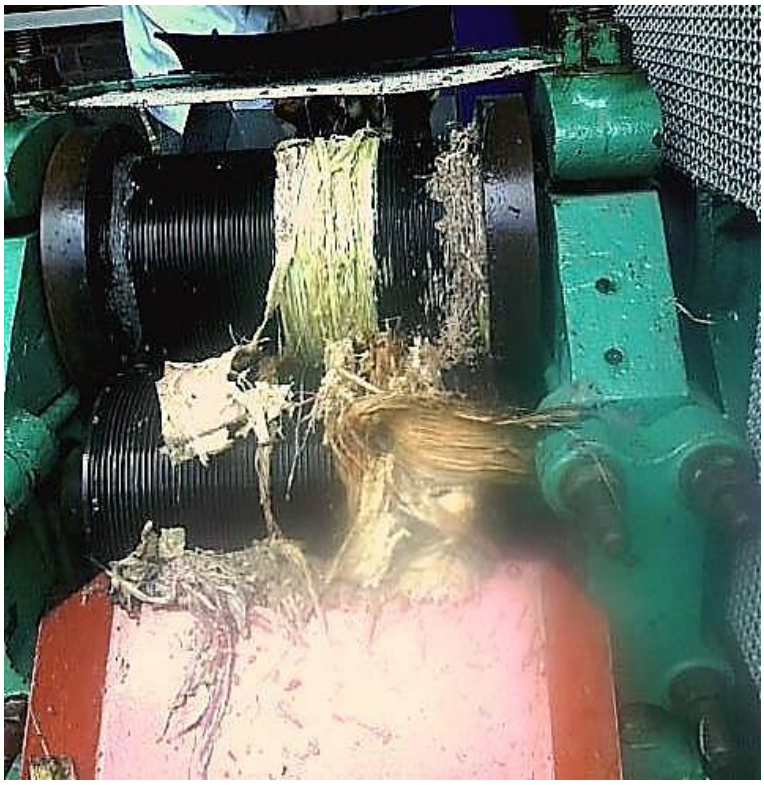

Figure 3.2: Extraction of BS from sheets of pseudostem using Pinette Emidecau Hydraulic Press

The fibres were processed into a needle punched, non-woven mat in a two-step process at the Council for Scientific and Industrial Research (CSIR) laboratories, Port Elizabeth. The procedure for the fibre processing is detailed in Appendix A3.1.

3.2.2 Chemical composition of banana sap

In order to determine the chemical composition of the banana sap, physiochemical analyses were performed (in triplicate). Mineral analysis of metals was determined by Inductively Coupled Plasma-Atomic Emission Spectroscopy (ICP-AES).

The amount of water present in the sap was confirmed by the Dean and Stark method, which involved continuously removing water that was produced during a chemical reaction performed at reflux temperature [123]. The sap was qualitatively analyzed for carbohydrates using the Molisch test [124]. Concentrated H_2SO_4 was carefully added to 2 mL of BS and 2 drops of α-naphthol in 95% ethanol in a test tube until a violet colour was observed.

Spectrophotometric analysis of total phenols was carried out using a Perkin Elmer UV/VIS spectrophotometer. The total phenolic content of extracts was determined using the Folin-Ciocalteu method [125]. The extracts were oxidized with Folin-Ciocalteu reagent, and the reaction neutralized with sodium carbonate. The absorbance of the resulting blue colour was measured at 765 nm after 60 min. Gallic acid (GA) was used as a standard and the total phenolic content was expressed as mg GA equivalent/L of extract. The standard curve was prepared using concentrations 50-500 mg/L.

High Performance Liquid Chromatography (HPLC) analysis of sugars was performed using the Perkin Elmer 250 Binary pump HPLC unit. A refractive index detector, Rheodyne 7125 manual injector, Phenomenex Rezex H organic acid column and Clarity software from Data Apex version 2.4.04.139 was used. The mobile phase was made up of 0.0025M H_2SO_4/H_2O. Chromatograms were then recorded, and the peak areas from the sample were identified by comparison to pure standards of 0.1% concentration.

Gas Chromatography-Mass Spectrometry (GC-MS) analysis of the organic compounds was performed using the Agilent Technologies 6890 Series GC coupled with an Agilent 5973 Mass Selective Detector, driven by Agilent Chemstation

software. The samples were prepared by liquid-liquid extraction using dichloromethane, ethyl acetate and hexane to extract the polar, medium polar and non- polar components. All solvents were of high purity gas chromatograph grade. The organic extracts were concentrated by rotary evaporator (rotavap) and analyzed by GC-MS.

3.2.3 Chemical composition of banana fibre

Fibre composition was determined through a number of tests conducted by the Animal Sciences Department at North Dakota State University. This included dry matter testing, neutral detergent solutions and acid detergent solution characterization, as well as starch spectrophotometry. These measurements allowed for the collection of percentage dry matter, as well as percentage cellulose, hemicellulose, lignin, starch, and ash. Dry matter determination was done according to Association of Official Analytical Chemists (AOAC) standard 930.15, and the samples were weighed at room temperature, heated at 100 °C for 24 hours, cooled in a desiccator, and then re-weighed for a second time. Neutral detergent fibre, acid detergent fibre, and acid detergent lignin analysis were performed using an ANKOM$^{200/220}$ Fiber Analyzer (ANKOM Technology, Fairport, NY) according to methods in the USDA Agricultural Handbook No. 379 [126].

The determination of starch was performed after an acid and enzymatic isolation using a micro-titre reading with a SPECTRAmax 340 Microplate Reader in accordance with the literature [127].

3.2.4 Chemical treatment of banana fibre

The fibres were chemically treated by immersing in 2% sodium hydroxide (reagent grade) for 24 hours at room temperature. After the alkaline treatment the fibres were rinsed with water and 10% acetic acid solution (reagent grade), thereafter they were rinsed with water again until a neutral pH was obtained. The fibres were dried in an oven at 80 °C overnight.

3.3 Resin preparation

Since the resins prepared in this research were based on unsaturated polyester resin (UPR) chemistry using MA and PG a brief introduction to this chemistry is given.

MA is bi-functional because it has two acid groups and also because of its unsaturated − CH:CH− grouping [128] as shown in Figure 3.3

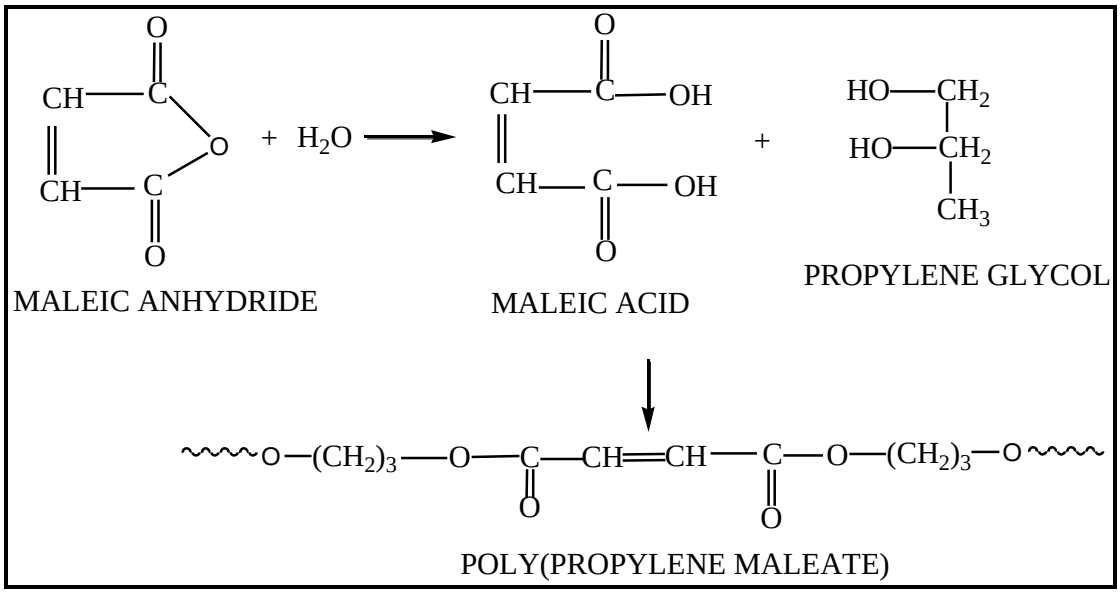

Figure 3.3: Schematic diagram of the formation of polypropylene maleate resin

The polyester resin formed in this reaction was a linear polymer containing reactive double bonds [128] cross-linked with a vinyl reactive monomer, styrene as shown in Figure 3.4. The cross-linking reaction between the styrene and the double bonds was highly exothermic and the temperature was controlled at 50 °C.

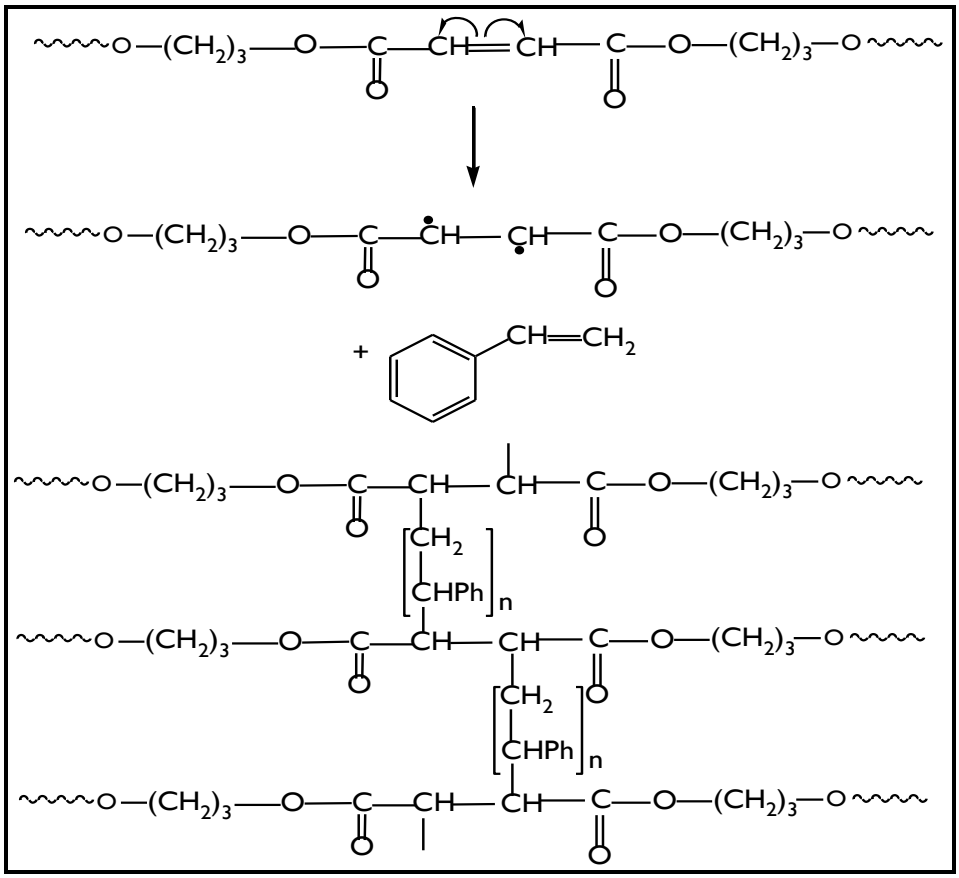

Figure 3.4: Cross-linking of polypropylene maleate with styrene monomer

3.3.1 Preparation of control and BSM bio-resin

The following section details the method employed to synthesize and characterize the control resin and BSM bio-resin. The materials used for the preparation of the resins are summarized in Table 3.3.

Table 3.3: Materials used for the preparation of the resins

Control resin	BSM bio-resin
Equal molar masses of MA+ PG + 10% excess PG	Equal molar masses of MA+ PG +10% excess PG + BS (30-64%)

A reactor flask as shown in Figure 3.5 was set up with a heating mantle, mechanical stirrer, condenser, temperature probe and water trap.

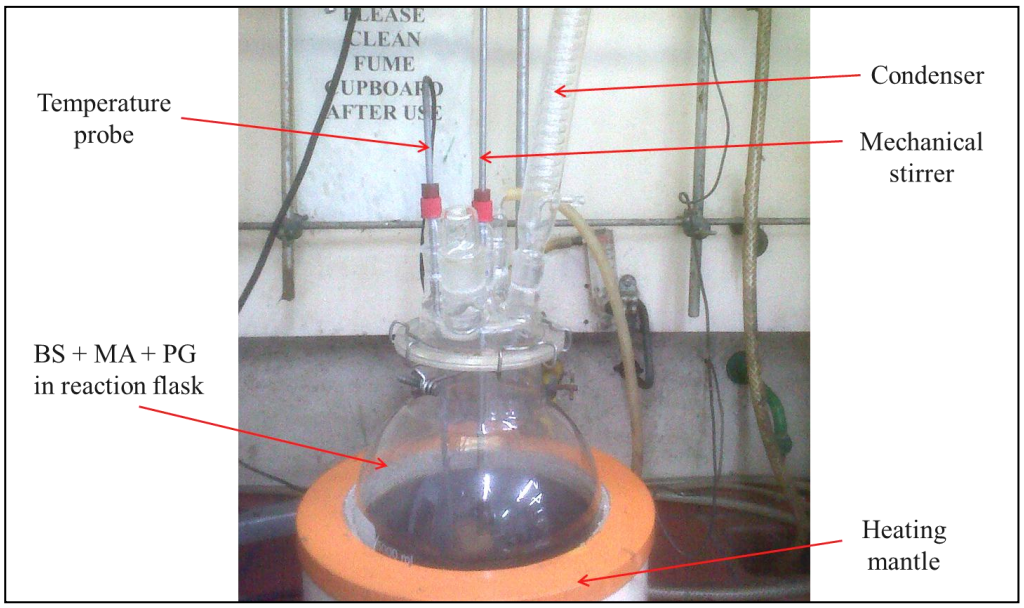

Figure 3.5: Experimental setup for the processing of the control and BSM bio-resin

PG was then transferred into a 2 litre round bottomed flask and allowed to melt at 100 °C in the heating mantle. MA was then slowly added to maintain a slurry. In the experiment for BSM bio-resin synthesis, varying concentrations of BS (30-60%) as shown in Table 3.4 were added to the MA and PG to determine the final optimum amount of BS to add to the cook.

Table 3.4: Percentage composition of banana sap (BS) in banana sap maleate resin (BSM)

Sample	% Composition BS
BSM 0	0
BSM 1	30
BSM 2	40
BSM 3	50
BSM 4	60

Thereafter 50 ppm hydroquinone; a stabilizer, was added to the flask to prevent premature gelling. The heating times, batch and vapour temperatures were recorded (See Appendix A3.2). Nitrogen was bubbled into the flask at a flow rate of 1 mL

/min to create an inert atmosphere. At the end of the reaction some of the solvent, in this instance PG, was distilled off. Therefore, a 10% excess was initially added to accommodate for this loss. Under good agitation, the temperature was slowly increased to 150 °C at 1 °C/min intervals followed by a ramp from 150 °C to 200 °C at 0.5 °C/min.

The acid number, which is a measure of carboxylic acid in the polymer, was measured every hour. The titration method as shown in Appendix A3.3 was used to measure the acid number of the banana sap maleate according to ASTM D 1386[3] method [129] which is defined by the amount of potassium hydroxide in milligrams required to neutralize 1 g of sample. Viscosity measurements were performed using a Cone and Plate viscometer. The molecular weight distribution was done by gel permeation chromatography. During the processing of the resin, samples were taken every hour, and then every half-hour (towards the end of the processing) to measure acid number, viscosity and molecular weight distribution. When the acid number was below 50 and the viscosity was between 5-8 poise, the reaction was terminated and the resin was thinned with styrene containing inhibitors.

3.3.2 Dilution of bio-resin

As previously mentioned, once the resin was cooked, it was necessary to for it to be thinned or diluted in order to prevent gelling. The resin was diluted with a co-monomer namely styrene, whose function was two-fold. Styrene helped tailor the viscosity of the resin to an acceptable level and also modified the property of the cured polymer and biocomposite. In order to prevent premature gelation and improve the shelf life of the resin, initiators were added to the styrene and mixed with the resin. The hot resin was added to 35-40% styrene to which 100 ppm of *tert*-hydroquinone (THQ), 50 ppm of di- *tert*-butylcatechol (TBC) and copper napthenate were added to stabilize the resin. The styrene was maintained at a temperature of 50 °C. Viscosity, % volatiles and density of the resin with styrene was measured and compared to the specifications of a similar industry sample. Viscosity measurements were taken by placing a 500 mL sample in a water bath at 25 °C for one hour. The

[3] ASTM D1386 test method for acid number of synthetic and natural waxes Vol 15.04

viscosity was measured with an ICI viscometer with a spindle number 5 at 10 rpm. Since 35-40 % of styrene was added to resin, the value for the volatiles was between 35 and 40 %. The volatiles were determined by measuring the mass of the resin before and after heating for one hour at 125 °C. The density was measured using a density cup.

3.3.3 Curing of bio-resin

Cure times were controlled by adjusting the amount of catalyst and accelerator. Peroxy catalyst such as Methyl Ethyl Ketone Peroxide (MEKP) liberated free radicals at ambient temperatures using certain metal accelerators such as cobalt napthenate to aid in the curing process as shown in Figure 3.6.

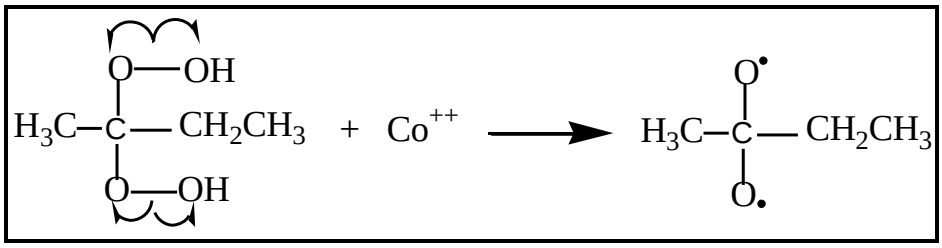

Figure 3.6: Free radical formation of MEKP with Co^{2+} taking place during the curing of the resin

To measure the gel times, 100 g of the resin was weighed out into a plastic cup and covered with aluminium foil and then equilibrated in a water bath at 25 °C for 30 minutes. Cobalt naphthenate (1%) accelerator was weighed and added to the resin. 1% of MEKP catalyst was added and stirred for one minute and the timer was immediately started. The resin was continuously stirred until the product started to gel. Thereafter the clock was stopped, and the gel time recorded. The thermometer probe was quickly attached to the cup, and the temperature and the product curing times were recorded.

3.4 Preparation of biocomposite

As mentioned previously, a biocomposite material comprises of reinforcing fibres embedded in the matrix system. The matrix systems consist of resin polymer, initiator and catalyst. The structural properties of the fibre-matrix interface are important for the mechanical and physical properties of composite materials. The matrix has the function to provide a physical form for the composites by binding fibres together and distributing the fibres in a predetermined manner in the composites. The matrix also transmits the load to the reinforcing fibres and protects the fibres from environmental attack. The most widely reported fibre loading is from 20% to 50% [38, 40-42, 130]. In this study the researcher decided to use 30% fibre loading using the non-woven banana fibres to create laminates of 3-4 mm thickness for the various mechanical tests.

There are several different routes for composites manufacturing. Each distinct route has its own speciality and suitability. Some of the most popular manufacturing routes are [131]:

- Spray Lay-up
- Vacuum Bagging
- Filament Winding
- Pultrusion
- Resin Transfer
- Infusion Processes
- Prepreg Moulding
- Low-Temp Prepreg
- Resin Film Infusion
- Wet/Hand Lay-up

In this research, only the vacuum assisted resin infusion moulding (VARIM) technique as shown in Figure 3.7 was used. The advantages of using vacuum infusion is the low cost due to the reduced tooling costs, occurrence of low volatile styrene emissions, use of higher fibre volume fractions, low void content, better fibre wet-out due to pressure and resin flow throughout the structural fibres [29].

3.4.1 Vacuum assisted resin infusion moulding (VARIM)

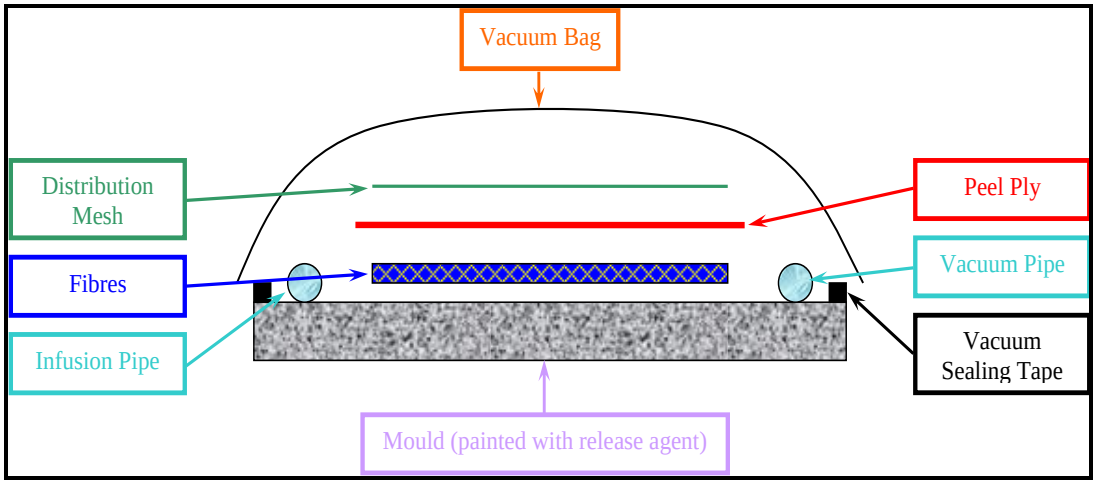

Figure 3.7: Schematic diagram of VARIM technique [131]

The non- woven mat fibres were infused with the control and BSM resins by vacuum assisted resin infusion moulding. In this technique a vacuum was used to impregnate the banana fibres with BSM and control resin. Figure 3.7 shows a schematic diagram of this process. A glass sheet was polished and shone five times with a release agent, which served in preventing the composite panel from adhering to the glass surface. The fibres were then laid out on the glass panel, and a peel ply and distribution mesh were placed on top of these. The peel ply was used to prevent the adhesion of the fibres to the distribution mesh. The distribution mesh assisted the resin flow process. Infusion and vacuum pipes were laid and the entire setup was covered with a vacuum bag which was sealed with vacuum sealing tape. The infusion pipe was initially closed off, and the vacuum pipe was connected to a vacuum pump. The pump was turned on and all the air inside the vacuum bag was removed. The infusion pipe was then inserted into the resin mixture, that was well mixed with 1% cobalt napthenate and 1% MEKP, and opened. Once all the fibres were wetted, the infusion pipe was closed and the pressure was held constant during curing process at room temperature for 24 hours. The biocomposite sheet was post cured at 80 °C for three hours. Figure 3.8 shows the infusion of the fibres with the BSM resin using the VARIM technique.

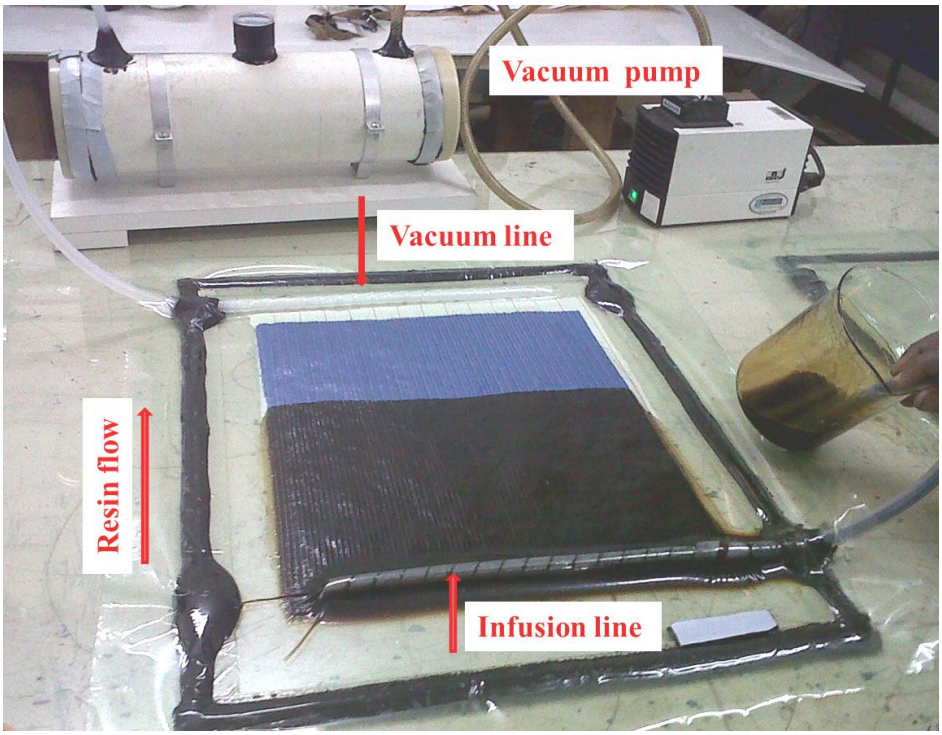

Figure 3.8: Method of vacuum infusion for BSM resin onto banana fibres

3.5 Characterization techniques and basic procedures

This section presents the various techniques used to characterize the bio-resins and biocomposites produced through the chemical functionalization of banana sap and banana fibres. A check list is given in Table 3.5.

Table 3.5: Checklist of characterization techniques conducted in this study

Technique	Reason for test
FTIR	Determination of functional groups
TG/DSC	Determination of degradation temperature, melting and crystallization temperatures
HDT	Deflection temperature under load
DMA	Elastic and viscoelastic properties
XRD	Determine amorphous/crystallinity
SEM	Study surface structure and morphology
Water absorption	Moisture uptake
Swelling test	Swelling resistance
Chemical resistivity	Resistance to water and harsh chemicals
Tensile test (ambient + elevated temperature)	Material strength
Tensile modulus (ambient + elevated temperature)	Measure of stiffness of material
Flexural test (ambient + elevated temperature)	Flexural strength
Flexural modulus (ambient + elevated temperature)	Resistance to deformation under load
Pull-out test	Study of fibre/matrix interface
Impact test	Resistance to impact
Delamination	Separation of reinforcement from matrix
Biodegradability test	Disintegration of biocomposite to give CO_2, water, inorganic compounds and biomass

3.5.1 Fourier transform infrared spectroscopy (FTIR)

Functional groups of the resins and the fibres were determined by the use of a Varian 800 FTIR, Scimitar Series instrument with Attenuated Total Reflectance (ATR) in

the range of 400-4000 cm^{-1}, and a resolution of 2 cm^{-1} for each sample. Whilst the resins were being processed, approximately 1g of sample was taken for analysis every hour and FTIR measurements were done. The fibres were cut and milled to provide a size of sample between 100-200 μm which was then analyzed to determine the functional groups.

3.5.2 Thermal analysis (TA)

Thermogravimetry (TG) measured the mass of a sample as a function of temperature and time. Differential scanning calorimetry (DSC) is a technique whereby the temperature change occurring whilst a chemical reaction or phase change took place in the polymer, for example crystallization, was monitored until the reaction was complete. The TG and DSC tests were performed using the TA SDT Q600 instrument at a temperature range of 40-400 °C, with a heating rate of 10 °C/min under nitrogen flow of 50 ml/min. TA techniques were also used to analyse the curing behaviour of the bio-resin, and isothermal and dynamic methods were used.

Kinetic studies were investigated on how different experimental conditions can influence the speed of a chemical reaction and give information about the reactions mechanism. Cure kinetics is an intregral aspect of thermosetting resin as they establish the optimum processing conditions. While extensive cure kinetic studies have been conducted on unsaturated polyester resin, research on bio-resins is limited.

Reaction kinetics was studied using the isothermal mode of the DSC. In order to select suitable temperatures for the isothermal experiments, a dynamic DSC scan from 40-500 °C at a heating rate of 5 °C/min was first obtained.

Samples between 10-15 mg were placed in the DSC pans. Dynamic scans were performed at four different heating rates: 5, 10, 15, 20 °C/min from 30-500 °C. The cured samples were cooled to 30 °C at a rate of 10 °C/min. To complete the heat-cool-heat cycle, the sample was then reheated to 500 °C to confirm the nonexistence of residual curing.

Two dynamic kinetic models based on multiple heating rates that are useful in determining the activation energy of the curing reaction have been proposed by

Kissinger [132] and Ozawa-Flynn-Wall [133]. This dissertation used the two models to determine the activation energy of BSM bio-resin.

3.5.3 Heat distortion

The heat distortion temperature (HDT) was performed on the DMA using three point bending clamps over the temperature range of 25-150 °C at a heating rate of 5 °C/min.

3.5.4 Dynamic Mechanical Analysis (DMA)

The Dynamic storage modulus (E′), loss modulus (E″) and the loss or damping factor (tan δ) of the BSM and control composites were measured using the dual cantilever clamp on a Dynamic Mechanical Thermal Analyzer, DMA Q800, TA Instruments. The specimen dimensions were 25 x 10 x 3 mm^3. The properties were determined over a temperature range of 25-350 °C at a heating rate of 5 °C/min, frequency of 10 Hz and amplitude of 50 µm.

Figure 3.9 shows the viscoelastic spectrum for an amorphous polymer as a function of temperature adapted from Perkin Elmer [134].

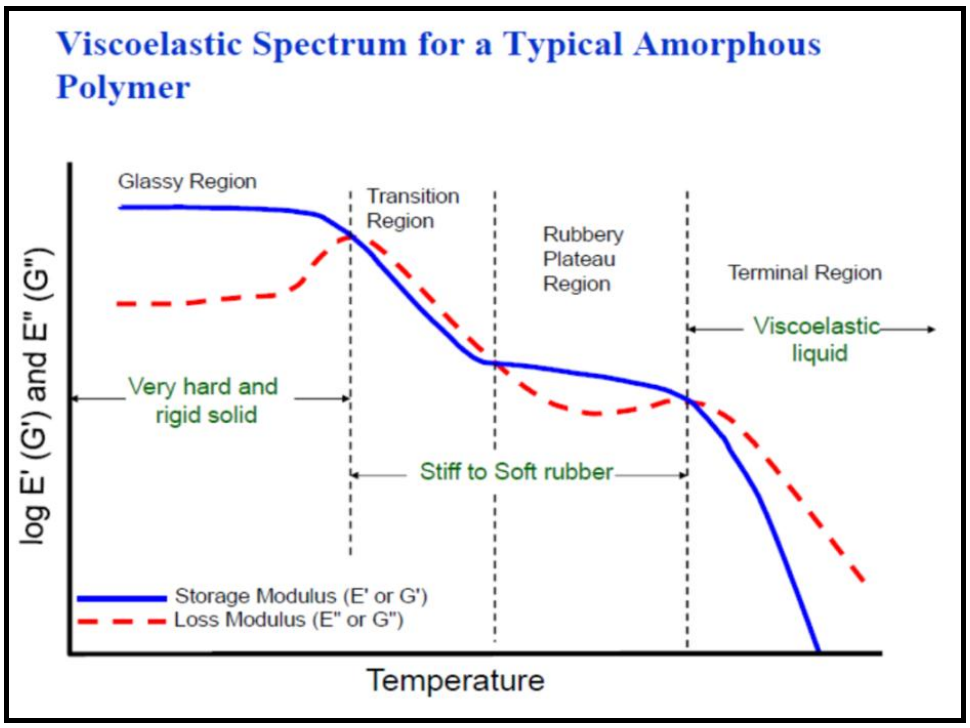

Figure 3.9: Viscoelastic spectrum for a typical amorphous polymer [134]

3.5.5 X-Ray Diffraction analysis (XRD)

Amorphous polymers are randomly oriented and are intertwined whereas semi-crystalline polymers pack together in ordered regions as shown in Figure 3.10. The crystalline region is shown by the neat or orderly packing of the polymer chain whereas the amorphous region is indicated by spaghetti-like polymer chains.

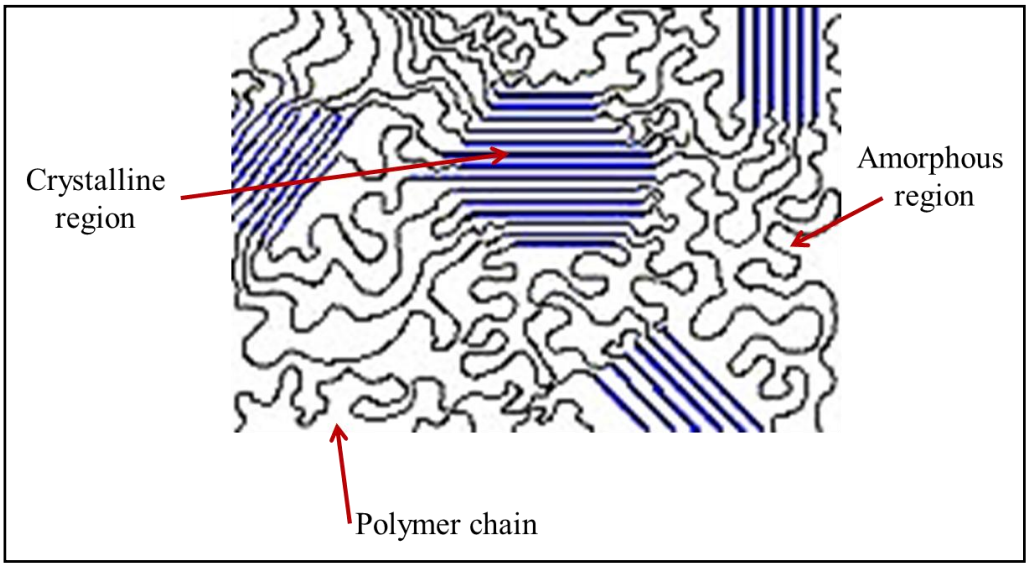

Figure 3.10: Amorphous and semi-crystalline polymer morphologies [135]

XRD patterns were carried out for dried and finely grounded neat resin and composite samples on a PANalytical Empyrean XRD instrument using Cu and Kα radiation generated at 45 mA and 40 kV.

When an X-ray beam hits a sample, and is diffracted, the distance between the planes of the atoms that constitute the sample can be determined by applying Braggs Law (equation 3.1).

$$n\lambda = 2d\sin\theta \tag{3.1}$$

Where n is the order of the diffracted beam, λ is the wavelength of the incident beam, *d* is the distance between the adjacent planes of the atoms (*d* spacing), and θ is the

angle of incidence of the x-ray beam. Since λ is known and θ can be measured, then *d*-spacing can be calculated.

3.5.6 Scanning Electron Microscope (SEM)

Scanning electron microscope was used to observe the surface structure and morphology of the treated and untreated banana fibres as well as the neat resins and the fracture surface of the biocomposites. SEM analysis of all the polymer and composite samples were performed using an environmental scanning electron microscope (EVO 15 HD, Carl Zeiss) at an accelerating voltage of 20 kV.

3.5.7 Water absorption

The water absorption test was done according to ASTM standard test method D570[4]. The dimensions of the test samples were 61 mm x 61 mm x 1 mm. The sample was first dried in an air oven at 50 °C for 24 h, cooled in a desiccator and immediately weighed to the nearest 0.001 g which was then taken as the dry initial weight of the sample, M_o. The specimen was immersed in a container of distilled water maintained at a temperature of 25 °C for 24 hours. After 24 hours, the specimen was dried and reweighed to constant weight, designated as M_1. The analysis was done in triplicate and the percentage of water absorbed by the composite material was calculated by using weight difference between the samples immersed in water and the dry samples using equation 3.2.

$$\Delta M(t) = \frac{m_t - m_0}{m_0} \times 100 \tag{3.2}$$

where, ΔM_t is moisture uptake at time t, m_t and m_o are the mass of the wet weight and dry weight at time t, respectively.

The diffusion of water in the composite medium was studied using Fick's steady state flow by applying equation 3.3:

[4] ASTM D570. (1995). Standard test method for water absorption of plastic materials.

$$\frac{M_t}{M_\infty} = \frac{\sqrt[4]{D_t}}{L\sqrt{\pi}} \tag{3.3}$$

Where M_t is the weight of water content at time t, M_∞ is the equilibrium water content, L is the sample thickness and *D* is diffusion coefficient whilst $M_t / M_\infty \leq 0.6$ was maintained.

The movement of the solvent molecules in the polymer segments was characterized by the diffusion coefficient. The absorption of water by the natural fibre was related to the permeability of the water molecules through the biocomposite material. Therefore, the sorption coefficient are related to the equilibrium sorption and is calculated by the equation 3.4:

$$S = M_\infty / M_t \tag{3.4}$$

Where, M_∞ and M_t are the percentage of water uptake at infinite time and time *t*.

The permeability coefficient P, (mm^2/s), which implies the net effect of sorption and diffusion and is given by the equation 3.5:

$$P = D \times S \tag{3.5}$$

3.5.8 Swelling tests

Circular samples of the BSM and control resins (diameter approx. 2 cm) of ASTM standard D5890[5] were weighed and immersed in test bottles with airtight stoppers containing toluene at 80 °C. The initial weight, swollen weight and deswollen weights were recorded using an analytical balance.

The swelling index measures the swelling resistance of the BSM and control bio-resins and was calculated using the equation:

$$\text{Swelling index } \% = \frac{A_s}{W} \times 100 \tag{3.6}$$

[5] ASTM 5890- Standard Test Method for Swell Index of Clay Mineral Component of Geosynthetic Clay Liners

Where A_s was the amount of solvent absorbed by the sample, *W* was the initial weight of sample before swelling.

The extent of cross-linking can be determined from the reciprocal swelling values 1/Q where Q is the amount of solvent absorbed by 1 g of sample:

$$Q = \frac{\text{Swollen wt.} - \text{dried wt.}}{\text{Original wt.}} \times \frac{100}{\text{formula wt.}} \qquad (3.7)$$

3.5.9 Chemical resistivity tests

Chemicals can affect the strength, flexibility, surface appearance, colour, dimensions or weight of plastics. Chemical attack on the polymer chain results in the reduction of chemical properties such as oxidation, reaction of functional groups and depolymerization. Furthermore, physical changes take place such as adsorption of solvent resulting in the softening and swelling of the polymer, permeation of the solvent through the polymer and dissolution in the solvent [97].

The immersion test was adapted using ASTM D 543[6]. The samples were visually observed and classified as: high resistance with no attack and possibly slight absorption, or limited resistance with a slight attack by absorption or swelling, and no resistance where the material will decompose or dissolve within a specified time. A specimen sample of 2 cm x 2 cm of the control and BSM composites were immersed for 30 days at room temperature in the following solutions: water ethanol, benzene, acetone, chloroform, petrol, 10% H_2SO_4, 10% HCl, 10% HNO_3, 10% NaOH. The initial masses were recorded, and after 30 days the specimens were reweighed and the % change in weight were recorded.

3.6 Mechanical properties

The standard mechanical properties were determined by the procedures found in ASTM standards for plastics. The mechanical properties studied were tensile strength

[6] **ASTM D543 - 06 Standard Practices for Evaluating the Resistance of Plastics to Chemical Reagents**

and modulus, flexural strength and modulus at ambient and elevated temperatures, impact, fracture test and creep.

3.6.1 Tensile properties

The tensile properties of the neat resins and biocomposite materials samples were tested on a LLOYD Universal Testing Machine with a crosshead speed of 1mm/min according to ASTM standard test method (D638). The test samples were rectangular in shape with dimensions 150 mm x 15 mm x 4 mm. The test specimen was held tightly by the two grips, the lower grip being fixed. The output data in the form of stress-strain graphs was computed from the console microprocessor.

3.6.2 Flexural properties

The flexural properties were tested on a LLOYD Universal Testing Machine with a crosshead speed of 1mm/min using the three point testing method adapted from ASTM standard test method (D790). The test samples were rectangular in shape with dimensions 64 mm x 12.7 mm x 4 mm.

3.6.3 Fibre pull-out tests

The resin was poured into cylindrical capsules as shown in Figure 3.11. One end of the treated and untreated fibre was immersed at a depth of 1 cm into the resin with the opposite end protruding from the resin. The resin was cured at room temperature. The fibre and resin ends were attached to the tensile clamps.

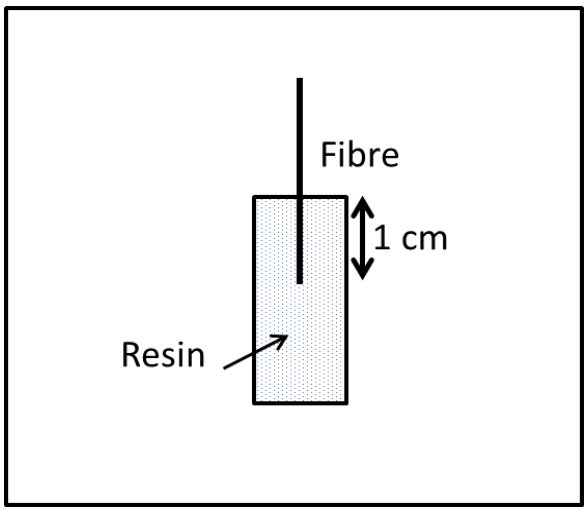

Figure 3.11: Schematic diagram for fibre pull-out test [84]

3.6.4 Impact tests

One of the major concerns in the use of natural plant fibre reinforced polymeric composites is their response to impact damage and the capacity of the composites to withstand it during their service life. In automotive applications such damage to materials may be introduced by bumps, crashes and falling foreign objects which can cause a severe reduction in load bearing capabilities of these materials [136]. Impact testing is about resisting impact and gives an insight to the material's toughness.

Drop weight impact testers

Cylindrical mass pieces of 242 g and 318 g were dropped vertically onto the square specimens of 50 mm x 4 mm thickness. The height of the fall was recorded. Since the mass either stops dead on the specimen or breaks it, the test was essentially recorded as pass or fail. The energy absorbed by a specimen was calculated by the product of impactor mass, impactor height and gravitational force (equation 3.8) from which it was dropped from increasing heights until the specimen fractured or broke. Both the mass and the drop height were varied till an indentation was observed.

$$\text{Impact Energy} = \text{mass} \times \text{height} \times \text{gravity} \qquad (3.8)$$

3.6.5 Hardness tests

The Barcol hardness test was used to determine the indentation hardness of materials through the depth of penetration of an indenter.

3.6.6 Fracture toughness: Single Edge Notched Bend (SENB)

The ASTM D 5045–93 testing standard was used as the guideline for the SENB test coupons [137]. Each specimen had an initial crack length of 5 mm. Specimens were subjected to this test using a three-point-bend fixture. SENB tests were done on the Lloyds universal testing machine fitted with a 5 kN load cell at a cross-head speed of 10 mm/min. The dimensions of the test specimen for plane strain conditions are shown in Figure 3.12 (a) and (b) [138].

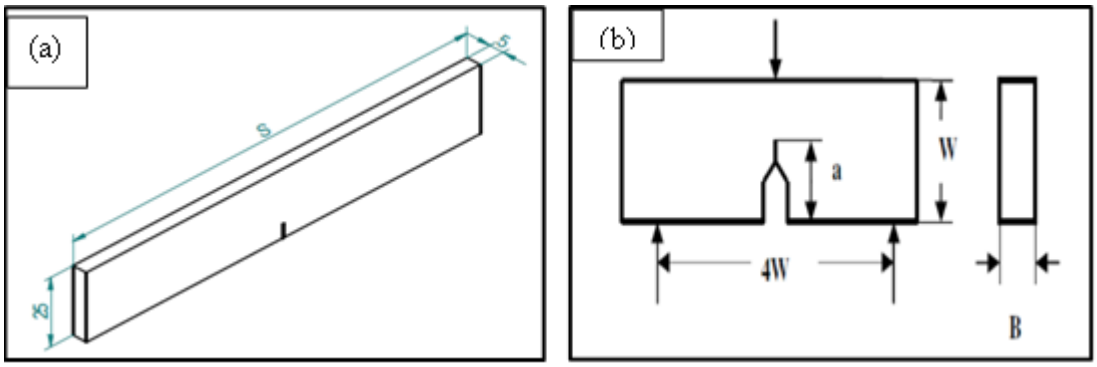

Figure 3.12: (a) and (b) Dimensions of SENB specimen [138]

This test was performed to determine the Mode I fracture toughness (K_I) of the manufactured composite structures. Fracture toughness measures the resistance of a material to the propagation of a crack. K_I was evaluated using equation 3.9.

$$K_I = \frac{P}{B\sqrt{W}} f\left(\frac{a}{W}\right) \tag{3.9}$$

Where,

K_I = stress intensity factor (MPa√m)

P = critical load (N)

B = thickness of specimen (m)

W = height of specimen (m)

f(a/W) = correction factor calculated in equation 3.10:

$$f\left(\frac{a}{W}\right) = \frac{3\frac{S}{W}\sqrt{\frac{a}{W}}}{2\left(1+2\frac{a}{W}\right)\left(1-\frac{a}{W}\right)^{\frac{3}{2}}}\left[1.99-\frac{a}{W}\left(1-\frac{a}{W}\right)\left\{2.15-3.93\left(\frac{a}{W}\right)+2.7\left(\frac{a}{W}\right)^2\right\}\right] \tag{3.10}$$

Where,

S = span length of the specimen (m)

a = crack length (m)

W = height of the specimen (m)

The Mode I strain energy release rates, G_I, for the SENB specimens was determined as follows,

$$G_I = \frac{K_I}{\mathrm{E}}^2 \quad (3.11)$$

Where,

G_I	=	Mode I strain energy release rate	(J/m^2)
E	=	Youngs Modulus	(GPa)

3.6.7 Creep tests

The creep test was performed using the DMA instrument (TA Instruments DMA Q800). An initial "scouting" experiment was performed to establish the optimum temperature range (the materials ambient temperature modulus and glass transition temperature) to conduct the creep experiment. The specimen was 4 mm thickness x 12.5 mm width x 50 mm length. The samples were tested using a dual cantilever clamp at a constant load of 1 MPa from 25-200 °C at 5 °C/min for 22 hours. The data was obtained from the TA Universal software, TA to obtain the creep compliance. For the Time-temperature superposition (TTS) analysis, the data was obtained using the Rheology Advantage Analysis software, TA to predict long-term creep deformation of the control and BSM composite samples from accelerated testing data at different temperature levels and smooth master curves were obtained.

3.7 Hybrid polymers (with nanoclays)

Biocomposites have the challenge of not having the desired mechanical strength compared to the traditional counterparts. A new class of composite material incorporating nanofillers or nanoclays has been investigated to improve mechanical, thermal and barrier properties of bio-based composite material [139, 140]. Many researchers have found that montmorillonite was the most commonly used layered silicate because of its high cation-exchange capacity, excellent swelling ability, high aspect ratio, ease of modification, commonly available and inexpensive [141-143]. Laoutid *et al*. indicated that the minimal amount of nanoclays (1-5% wt) added can improve the reinforcement of the polymer matrix by increasing flexural strength by up to 31 % and lowering the coefficient of linear thermal expansion [144]. Praveen *et al*. investigated the effect of nanoclay loading on the tensile and dynamic mechanical

properties of short banana fibre-filled styrene butadiene rubber composites. They found that nanoclay addition to the composites led to improved elongation at break and frequency damping properties [145].

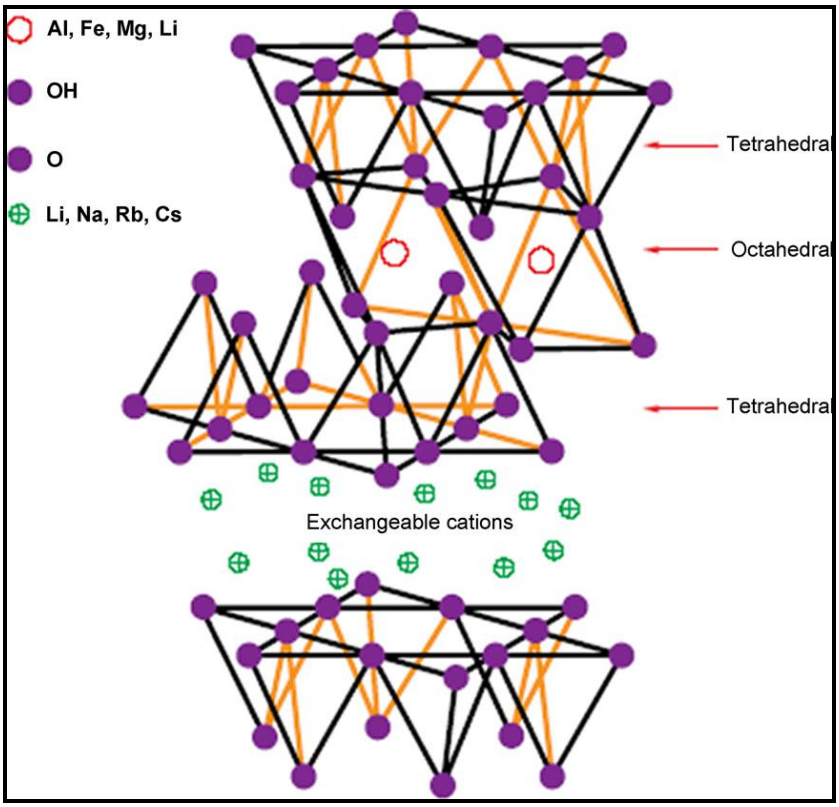

Figure 3.13: Structure of layered Montmorillonite silicate [140]

In this study it was decided to use Cloisite® 30B, a layered alkyl quaternary ammonium salt bentonite silicate shown in Figure 3.13. It was used as an additive to the bio-resin to improve the mechanical, thermal and mechanical properties.

1, 3 and 5% of Cloisite® 30B was added to the control resin and the BSM resin. The resins with the nanoclays were homogenised on an ultrasonic bath for one hour to ensure complete mixing. The accelerator and catalyst were then added and the resin was cured overnight at room temperature and post-cured for 3 hours at 80 °C.

3.8 Biodegradability tests

In this section different tests namely soil burial, microbial growth and respirometric tests were conducted to verify the biodegradability of the BSM bio-composite. A comparison was made to the control specimens.

3.8.1 Soil burial tests

Two biodegradability tests, namely soil burial test and microbial growth test were conducted. Both the control and BSM bio-composite samples with dimensions of 2 cm x 2 cm were weighed and buried in a large container of soil, to which soil nutrients were added. These tests were conducted at ambient temperature (25-30 °C). The biodegradation was monitored for 120 days. The specimens were weighed to record the wet mass and then washed and dried at 40 °C for 24 hours, thereafter they were re-weighed to record the dry mass.

3.8.2 Microbial growth tests

For the microbial growth test, *Aspergillus niger* (a fungi that is most commonly found in decaying vegetation or soil and plants) was grown on potato dextrose agar for five days. The spores were collected and suspended in sterile water. The sterile control and BSM bio-composites were inoculated with the spores and incubated at 30 °C for seven days. Change in fungal growth was observed and analyzed. Growth measurement of the fungi was determined by two methods namely dilution plating and optical density of culture suspension.

3.8.2.1 Growth measurement: Dilution Plating

1 g sample from the zone of maximum growth of the fungi was cut, weighed and soaked for 30 minutes in 0.1% peptone water at room temperature. The soaked samples were then homogenized / vortexed for 1 minute in a homogenizer / vortex-mixer. Dilutions up to 10^{-4} in 0.1% peptone water were prepared, following the serial-dilution method, of homogenized / vortexed samples and spot plated with 0.1 ml-0.01 mL inoculum, from 10^{-3} and 10^{-4} dilutions, in pre-sterilized Petri-dishes containing potato-dextrose agar medium. The plates were then incubated at 25 ^{o}C for 4-5 days in an incubator. The plates were checked for growth every day. The zone-diameter was recorded using an appropriate measuring scale.

3.8.2.2 Growth measurement: Suspension Culture

1 g sample from the area of maximum growth was cut, weighed and soaked for 30 minutes in 0.1% peptone water at room temperature. The soaked samples were then homogenized / vortexed for 1 minute in a homogenizer / vortex-mixer.

The homogenized /vortexed samples were added to pre-sterilized 250 mL Erlenmeyer flasks containing 50 mL potato-dextrose broth. The flasks were then incubated at 25 ^{o}C, at 150 rpm for 4-5 days* in an orbital-shaker incubator. The flasks were checked for growth every day. The optical density, which is a measure of light scattering or turbidity, for growth in absorbance units was recorded using a spectrophotometer (Merck, Spectroquant Pharo 300) at 600 nm after 2.5 times dilution of culture.

*60 hrs used in this experiment.

3.8.3 Respirometric tests

This section focuses on a respirometric method that provided a direct measurement of the oxygen consumed by micro-organisms in biodegradation processes from an air or oxygen-enriched environment in a closed vessel.

Biodegradation Test: The biometer flask technique developed by Chiellini research group, Biolab, University of Pisa [146] was used in this study to test the biodegradability of the composite and polymer samples as shown in Figure 3.14 labelled by (A) Lid with airtight seal, (B) Beaker containing KOH solution, (C) Top layer of coarse perlite particles, (D) Layer of composting soil, mixed with sample material and fine perlite, (E) Bottom layer of coarse perlite particles.

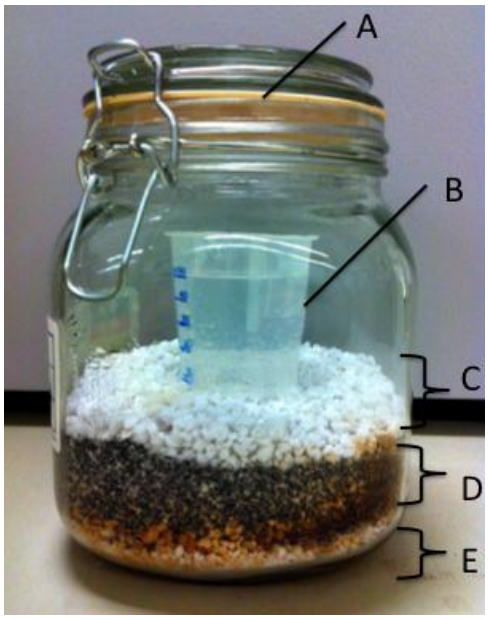

Figure 3.14: A biodegradation flask for respirometric testing

Compost inoculum that was three months old was sieved to a size of < 0.8 cm. Its physical and chemical characteristics were determined according to the ASTM D6400 standard [147] and the results are shown in Table 3.6.

Table 3.6: Physical and chemical properties of compost used in biodegradation test

Analysis of inoculum	
Respiration Rate	57.2 mg CO_2 per gram volatile solids in the first ten days
Total dry solids (%)	55
pH value	7.2
Moisture (%)	50 (wet basis)
Volatile Solids (%)	23 (dry weight basis)
Total Nitrogen (%)	0.9 (dry weight)

The compost was mixed with finely ground perlite particles in a 1:1 dry weight ratio to maintain proper humidity and aerobic conditions. The BSM composite test materials (Table 3.7) were pelletized to an average size of ≥ 100 μm and then added to the compost mixture in a ratio of 1:6 (w/w sample to dry solids of compost). Cellulose powder with a particle size of less than 20 μm (cellulose microcrystalline,

Sigma Aldrich, South Africa) was used as the positive control reference, since it was considered as a fully biodegradable material [148]

Table 3.7: Description of test materials used for biodegradation studies

S.N	Sample	Description	Amount (mg)	% Carbon	Carbon (mg)	Th CO_2 (mg)
1	BSMF_A	banana sap maleate + Fibre	5055	61.32	3099.73	11365.66
2	BSMF_B	banana sap maleate + Fibre	5033	61.32	3086.24	11316.20
3	BSMF_C	banana sap maleate + Fibre	5003	61.32	3067.84	11248.75
4	BSM_A	banana sap maleate	5005	65.49	3277.77	12018.51
5	BSM_B	banana sap maleate	5020	65.49	3287.60	12054.53
6	BSM_C	banana sap maleate	5024	65.49	3290.22	12064.13
7	CR_A	Control Resin	5001	66.13	3307.16	12126.26
8	CR_B	Control Resin	5017	66.13	3317.74	12165.05
9	CR_C	Control Resin	5003	66.13	3308.48	12131.11
10	CRF_A	Control Resin+Fibre	5012	60.17	3015.72	11057.64
11	CRF_B	Control Resin+Fibre	5011	60.17	3015.12	11055.44
12	CRF_C	Control Resin+Fibre	5010	60.17	3014.52	11053.23
13	Cellulose –A	Microcrystalline cellulose	5001	42.3	2115.42	7756.55
14	Cellulose –B	Microcrystalline cellulose	5005	42.3	2117.12	7762.76
15	Cellulose –C	Microcrystalline cellulose	5009	42.3	2118.81	7768.96

The mixture was then placed in a 1000 mL glass airtight flask. The compost and pelletized particle mixture was placed between two layers of wetted perlite, each being 15 g in mass. Water was added to the perlite in order to create a moist environment. Finally, a beaker containing 40 ml of potassium hydroxide solution (0.5 N KOH) was placed on the upper layer to trap emitted carbon dioxide. The BSM composite and control samples were tested in triplicate and the flasks were kept in an IsoTemp Oven which maintained the samples at the optimum composting temperature of 58 ± 2 °C. The conditions within the oven and flasks were aerobic. The flasks were periodically removed from the oven and the KOH solution was titrated with 0.1N HCl. After each titration, the beaker was washed and refilled with fresh KOH solution. The moisture in the test flask was recorded with a moisture analyzer. The moisture content of each flask was measured with a moisture analyzer

and was maintained between 50-55% by measuring the weight loss due to evaporation.

The biodegradation of the material was tracked by trapping all of the emitted CO_2 in the KOH solution. The carbon dioxide emitted by organic metabolization of the material was representative of the total degradation. Gaseous CO_2 emitted reacted with the KOH in the beaker. Eqn. 3.12 below describes this:

$$2KOH + CO_2 \rightarrow K_2CO_3 + H_2O \tag{3.12}$$

The beaker containing KOH was removed from the biodegradation flask and barium chloride (1N $BaCl_2$) was added to the KOH-K_2CO_3 solution. This reaction is shown below (Eqn. 3.13):

$$K_2CO_3 + BaCl_2 \rightarrow + BaCO_3 + 2KCl \tag{3.13}$$

The barium carbonate formed in Eqn. 3.20 appeared as a cloudy white precipitate. The remaining amount of KOH in the solution was determined by titrating with 0.5N HCl, using phenolphthalein as an endpoint indicator (Eqn. 3.14).

$$KOH + HCl \rightarrow H_2O + KCl \tag{3.14}$$

The theoretical amount of carbon dioxide produced by total oxidation of incubated materials in each flask ($ThCO_2$ in g per vessel) was calculated using the following expression (Eqn. 3.15):

$$ThCO_2 = M_{total} \times C_{total} \times {}^{44}/_{12} \tag{3.15}$$

where, M_{total} is the total dry amount of constituent or plastic materials (g) added to the compost, C_{total} is the relative amount of total organic carbon (g) in the total dry solids, 44 is the molar mass of carbon dioxide and 12 is the atomic mass of carbon.

The rate and extent of biodegradation of the materials listed in Table 3.7 was evaluated in compost environments under controlled conditions according to the ASTM D5338 method [149]. A biodegradation curve was obtained by plotting

released CO_2 (%) versus composting time. Biodegradation was calculated as the percentage of carbon in the polymer mineralized as CO_2 according to Eqn. 3.16:

$$\text{Biodegradation}\ (\%) = (CO_2)s\text{-}(CO_2)c/ThCO_2 \times 100 \quad (3.16)$$

where $(CO_2)s$ and $(CO_2)c$ are the amount of CO_2 produced in the sample and in the control (blank) respectively.

The respirometric test was conducted in a biometer flask in a controlled environment where the temperature was between 58-60 °C, pH 7-8 and moisture 50-55%. These conditions were suitable for mesophilic and thermophilic microorganisms (bacteria and fungi) in organic manure compost environment.

After 55 days of incubation a known amount of sample was recovered from respective test flasks to characterize the changes in structural and thermal properties of BSM, BSMF, CR and CRF test materials. The recovered samples were easily distinguishable; further washed with de-ionized water and dried in oven at 40 °C for 4 hrs. These were analyzed using TGA, DSC, FTIR and SEM techniques.

3.9 Summary

This chapter explained the method used in the preparation of the bio-resin and biocomposite in comparison to the control specimens. The materials used were defined. An explanation of the various techniques and its applicability in this study was given. The next chapter discusses the chemical composition of the banana sap and its role in the formulation of the bio-resin. The synthesis and characterization of the bio-resin is presented.

CHAPTER 4– RESULTS AND DISCUSSION: THE SYNTHESIS AND CHARACTERIZATION OF THE BIO-RESIN FROM BANANA SAP

Introduction

This chapter focuses on the analysis of the banana sap (BS) and the synthesis and characterization of the bio-resin (BSM). Since physical and chemical analysis results of BS were not available, it was deemed critical to develop the knowledge of results. The first part of this chapter deals with the findings and analysis of BS and its purpose in the formulation of the bio-resin. Chemical compounds present in the sap were identified and predictions were made of the reaction with the bio-resin. The second part of this study involves the synthesis of a bio-resin[7] using BS. Throughout this study comparison is made to a control sample.

4.1 Characterization of banana sap

The BS was characterized in order to understand its chemical and physical background and to foresee its role in the bio-resin formulation.

4.1.1 Physical testing of BS

Since the water content of BS was over 90% [91], its chemical and physical properties were compared to that of water. Table 4.1 shows a comparison of the physical properties of BS to deionized water.

Table 4.1: Physical properties of BS compared to water

Physical parameter	Banana sap	Water
Total dissolved solid (TDS) (%)	0.88	-
pH	5.45	7.00
Conductivity (mS/cm)	6.67	5.89
Density (g/cm^3)	1.0030	0.9970

[7] Extracts from Chapter 4 have been published as "Formulation of a novel bio-resin from banana sap", Industrial Crops and Products, 43, (2013), 496-505.

Interferences by inorganic and organic substances shown by TDS act as a benchmark indicator for the species of *Musa Cavendish* analyzed. BS is acidic in nature (pH 5.45) which could be attributed to the tannic acid in the sap [150]. Literature reviewed showed that traditional medicine capitalized on the astringent property of BS related to the pH for the treatment of a variety of ailments [151]. The presence of ions in the BS was confirmed by a conductivity reading of 6.67 mS/cm which was further verified by ICP-AES shown in Table 4.2. The larger value of the conductivity indicated that more ions were present in the BS than water.

4.1.2 ICP-AES analysis of BS

The elemental values shown in Table 4.2 are indicative of this species of banana plant and the results may vary from species to species because of climate and locality variation. As expected it was found that potassium and magnesium were the most abundant elements present in the BS. In another study conducted in Brazil with indigenous banana plants, Feriotti and Iguti found that the BS contained 874 $mg.L^{-1}$ of potassium, 88 $mg.L^{-1}$ sodium and 116 $mg.L^{-1}$ of magnesium [152].

Table 4.2 : Elemental analysis of banana sap by ICP-AES

Element	Banana sap (mg/L)
Potassium	200
Magnesium	100
Iron	7.3
Silicon	7.0
Copper	6.5
Sodium	5.1
Sulphur	3.2
Phosphorus	1.8
Calcium	1.5

4.1.3 Qualitative and quantitative analysis of carbohydrates

Carbohydrates are synonymous with the term saccharide. The carbohydrates (saccharide) are categorized into monosaccharides, disaccharides, oligosaccharides

and polysaccharides. This study focuses on monosaccharides and disaccharides which are commonly referred to as sugars [153].

A positive Molisch test (Figure 4.1), indicative of a purple colour, obtained for BS indicated the presence of carbohydrates.

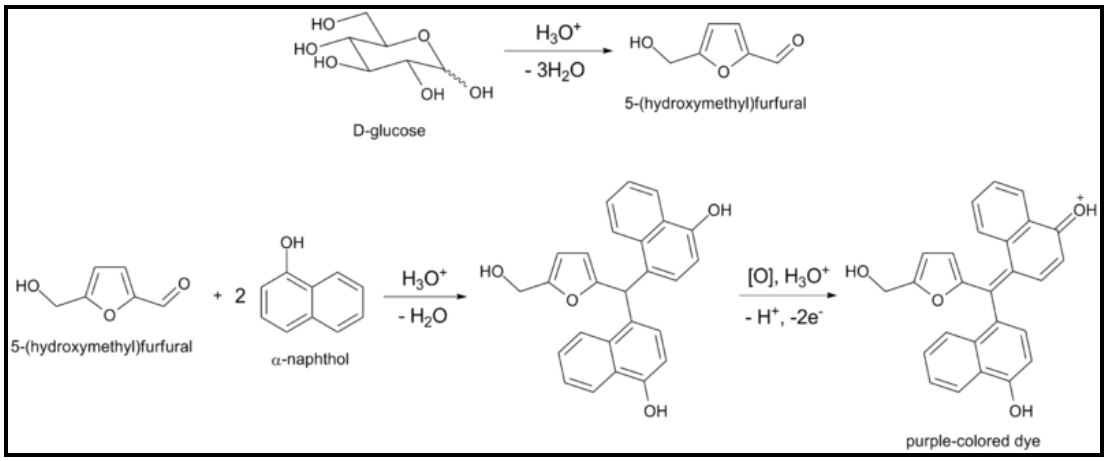

Figure 4.1: Reaction scheme showing a positive Molisch test for carbohydrates [154]

As a consequence of the positive Molisch test, the concentration of carbohydrates in the BS was further quantified by HPLC analysis. Two sets of HPLC analysis were performed. Firstly the initial BS that was added to the processing of the bio-resin was analyzed and secondly the solvent (normally water) expelled during the polycondenzation reaction of the bio-resin synthesis was analyzed. Figure 4.2 shows the retention times and areas of the calibration standard solutions of 1% sucrose, glucose and fructose. BS was sequentially quantified by matching the area and retention time with the respective standards. Table 4.3 lists the concentration of sucrose (0.021%), fructose, (0.036%) and glucose (0.04%) quantified by HPLC in BS by the calibration standard method. It was important to further analyze these sugars that were reported by other researchers as possible cross-linkers [117, 155, 156].

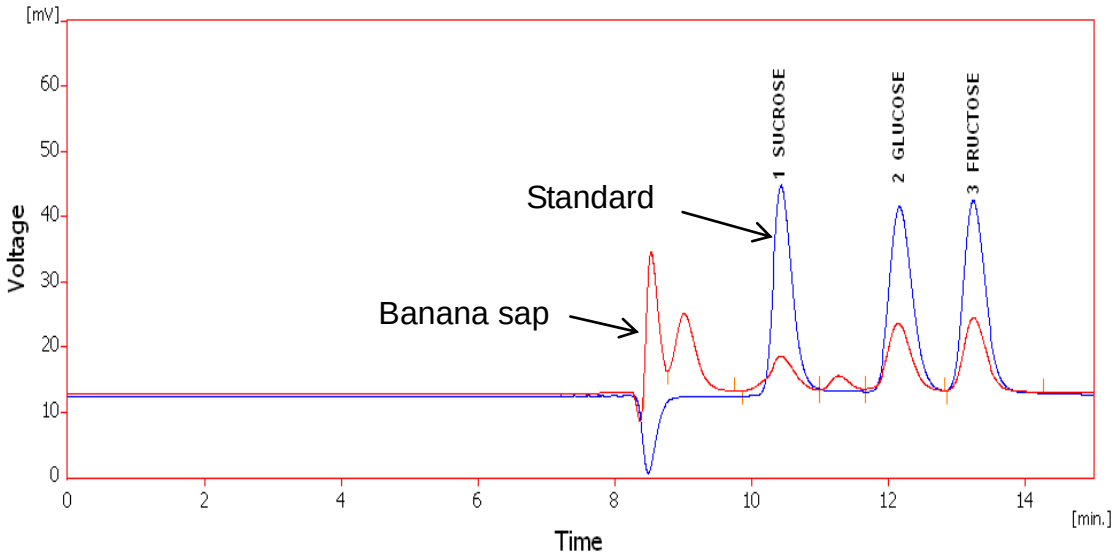

Figure 4.2: HPLC analysis and quantification of carbohydrates in BS

Table 4.3: Concentration of sugars present in initial banana sap and the condensate collected during the polycondenzation reaction

Sugars	Sugars in initial sap (%)	Sugars in condensate (%)
Sucrose	0.021	0.016
Glucose	0.036	ND*
Fructose	0.040	ND*

*ND-Not detected

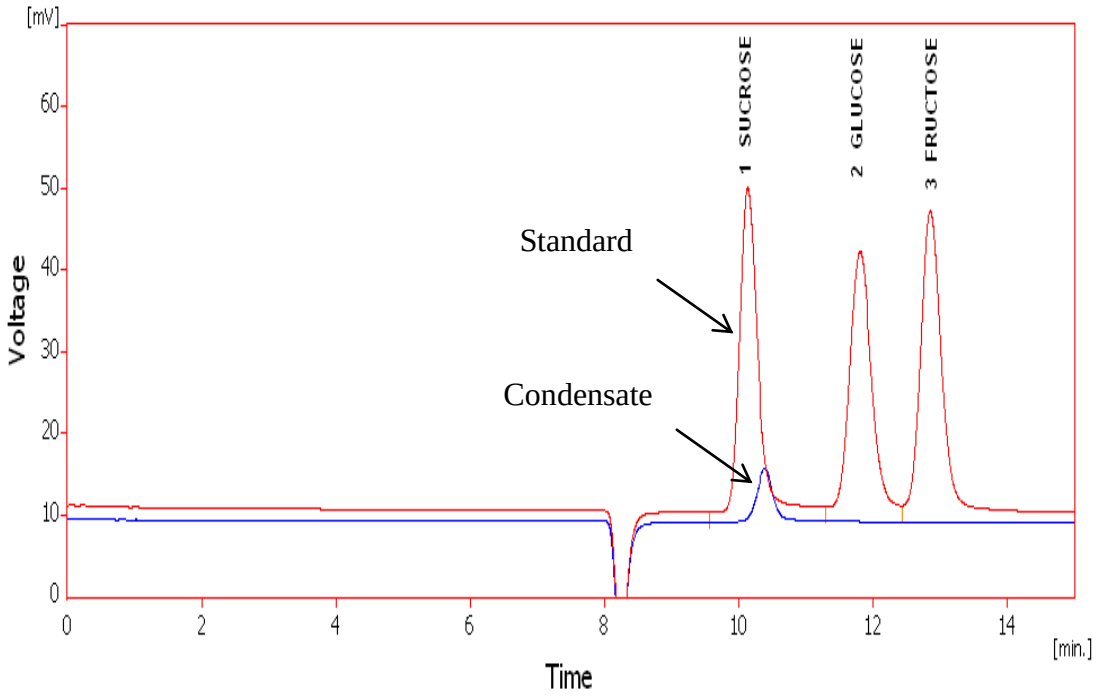

Figure 4.3: HPLC analysis and quantification of carbohydrates in the condensate

The condensate formed as a by-product of the reaction between MA, PG and BS was analyzed by HPLC to verify if the sugars in the sap contributed to the resin formation or if they were expelled with the water. Figure 4.3 shows that only sucrose (0.016%, Table 4.3) was present in the condensate which was 23 % less than the original amount of sucrose. Sucrose, a disaccharide, was hydrolyzed into glucose and fructose, hence the lower concentration in the condensate suggesting that glucose and fructose, being monomers, attached themselves onto the backbone of the maleate. Hirose *et al.* studied the effect of combining glucose and ethylene glycol and then adding it to succinic anhydride to form an ester-carboxylic acid derivative [117]. Furthermore, Narain *et al.* synthesized and characterized the behaviour of the water soluble polymers derived from gluconolactone with hydrophilic and hydrophobic monomers [155]. Further to this, a similar reaction procedure of polycondenzation was applied by Jhurry and Deffieux for the synthesis of polyurethanes from diisocyanate and sucrose by a reaction based polymers with sucrose in the main

chain [156]. From the work done by these researchers it is evident that sugars such as glucose and fructose can be effectively used as cross-linkers in biopolymers.

In this study, two possible synthetic pathways are shown in Figures 4.4 and 4.5 for the possible reactions of glucose and fructose with the maleic acid-propylene glycol polymer backbone. Fructose and glucose have at least two reactive ends that connected to the polymer chains. As seen in Figures 4.4 and 4.5 the polymer chains were lengthened resulting in a higher molecular mass compared to the control resin. Tillet *et al*. showed that a lower molecular-weight range often required a cross-linking step to obtain satisfactory mechanical properties [157]. The molecular weights of the BSM and control resins were 2179 and 2114 $g.mol^{-1}$ respectively. It is also important to note that BS is a complex matrix with many chemical compounds as shown by HPLC and GC-MS. It is also possible that the other components could have contributed to the increase in the strength of the material. In another study, Lamaming *et al*. showed that by adding glucose and sucrose to binderless particle boards increased the modulus of rapture and internal bond strength [158].

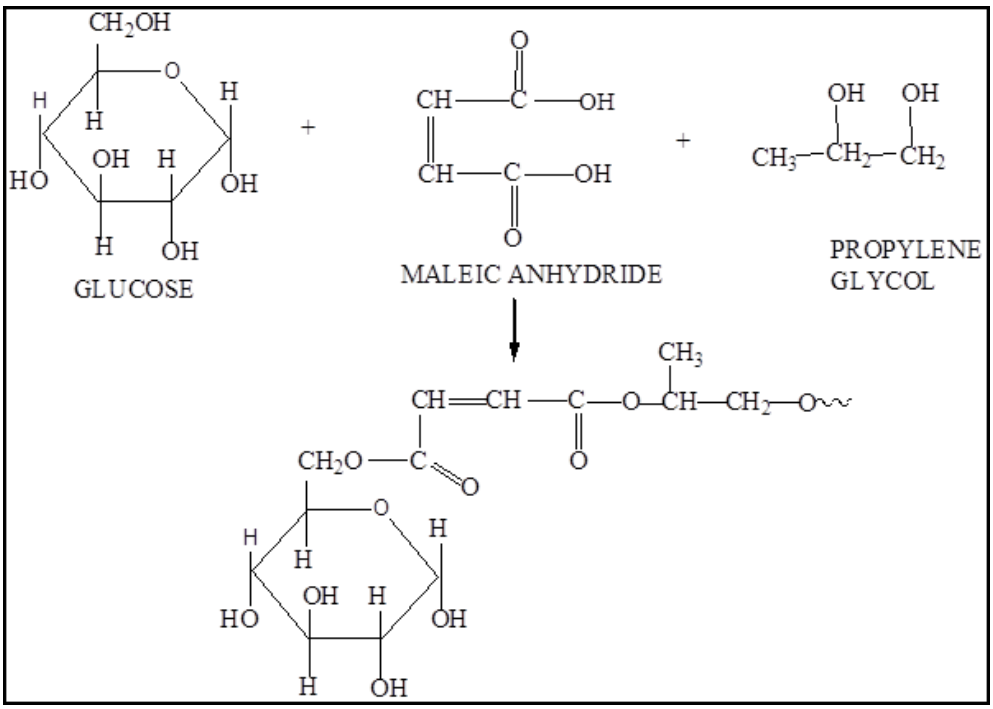

Figure 4.4: A possible reaction scheme of the product formed when glucose is attached to maleic acid- propylene glycol polymer backbone

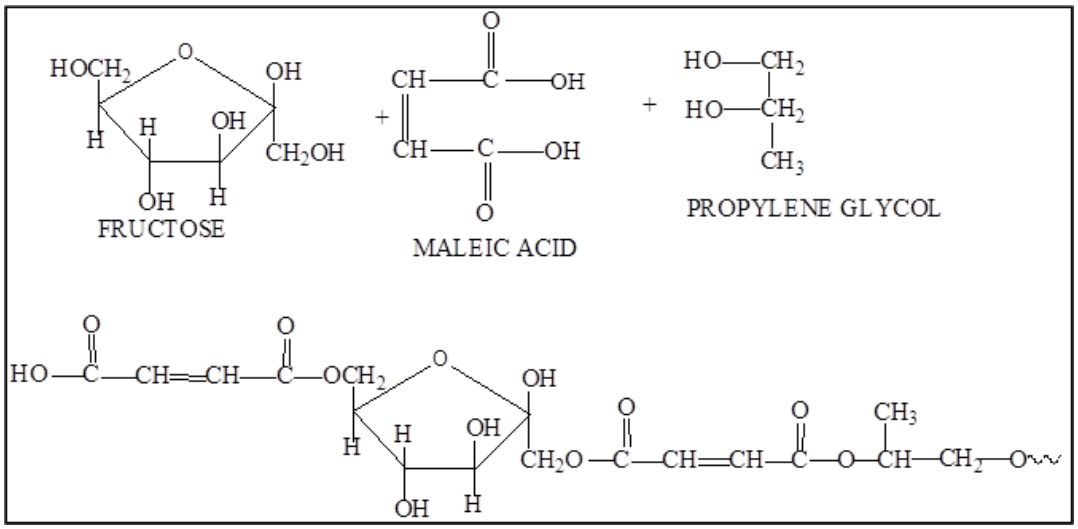

Figure 4.5: A possible reaction scheme of the product formed when fructose is attached to maleic acid-propylene glycol polymer backbone

4.1.4 Analysis of phenolic compounds

The BS collected from the pseudostem was initially clear; however upon exposure to air, it immediately turned brown due to oxidation. This led to the investigation of the presence of phenolic compounds in BS. Chemically, the phenolic compounds were oxidized into quinones which rapidly combined into a dark polymer residue [159]. The immediate darkening of the BS prompted a quantitative analysis of phenolic compounds in the sap by UV/VIS. Confirmation of the phenolic compounds was further verified by GC-MS (Table 4.4).

The quantitation of phenolic compounds was obtained from a linear calibration of the spectral analysis by UV-VIS (Figure 4.6) against a gallic acid standard. The phenol content of the sap was found to be 122 mg/L.

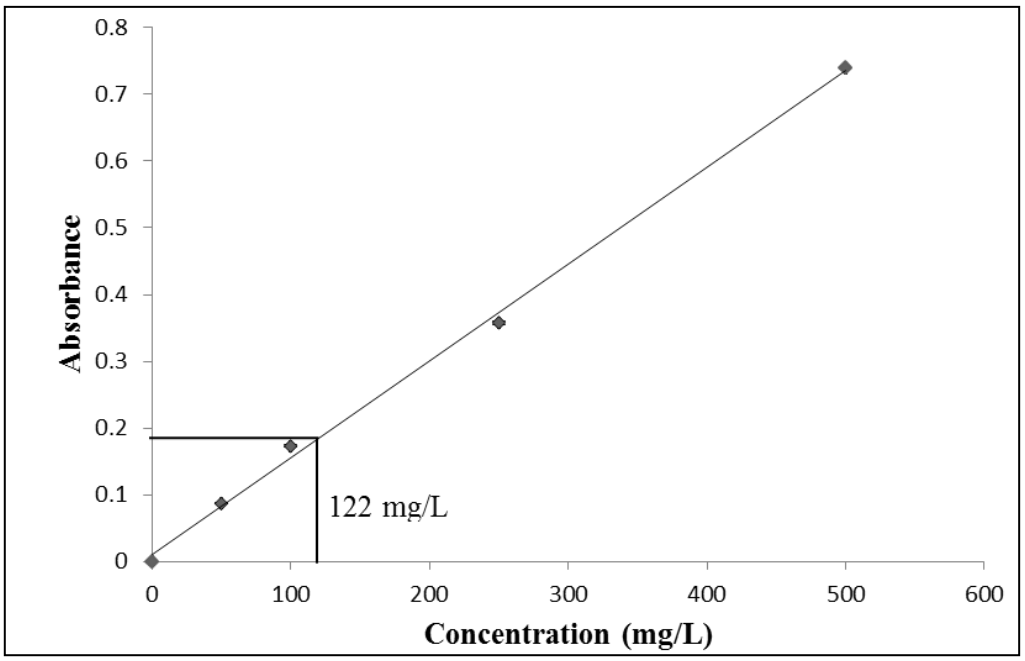

Figure 4.6: Quantification of total phenolic compounds in BS by UV/VIS spectroscopy

4.1.5 GC-MS analysis of banana sap

The purpose of analyzing the BS extracts by GC-MS was to identify the major components of possible reactions that could have taken place during the condensation reaction. Extraction of compounds from BS was conducted using dichloromethane (DCM) (polar), ethyl acetate (medium polarity) and hexane (non-polar) as shown in Table 4.4.

The DCM and ethyl acetate extracts showed the commonality of ester compounds from the BS. The phenolic compounds were extracted into the ethyl acetate fraction confirming the polar nature of the phenolic compounds. The GC of the DCM extraction (Figure 4.7) indicated an abundance of hexadecanoic acid (72.72%), 1, 2-benzenedicarboxylic acid and bis (2-methylpropyl) ester (6.39%). The ethyl acetate extraction (Table 4.4), produced 2, 4 bis 1,1 dimethyl ethyl phenol (75%), 1,2-Benzenedicarboxylic acid and bis (2-methylpropyl) ester (5%) (synonym: isobutyl

phthalate). The hexane extraction (Table 4.4) indicated the presence of the 1,3dimethyl benzene (34%) and ethyl benzene (15%).

The phenolic compounds were confirmed by the UV/VIS and GC-MS methods. It is possible that these esters and phenolic compounds self-polymerize before attaching themselves to the maleate backbone.

Table 4.4: Identification of most abundant compounds extracted from BS by GC-MS

DCM extract	Abundance %	Ethyl acetate extract	Abundance %	Hexane extract	Abundance %
Hexadecanoic acid	72.72	2,4-bis-1,1-dimethylethyl phenol	51.4	1,3 dimethyl benzene	34
1,2-Benzene dicarboxylic acid, butyl 2 methylpropyl ester	6.39	1,2,3 trimethyl benzene	12.2	Ethyl benzene	
6, 10, 14 trimethyl- 2-Pentadecanone	5.14	1-ethyl-3-methyl Benzene	7.3	3 methyl heptane	15
Dihydro-5-pentyl 2(3H)-furanone	4.8	1,2-Benzene dicarboxylic acid, bis (2methylpropyl) ester	2.6	2 methyl heptane	12.6
Dibutyl phthalate	3.18				9

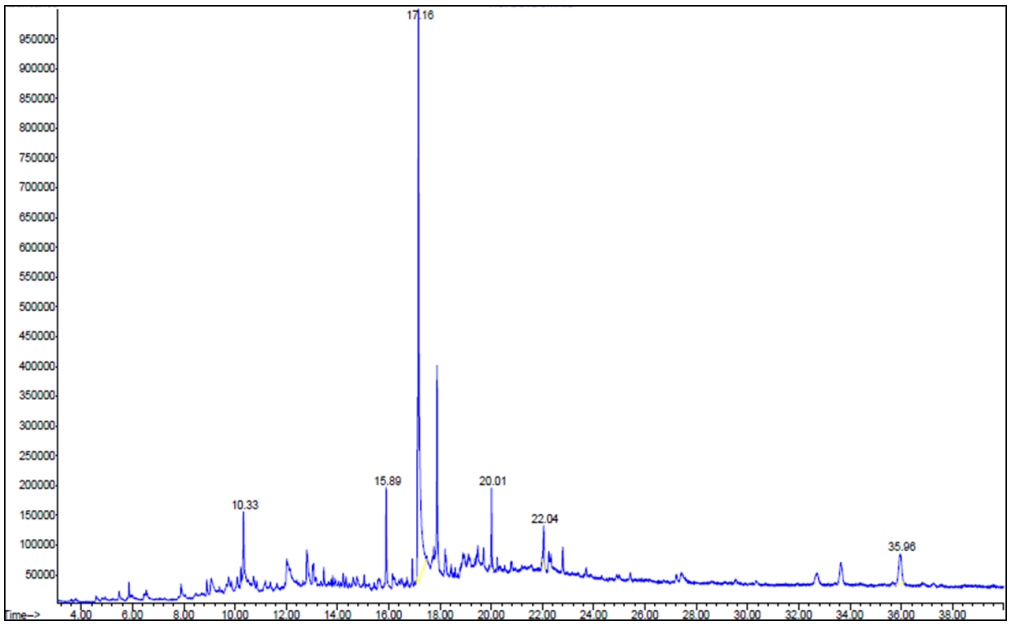

Figure 4.7: Gas chromatogram of the DCM extract of BS

As mentioned earlier, BS is a complex matrix with various components. In the current work, it is possible that hexadecanoic acid (which is commonly known as palmitic acid) present in the BS, together with MA, reacted with the PG to form the hybridized BSM resin. Research elsewhere has shown that derivatives of hexadecanoic acid can be isolated into monomers and are used as starting material for a wide range of bio-polyesters [160]. Stales *et al.* showed that 1,2-Benzenedicarboxylic acid-1,2-bis(2-methylpropyl) ester otherwise known as isobutyl phthalate behave as a plasticizer [161]. Plasticizers are chemical substances used to soften PVC to produce flexible and durable goods such as floors, cables and wall coverings.

4.2 Synthesis of control and BSM resins

Banana sap was the major component in the manufacture of the resin; hence the chemical analysis performed in the previous sections on the BS gave a better understanding of the mechanisms that occurred.

During the condensation polymerization process, propylene glycol and maleic anhydride reacted with the BS to form a hybrid unsaturated polyester resin and water

as a by-product. This water was analyzed by HPLC (Figure 4.3) as discussed in section 4.1.3. The acid number, which is an indication of the measure of carboxylic acid, of the resin was periodically measured during the processing of the resins as shown in Table 4.5A and B. Generally, an acid value less than 50 is desirable [128] and it was found that BSM and control resins had acid values of 43 and 44 respectively.

A comparison of the acid values and viscosities of the control and BSM resins showed that with an increase in reaction time there was a corresponding decrease in the acid numbers. In Table 4.5A and Figure 4.8A the acid number of the control sample decreased from 125 to 44 and the viscosity increased from 0.9 to 4 poise. In Table 4.5A an increase in acid value of the control resin between the 13th and 14th hour of the experiment from 83.9 to 87.2 was observed. This was due to increasing temperatures during the resin processing when PG was lost. To overcome this spike in temperature and acid value, 50mL of PG was added to the cook to stabilise the reaction.

Table 4.5A: Acid value and viscosity values of control resin

Time (hours)	Acid value	Viscosity (Poise)
5	124.5	0.9
6	105.4	1.1
7	100.8	1.3
9	99.2	1.9
10	96.7	2.1
11	89.6	2.8
12	80.7	3
13	83.9	3.1
14	87.2	4
15	72.4	4.9
16	58.7	4
17	44.4	4.1

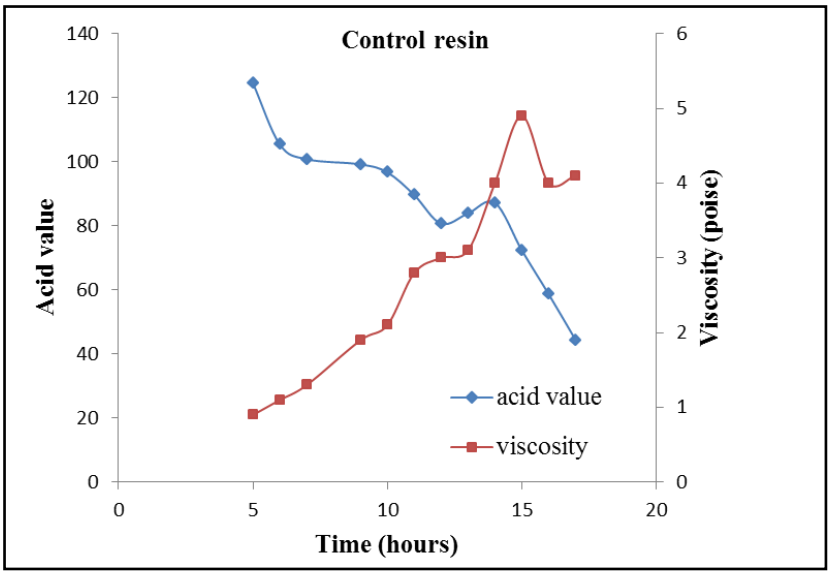

Figure 4.8A: Correlation of acid value and viscosity as a function of time of the control resin

In Table 4.5B and Figure 4.8B the acid value for BSM bio-resin decreased from 147 to 43 and the viscosity increased from 0.1 to 6 poise. With a decrease in acid value and an increase in viscosity the polymer chain length grew with time shown by the increase in molecular weight as shown in Figure 4.10. Since the initial acid value of 147 of the BSM bio-resin was higher than the control resin due to the water in the BS, the processing of the BSM resin took a longer time.

Table 4.5B: Acid value and viscosity values of BSM bio-resin

Time (hours)	Acid value	Viscosity (Poise)
15	147.1	1
16	96.1	2.5
17	86.7	2.8
18	76.2	4
19	69.7	4.9
20	63.1	6.9
21	61.1	11
22	44.8	5
23	43	6

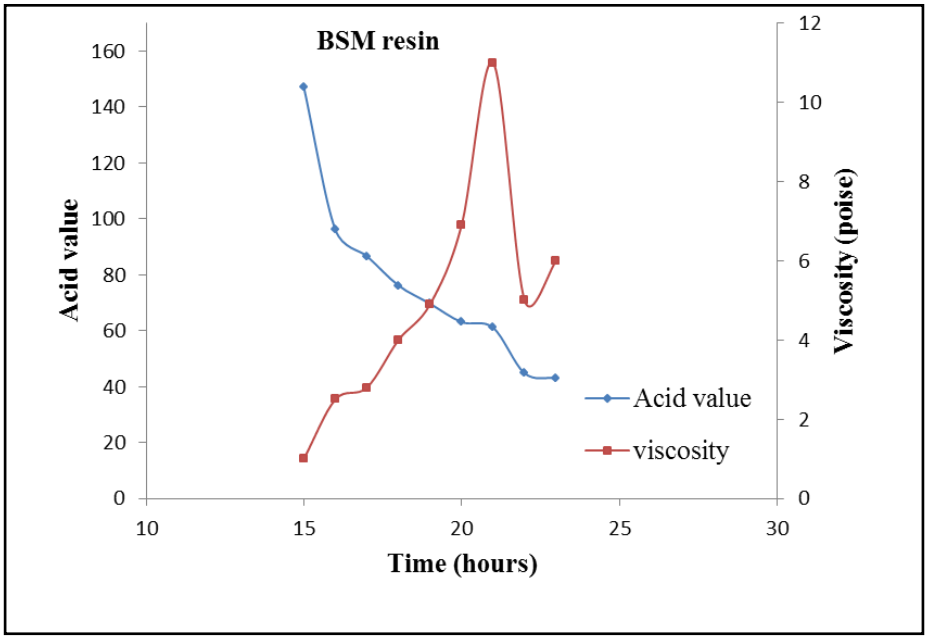

Figure 4.8B: Correlation of acid value and viscosity as a function of time of the BSM bio-resin

Unsaturated polyester resins are important in the industrial field and the molecular weight at most is between 1000 and 2500 g/mol and it is not an overstatement to say that molecular weights above 3000 can be achieved [162]. Since it was desirable to obtain a polymer chain of the above molecular weights it was found that further processing of the resin to obtain lower acid value, higher viscosity and molecular mass resulted in the resin gelling and being completely charred as shown in Figure 4.9. The optimum values the BSM bio-resin was: acid value < 50, viscosity between 4-6 poise and molecular weight of 2000-2500 g/mol.

Figure 4.9: Consequence of cooking the resin to obtain larger molecular weights

It was also observed that as the acid value decreased, the viscosity and the molecular weight increased. As the acid-glycol esterification reaction proceeded, an increase in viscosity and molecular weight at the end of the processing was recorded. Visual observation showed the thickening of the bio-resin. Here the large polymer chains started to join together and thus the molecular weight increased. Figure 4.10 showed the increase in molecular weight growth with time. The BSM resin had a molecular weight (MW) of 2179 units and the control resin had a molecular weight of 2114 units. The higher molecular weight of BSM was contributed by the cross-linking of glucose, fructose and possibly other components of the BS attached to the maleate backbone as proposed in Figures 4.4 and 4.5 respectively.

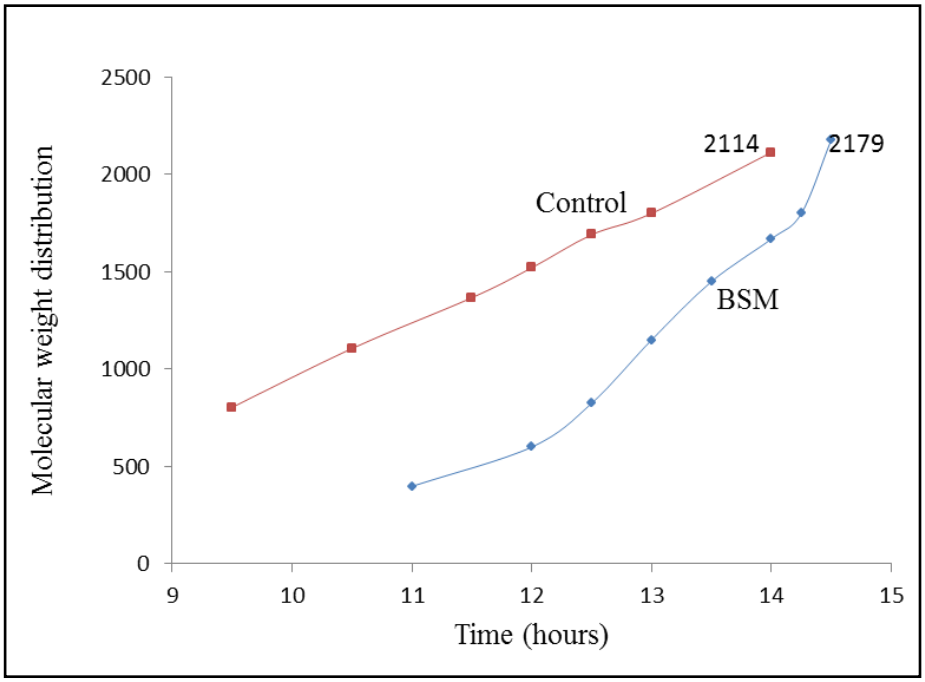

Figure 4.10: Molecular weight distribution of the control and BSM bio-resin

4.3 Characterization of control and BSM resins

Various analytical and mechanical testing performed on the BSM and control resins will be explained in this section.

4.3.1 Physical testing

Table 4.6 illustrates the comparison of the results of the control and BSM resin to an industry standard resin that was also an unsaturated polyester resin. Although the viscosity, density and gel times of the control and BSM were similar to the industry resin, there were inconsistencies with the acid value. The starting materials for the industry resin were different to MA and PG resulting in a lower acid value which was a measure of the amount of carboxylic groups on the polymer chain.

Table 4.6: Specifications of the control and BSM resins as compared to an industry resin*

Test	Industry Resin*	Control resin	BSM resin
Acid value (mg KOH/g resin)	18-26	44	43
Volatile content	39-43	39	40
Viscosity at 25°C (Brookfield sp 3 500 rpm)	200-300	300	200
Stability at 120°C (hours)	4	4	2.5
at ambient (months)	6	-	-
Rel. density at 25°C ($g.cm^{-3}$)	1.10	1.098	1.093
Time to gel (min)	20-25	28	20
Time to peak (min)	40-50	36	31
Peak exotherm (°C)	140-160	203	207

*The name of the industry resin cannot be disclosed due to confidentiality

4.3.2 Gel time, time to peak, cure time, peak exotherm

The gel times of 28 minutes and 20 minutes were obtained for BSM and control resins respectively as shown in Table 4.6. The time-to-peak of 36 minutes and 31 minutes were obtained for the BSM and control resins respectively. However these gel and cure times can be lengthened or shortened by varying the amount of cobalt naphthenate and MEKP to accommodate the size of the laminate to be prepared.

The time-to-peak exotherm is the interval between the initial mixing of reactants (MEKP and cobalt naphthenate) of a thermosetting polymer until the highest exothermic temperature is reached. The resin continued to harden after it gelled until it obtained its full hardness and properties. This exothermic reaction proceeded quickly.

Table 4.7: A comparison of gel time, time to peak, cure time and peak exotherm of control resin by varying the amount of Co added

Variation of Co	Gel time (min)	Time to peak (min)	Cure time (min)	Peak exotherm (°C)
100g resin + 0.5g Co + 1g MEKP	39.00	52.17	91.17	198.7
100g resin + 0.8g Co + 1g MEKP	28.10	38.36	66.46	203.3
100g resin + 1.0g Co + 1g MEKP	16.30	24.19	40.49	206.4

The mass of the accelerator (cobalt) added to the control resin varied from 0.5 g, 0.8 g and 1.0 g and the catalyst (MEKP) was held constant at 1 g as shown in Table 4.7. The gel times decreased from 39 min to 28.1 min to 16.3 min respectively with the increasing amount of cobalt. The cure times decreased from 91.17 min to 66.46 min to 40.49 min, respectively. Controlling cure times was deemed an advantage as the cure times can be adjusted to suit the manufacturing process.

Table 4.8: Gel time, time to peak, cure time and peak exotherm of control resin compared to BSM resin

	Control Resin	**BSM Resin**
	100g resin +0.5g Co +1g MEKP	**100g resin +0.5g Co +1g MEKP**
Gel Time (min)	39.00	15.30
Time to peak (min)	52.17	22.07
Cure time (min)	91.17	37.37
Peak exotherm (°C)	198.7	207

Table 4.8 show the gel and cures times of the BSM and control resin with the accelerator and catalyst kept constant. BSM gelled at 15.30 min compared to the control resin at 39 min. This was possibly due to the BS in the resin behaving as an accelerator for the curing of the unsaturated resin. In addition the presence of glucose and fructose in BS serve as cross-linking agents in the resin formulation, thus lowering gel time. The gel time of the control resin was 39.00 min as compared to 15.30 min for the BSM resin. Similarly, the cure times of the control and BSM resins

were 91.17 min and 37.37 min respectively. The cure time of BSM bio-resin was more than halved with the result that using the BS in the formulation was cost effective and time saving. A typical graph of the relationship of temperature and gel time is shown in Figure 4.11. The duration of the curing can be controlled by carefully adjusting the amount of catalyst and accelerator to accommodate the panel size and the type of application so that the resin does not gel whilst being infused into the fibres.

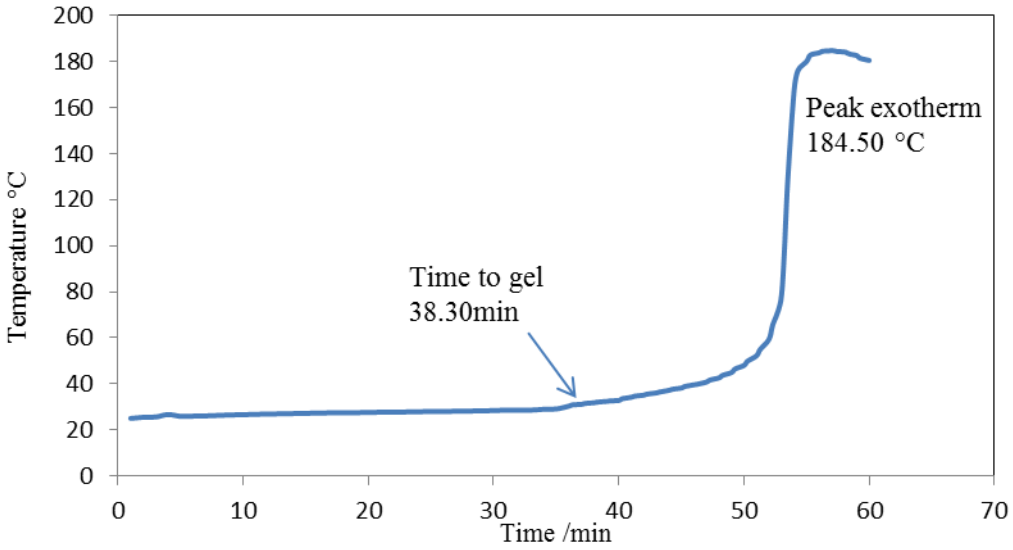

Figure 4.11: Gel time and peak exotherm profile of the resin

4.3.3 Adjustment of stability and gel time

The requirement of the stability test of the BSM resin was that it be stable for up to 4 hours in an oven at 120 °C. However, it was observed that the BSM resin failed this test and gelled within 2.5 hours at 120 °C (see Table 4.6). To improve the stability of the resin, 400 ppm of Ethanox®, an antioxidant was added. Ethanox® is used to enhance thermal stability, improve lubricant performance and reduce sludge formation of resins [163]. The shelf life of the BSM resin improved and the sample gelled only after 4 hours. But with improved stability, the gel times were compromised. When 400 ppm of Ethanox® was added, the gel time of the BSM resin increased to 38 minutes. To address this compromise, the amount of accelerator and catalyst the gel time can be adjusted as required.

4.3.4 FT-IR analysis of BSM and control resin

Fourier Transform Infra-Red analysis was performed on BS, PG, MA and the control and BSM resins. Figure 4.12 shows the FTIR scans of the functional groups of MA, PG and BS that were used as the starting material in the formation of the resin. The carbonyl groups of the MA are at 1855 cm^{-1} and 1776 cm^{-1}. The FTIR analysis of the PG and BS were dominated by hydroxyl moieties at 3310 cm^{-1} and 3320 cm^{-1}, respectively. The peak at 1628 cm^{-1} in the BS was attributed to the presence of ketones and 1030 cm^{-1} to C-O stretching. During the processing of the bio-resin the functional groups of MA, PG and BS react to form chemical bonds that are either enhanced or diminished as shown in Figure 4.13.

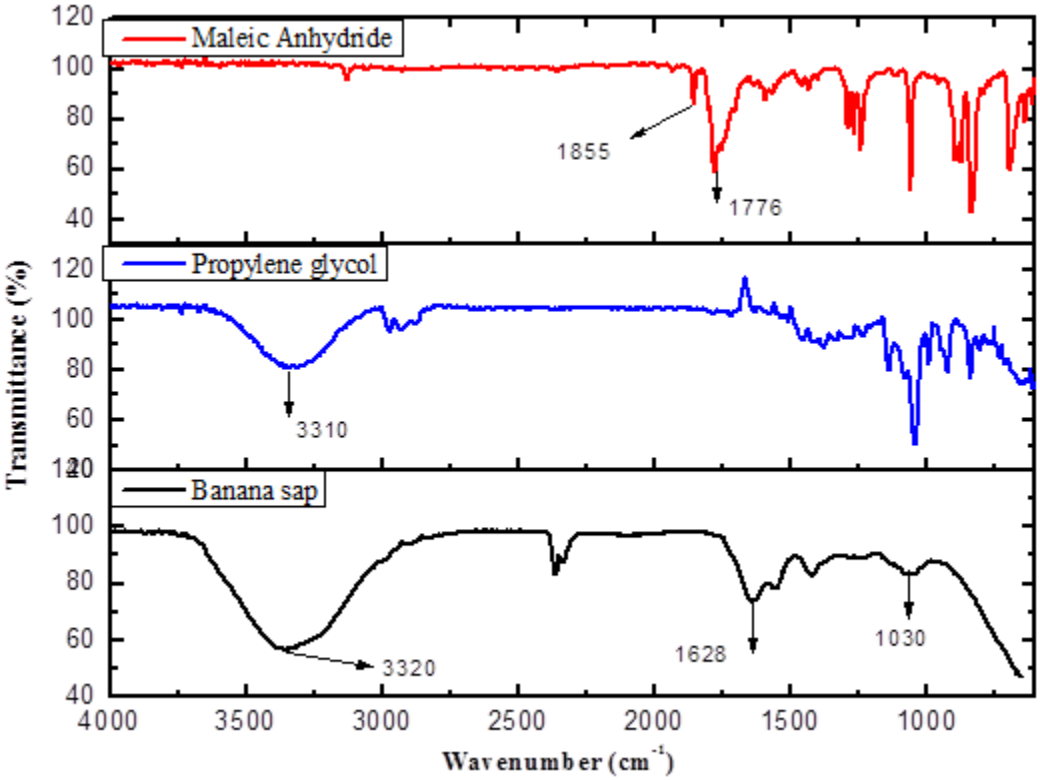

Figure 4.12: FTIR of starting materials of the resin namely banana sap, maleic anhydride and propylene glycol

The polyester chain grows as the acid and the hydroxyl groups combine to form ester and water is removed in the polycondenzation reaction as seen in Figure 4.13 during

the processing at 2 hours, 12, 13 and 15 hours. As the resin was processed and the water from the BS was removed, the O-H band at 3400 cm^{-1} slowly disappeared. The carbonyl stretch at 1709 cm^{-1} and 1716 cm^{-1} gradually became more pronounced as the esters were formed. The peak at 1640 cm^{-1} gradually disappeared as the -C=C- stretching bond broke.

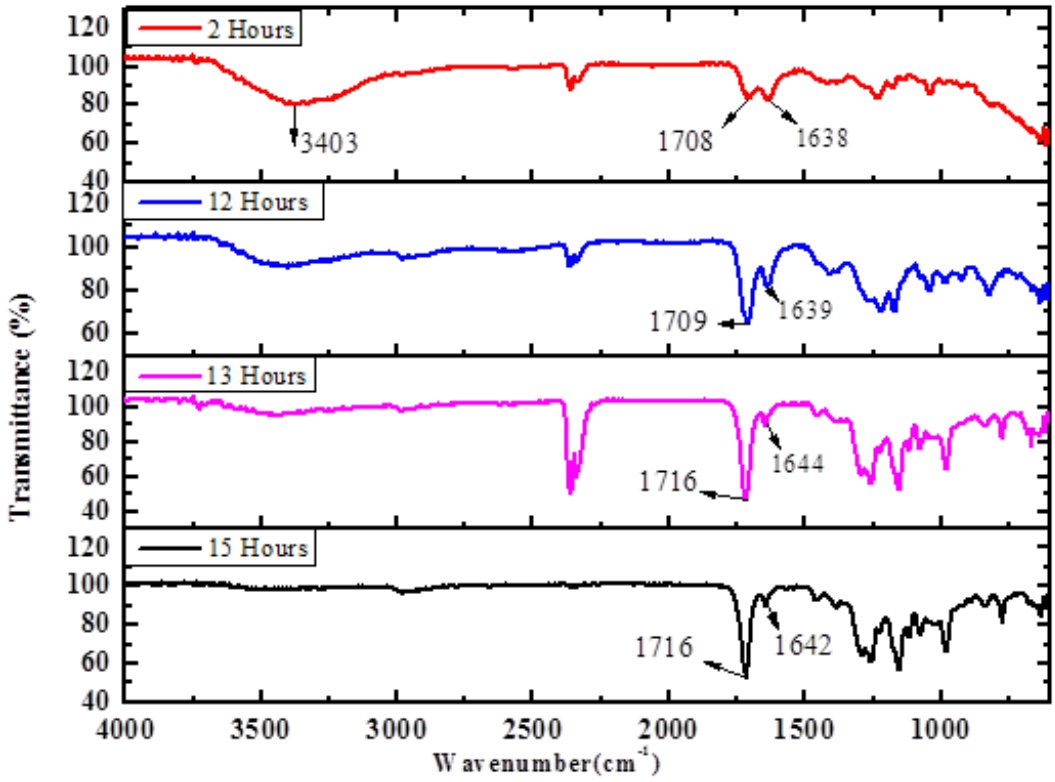

Figure 4.13: FTIR scans of the BSM resin during 2, 12, 13 and 15 hours of processing time

Figures 4.14 show the FTIR overlay scans of the cured control and BSM resins. It was noticed that the broad band associated with OH groups at 3530 cm^{-1} almost disappeared with the BSM bio-resin as the cured BSM bio-resin did not have any moisture in it. A strong absorption band at 2920 cm^{-1} was assigned to –C=C– functionality of the polyester group. A greater crosslinking in BSM showed a more intense double bond peak. The prominent peak at 1727 cm^{-1} representing the carbonyl peak (C=O) was more intense for the BSM bio-resin than the control resin. This functional group is associated with a larger ester group of the BSM. These ester

compounds in the BS were identified by GC-MS as shown in Table 4.4. There was a shift in wavenumbers from 1150 cm^{-1} to 1100 cm^{-1} from the control to BSM resins. These peaks are indicative of the –C-O-C- ester linkages and the shift was attributed to the addition of BS in the resin.

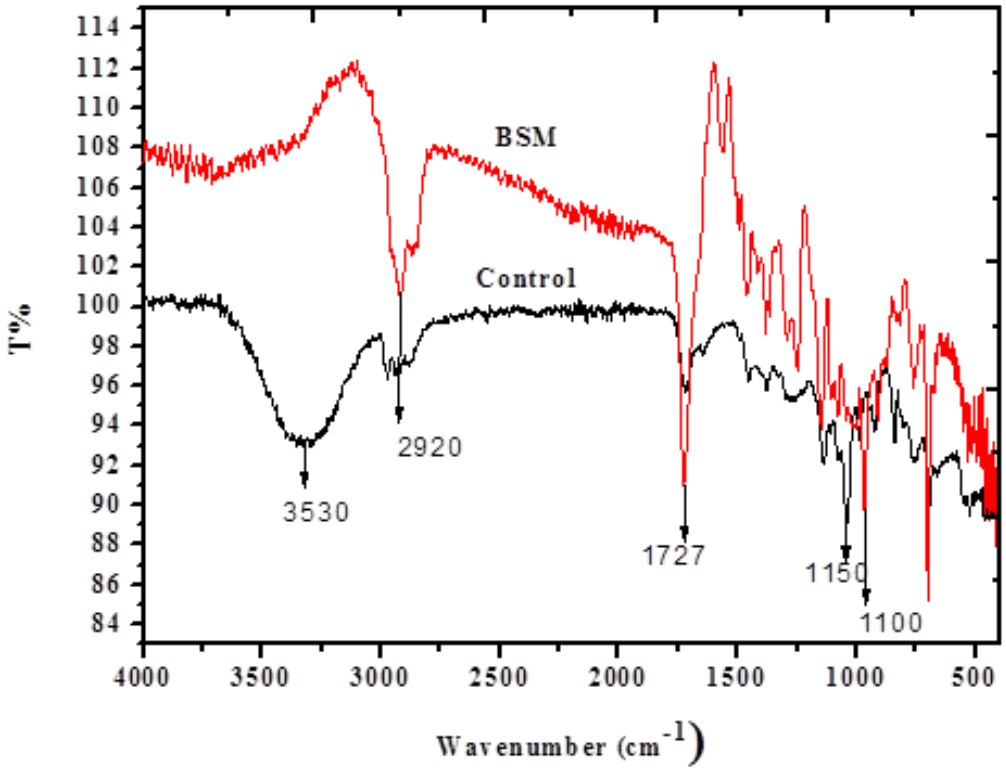

Figure 4.14: FTIR scan of an overlay of the cured control and BSM resins

4.3.5 Thermal analysis (TA) of BSM and control resins

Thermal gravimetric analysis provided information on the initial and final degradation behavioural patterns and decomposition of the BSM resin in comparison to the control resin. The thermogravimetric plots (Figure 4.15) show that the initial onset degradation temperature of the BSM resin at 352 °C and the control composite at 343 °C are comparable. In a separate reaction that looked at degradation patterns the final degradation of BSM resin was reached at 403 °C while that for the control composite was 392 °C. The weight loss at final degradation of BSM and the control were 6.2% and 9.9%, respectively. The presence of organics such as esters, sugars

and phenolic compounds from the BS [164] increased the thermal stability of the BSM resin resulting in increased thermal properties.

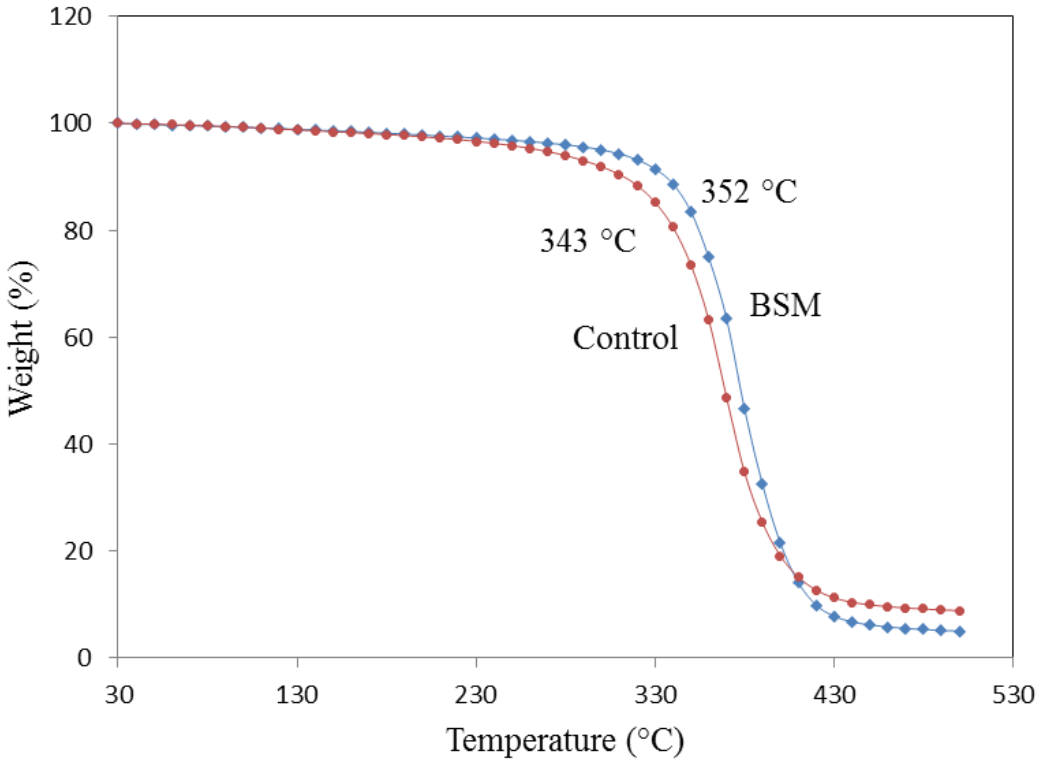

Figure 4.15: TG curves of BSM and control resin showing the onset degradation temperature

Figure 4.16 showed a shift in the DSC thermogram of BSM compared to the control resin. BSM resin had a higher melt and crystallization enthalpy than the control resin (Table 4.9) thus an indication that the BS resin was more stable and harder. A possible reason was due to the organics and sugars present in BS (GC-MS data Table 4.4 and HPLC data Table 4.3) which may have initiated cross-linking on the polymer backbone. The percent crystallinity was calculated based on 140 J/g for a 100% crystalline polymer (polyethylene terephthalate). BSM had a crystallinity of 58% and the control resin had 52%. Since, crystallinity is an indication of amount of crystalline region in the polymer with respect to amorphous content, it can be concluded that the BSM and control resins are both amorphous and crystalline. XRD results of the BSM resin and BSM biocomposite that give an indication of the

crystallinity are further explained in Figure 5.13, Chapter 5. Crystallinity influences many of the polymer properties such as hardness, modulus, tensile, stiffness and melting point [165].

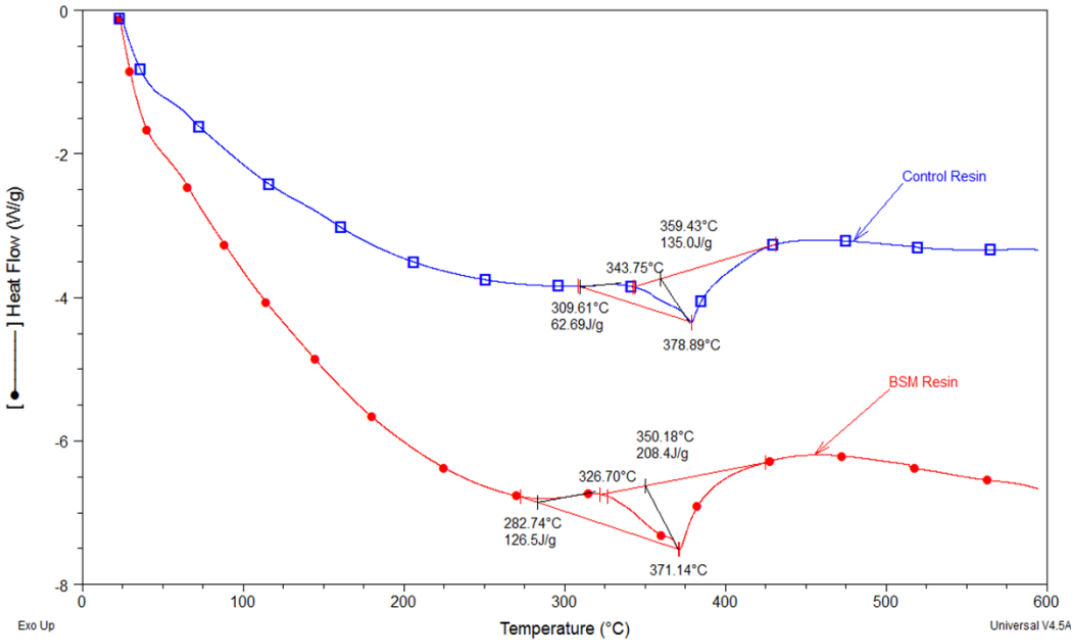

Figure 4.16: Comparison of DSC curves of BSM resin and control resin

Table 4.9: Crystallization temperature, melting point and enthalpy change of control resin and BSM resin

Sample	Melt enthalpy (J/g)	Crystallization enthalpy (J/g)	Degree of crystallinity (%)
Control Resin	62.7	135.0	52
BSM Resin	126.5	208.4	58

4.3.6 Kinetic studies on BSM and control resins

During the curing cycle of the resins, many complex physical and chemical changes take place [166]. For that reason it was deemed important to perform cure kinetic studies for thermosetting resins to obtain the ideal processing conditions that will provide the required structural performance for specific applications [166].

4.3.6.1 Dynamic kinetic analysis

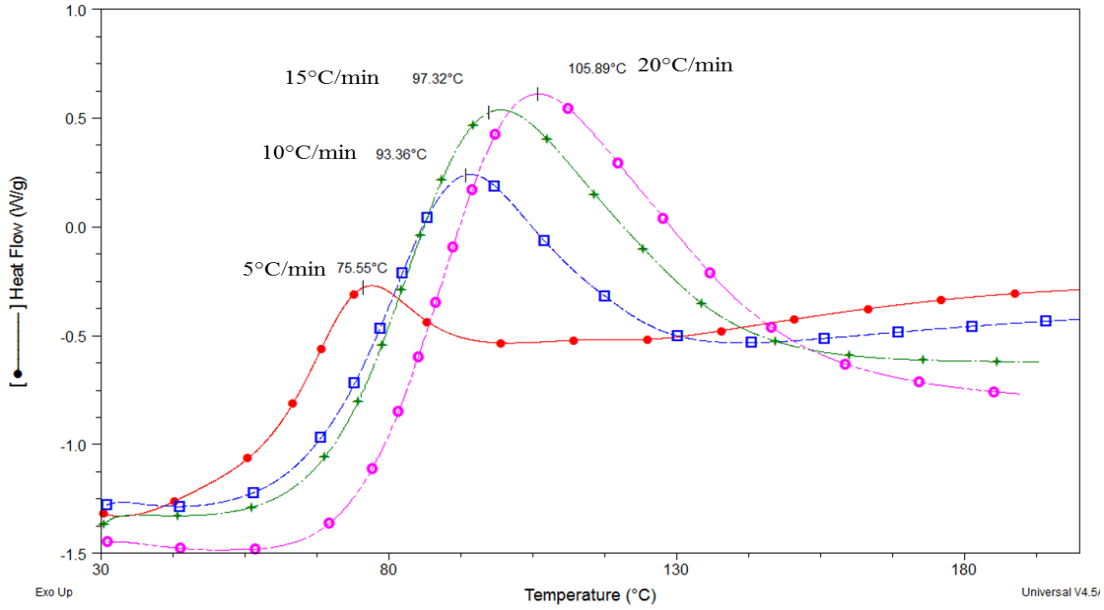

Figure 4.17: Dynamic DSC curves of BSM bio-resin at 5 °C/min (●), 10 °C/min (□), 15 °C/min (+) and 20 °C/min (○)

Figure 4.17 shows the DSC curves of the BSM bio-resin at ramp temperatures of 5 °C/min, 10 °C/min, 15 °C/min and 20 °C/min respectively. The total reaction heat ΔH_{total} which was determined as the area under the thermograms and the melt temperature, T_m, which was determined as the maximum peak of the exotherm is shown in Figure 4.18. With an increase in heating rate the reaction times were shorter and consequently the areas under the curves increased. Table 4.10 shows that the enthalpy (ΔH) values increased with increasing heating rates from 5 to 15 °C/min but decreased marginally at 20 °C/min. At lower heating rates, the calorimetric signal was smaller and consequently the cure times were longer. However, the decreased enthalpy value at 20 °C/min was associated with shorter curing times required for the reaction to occur [167]. The heating rate, q, and the melt temperature were used to calculate the values for the Kissinger and Ozawa-Flynn-Wall plots shown in Figure 4.19.

Table 4.10: Heats of reaction and peak temperatures at different heating rates

q (°C)	ΔH (Jg^{-1})	Tm (°C)	Tm (K)	Tm^2 (K)	1000/Tm (K)	Kissinger ($ln\ q/Tm^{2)}$)	OFW (ln q)
5	189.7	77.03	350.18	122626	2.86	-10.11	1.61
10	240.3	94.21	367.36	134953.4	2.72	-9.51	2.30
15	252.2	99.43	372.58	138815.9	2.68	-9.13	2.71
20	246.5	105.89	379.04	143671.3	2.64	-8.88	3.00

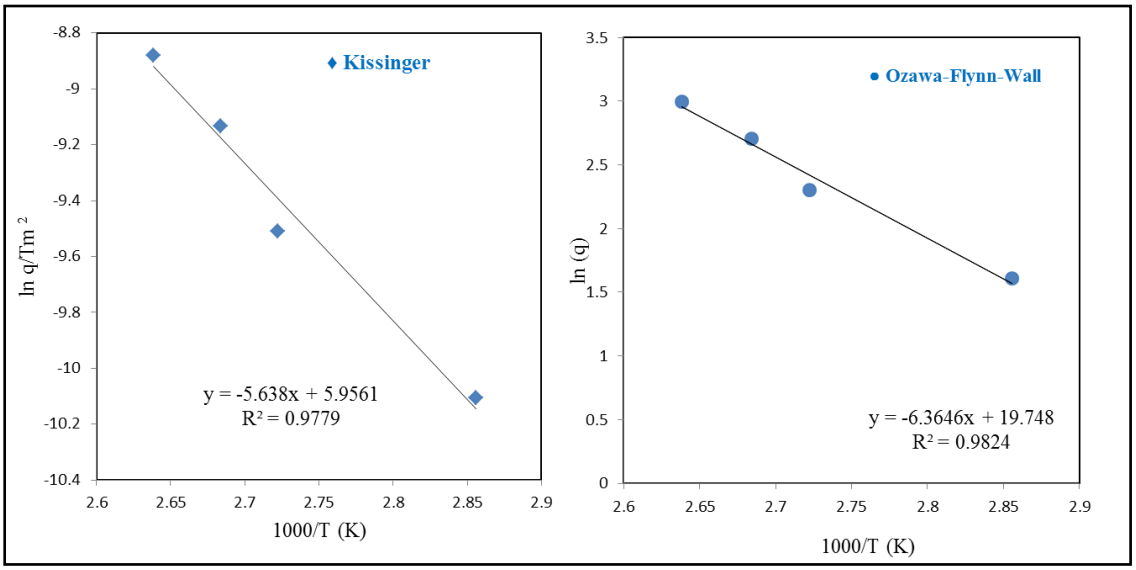

Figure 4.18: Kissinger's (■) and Ozawa-Flynn-Wall (●) plots of ln q versus temperature

The activation energy (E_a) of the BSM bio-resin defined as the minimum amount of energy required for a chemical reaction to occur, was determined by the application of Kissinger and OWF methods from the gradients of Figure 4.18 for the BSM resin system. The value of the activation energy using Kissinger's method was calculated (shown below) using equation 4.1 as referred to by Rantuch *et al.* [168].

$$E_a = -aR \tag{4.1}$$

where, a is the slope from Kissinger's plot (-5.638) and R is the universal gas constant (8.314 J $K^{-1}mol^{-1}$).

The value for the activation energy using the OFW method was calculated using equation 4.2 as referred to by Rantuch et al. [168].

$$E_a = -\frac{bR}{1.0516} \quad (4.2)$$

where, b is the slope of the OFW plot (-6.3646) and R is the universal gas constant (8.314 J $K^{-1}mol^{-1}$).

Activation energy of 46.87 J mol^{-1} was obtained by applying Kissinger's method, while a slightly higher value of 50.32 J mol^{-1} was obtained using the OFW method. These results were consistent with other researchers who also found activation energies from the OFW method to be marginally higher than the values obtained by the Kissinger method [169] [170]

In another study, Pistor *et al.* investigated the influence of glass and sisal fibers on the cure kinetics of UPR [167]. They reported that the neat UPR had an E_a of 43.9-47.2 $J.mol^{-1}$ and the addition of the fibres to the resin resulted in higher E_a. Other researchers have reported E_a values of pure UPR as 40.7 J mol^{-1} [171].

The E_a for BSM resin was 50.60 J mol^{-1} which is higher than that reported by Pistor *et al.* [167] and Kosar and Gomez [171]. Since BSM had other chemical components such as sugars and esters in its composition, it therefore required more energy for the chemical reaction to occur than the UPR resulting in a higher E_a.

4.3.7 Heat distortion temperature (HDT)

If a plastic is subjected to heat it will become pliable and will easily distort under load and it may not perform the function intended especially if that function is structural [97]. HDT was used to measure the temperature of a polymer that deforms under a specific load. Figure 4.19 show the HDT values of BSM and control resin occur at 91.40 °C and 93.04 °C, respectively. Deformation of the BSM resin takes place at a higher displacement but lower temperature as compared to the control resin. The HDT value of a material depends on the compactness and the glass transition temperature and the changes of hardness with temperature play a critical role. Yang and Puckett produced UPR's with different acids and marginally higher values were reported for HDT. The HDT results obtained are comparable to a producer of UPR and vinyl ester resins [172] where similar values were reported.

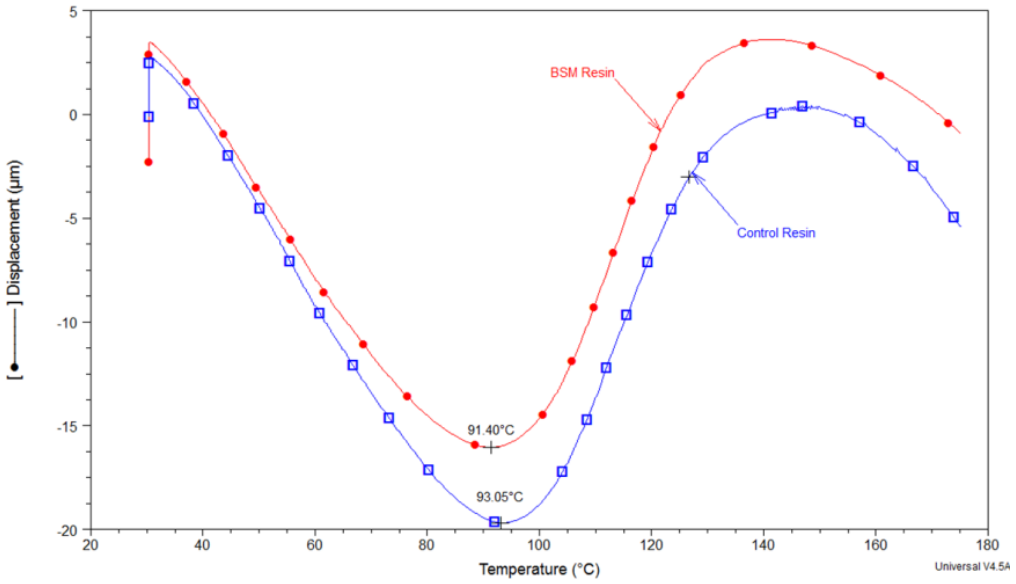

Figure 4.19: HDT curve of BSM and control resin

4.3.8 Dynamic Mechanical Analysis (DMA)

The viscoelastic properties of the BSM and control resins were determined by using the DMA. The DMA is the preferred method of determining the glass transition (T_g) or α transition, for polymers with rigid backbones. Glass transition is a major transition that occurs where the amorphous phase is converted to rubbery and glassy states in viscoelastic polymers as shown in Figure 3.9.

Figure 4.20 shows the plot of the storage modulus (E') of BSM resin as a function of temperature at three different frequencies namely 1, 10 and 100Hz. The viscoelastic properties of a material are dependent on temperature and frequency. The elastic modulus of a material decreased over a period of time if it was subjected to a constant stress. Pothan and co-workers reported that this is so because the material undergoes molecular rearrangement in an attempt to minimize the localized stresses [81]. They also reported that modulus measurements performed over a short period of time (high frequency) result in higher values and longer times (low frequency) produce lower results [81]. It was found that 1 Hz gave lower values and 100 Hz gave increased values. There were also electrical noises with the plots especially for the damping curves (not shown) and it was therefore decided to use 10 Hz in this experiment.

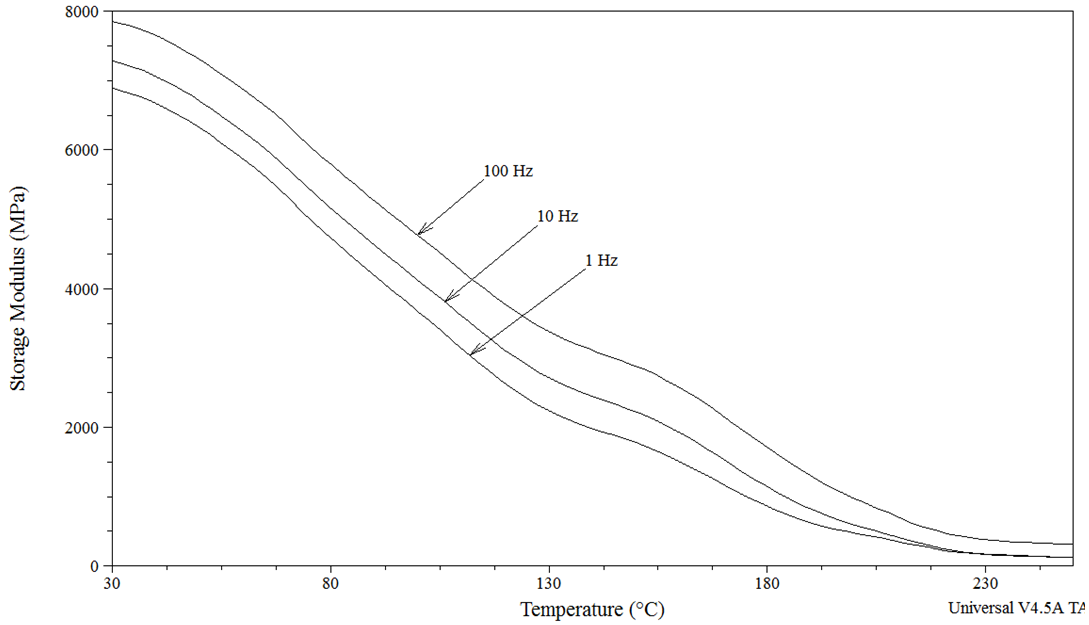

Figure 4.20: Effect of frequency on the storage modulus of BSM resin

The storage modulus as a function of temperature of the control and BSM resins as shown in Figure 4.21. The sudden decrease in storage modulus occurred at the lowest temperature and indicated physical softening of the resins. The initial storage moduli of BSM and control were 7320 MPa and 7591 MPa respectively. Although the initial change in the glassy region of the resins started at the same temperature, BSM had a lower modulus implying that softening of the bio-resin occurred at a lower modulus. However, between 136 °C and 160 °C the control curve plateaued out and decreased in a similar way as shown by the BSM resin. This region is the rubbery plateau region (Figure 3.9) during which the amorphous polymer changes from a stiff to soft rubber state.

Amorphous polymers are randomly oriented and are intertwined whereas semi-crystalline polymers pack together in ordered regions called crystallites. The T_g of the semi-crystalline polymer was lower than the amorphous polymer (Figure 3.10). The BSM resin showed a lower modulus value compared to the control resin which can be attributed to a larger degree of crystallinity of the BSM resin (Table 4.9)

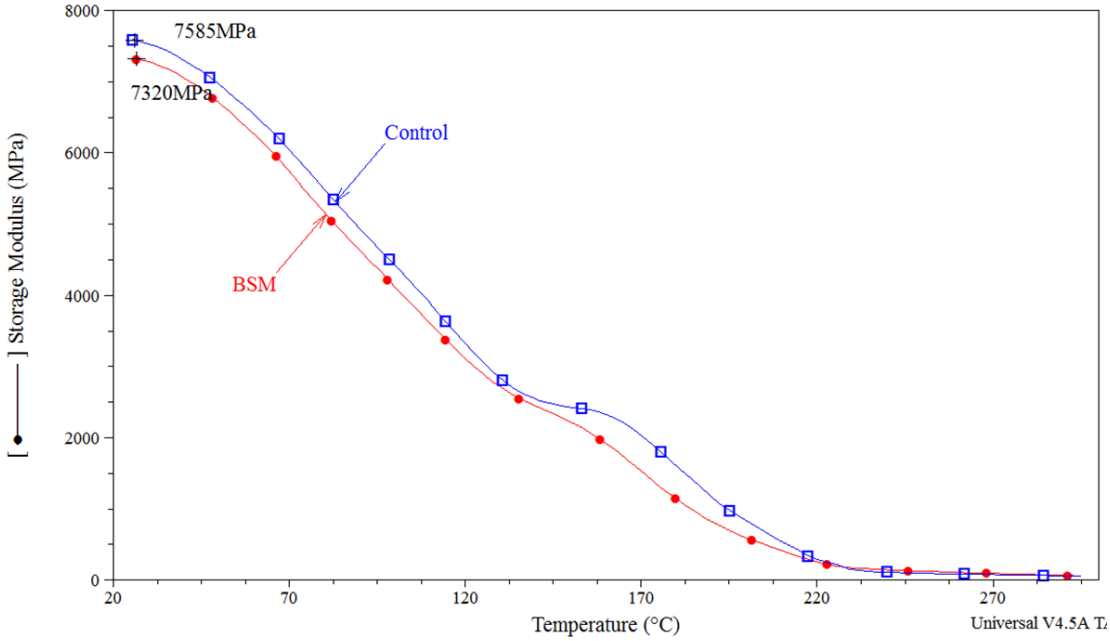

Figure 4.21: Variation in storage modulus (*E'*) as a function of temperature of BSM and control resin at 10 Hz

Figure 4.22 shows the peaks in loss modulus of BSM and control resins that occurred at the middle temperature and indicated segmental motion within the material. The loss moduli of the control and BSM resins increased with temperature until it reached T_g at 167 °C and 161°C respectively and thereafter it dropped back to the pre-transition values. From this softening region onwards, the loss modulus of control and BSM resins decreased sharply. However, the control resin indicated an increase in modulus value than the BSM resins since the control resin had a lower crystallinity value than BSM resin (Table 4.9).

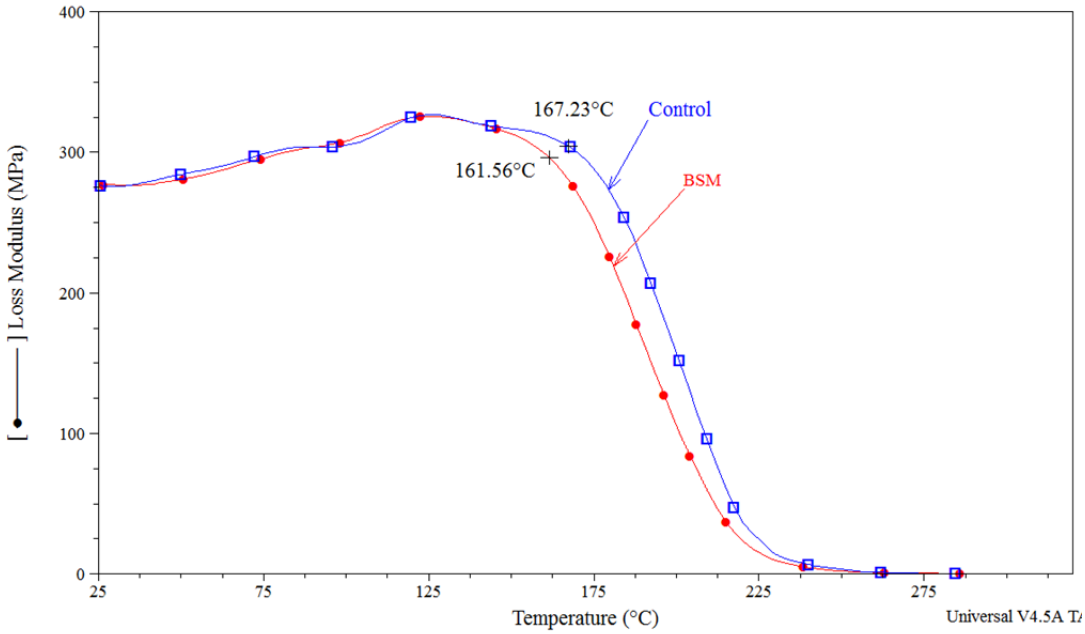

Figure 4.22: Variation in loss modulus (*E''*) as a function of temperature of BSM and control resins at 10 Hz

The peak in tan delta occurred at the highest temperature and indicated the midpoint of the material's transition between the glassy and rubbery states. The rapid rise in the tan delta curve coincided with the rapid decline in the storage modulus. The glass transition temperatures of the control and BSM resins were observed at 197 °C and 188 °C respectively as shown in Figure 4.23. The tan delta maximum values for BSM and control resins were 0.2021 and 0.1928 respectively. Since tan delta is the ratio of storage modulus to loss modulus, the BSM bio-resin had a higher elastic lower viscous part than the control resin. It was observed that the T_g obtained from loss modulus was several degrees lower than the T_g obtained from tan delta peak. The tan delta peak corresponded more closely to the transition midpoint of the decreasing storage modulus curve while the loss modulus denoted the initial drop from the glassy state into the transition [173].

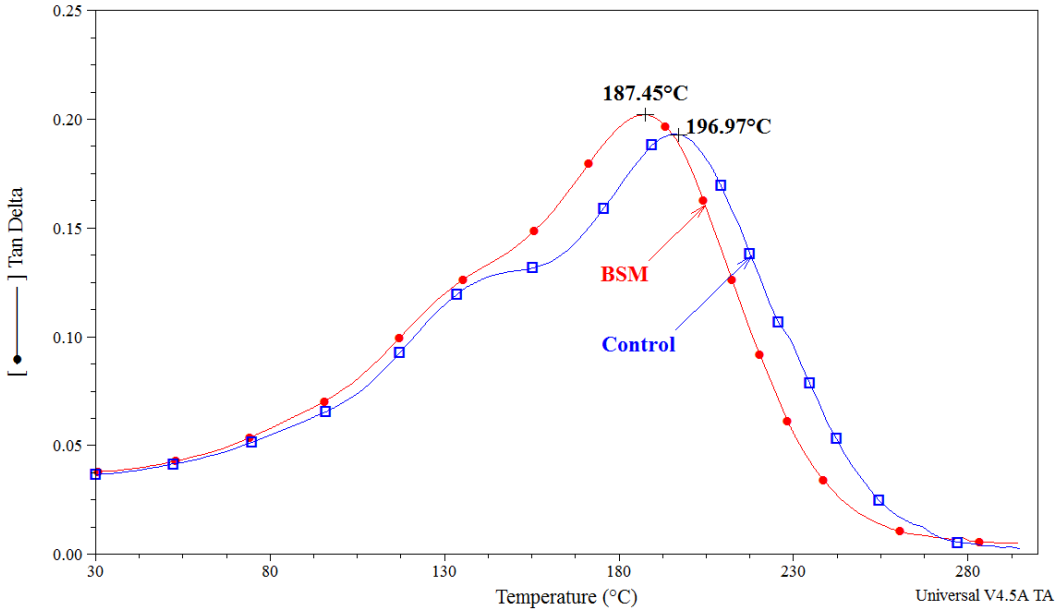

Figure 4.23: A plot of the tan delta of BSM and control resins as a function of temperature at 10 Hz

4.3.9 Mechanical properties of control and BSM resin

A parametric study of the mechanical properties was done using varying concentrations of BS to ascertain the optimum concentration of BS to be added to the maleate resin outlined in section 3.3.1.

Mechanical tests of the BSM bio-resins were compared to the control resin. Tensile strength, hardness, rigidity and brittleness, are the most fundamental mechanical properties that were analyzed and evaluated in order to characterize the formulated resin. Figure 4.24 shows the effect of increasing concentration of BS on the stress/strain behaviour of BSM compared to the control resin. It was noticed that with an increase of BS in the resin formulation the stiffness increased. However, BSM4 which had 60% BS decreased in stiffness. It was suggested that the maximum amount of BS to be added would be 50%. The addition of BS resulted in the dilution of PG-MA ratio. Higher concentrations of BS would dilute the bio-resin resulting in reduced crosslink density caused by reduced maleate content. The sites available for crosslinking with styrene decreased. It was suggested that self-crosslinking of the styrene may have occurred and the residual styrene left in the cured resin reduced the

mechanical properties of the resin thus rendering it brittle. It was also deduced that during the process of formation of the resin, varying amounts of the organics such as glucose and fructose from the BS reacted with maleate resin.

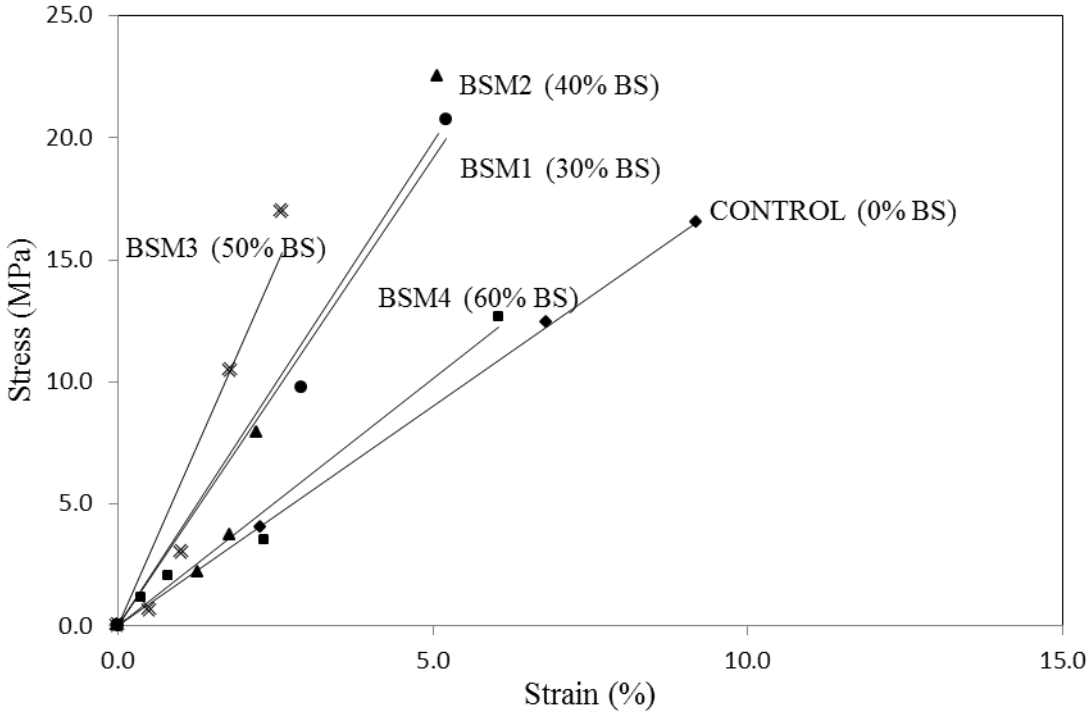

Figure 4.24: Effect of varying concentrations of BS on stiffness

Figure 4.25 show that by increasing the concentration of BS in the resin there was an increase in dynamic stiffness. The stiffness of the resin represented the resistance to deformation. However when 60% BS was added a decrease in stiffness occurred. Besides the BS diluting the maleate resin, compounds such as dibutyl phthalate and diphenyl esters present in the BS, shown in Table 4.4, can behave as plasticizers that may reduce interactions between segments of the polymer chain. These plasticizers have been reported to reduce the modulus [174]. It was also concluded that an optimum amount of 50% of the BS was added to the maleate in order for the reaction to reach completion to its fully cured state.

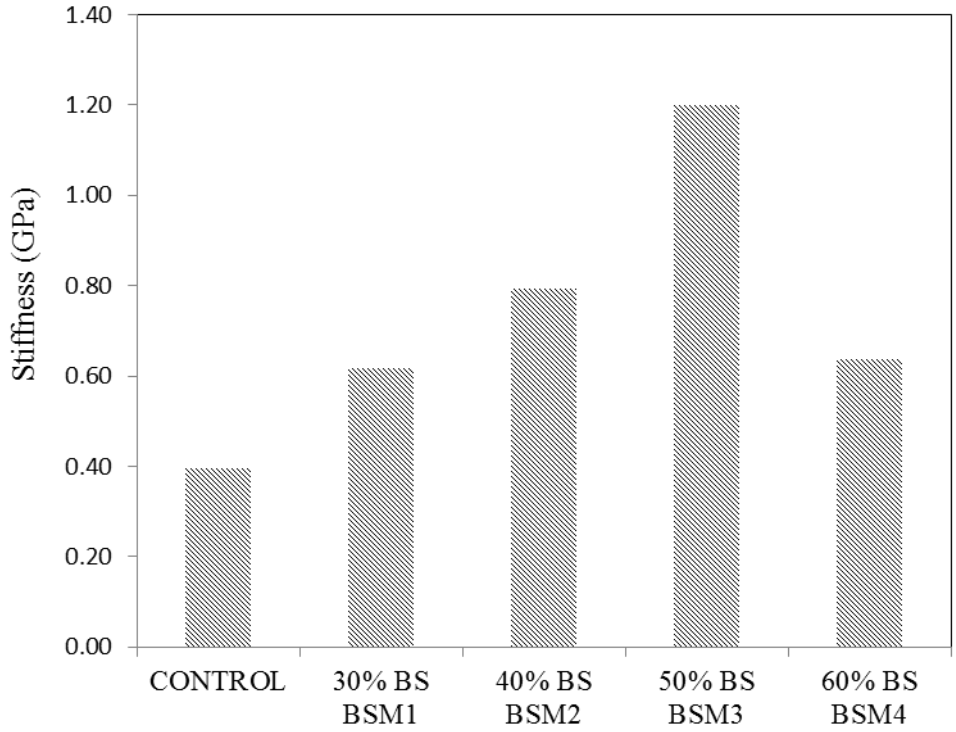

Figure 4.25: The effect of increasing BS concentration on stiffness compared to control resin

The three point flexural test shown in Figure 4.26 was carried out in accordance to the stipulated ASTM D790 method. Under static load BSM 1, 2 and 3 required 90 N, 160 N, and 270 N, respectively to extend the sample when compared to the control sample that broke at 40 N. BSM 4, however did not follow the trend. This sample had the most amount of BS which consequently led to the reduced maleate concentration and saturation for crosslinking with styrene. The brittle nature of this sample resulted in the sample breaking at a load of 50 N.

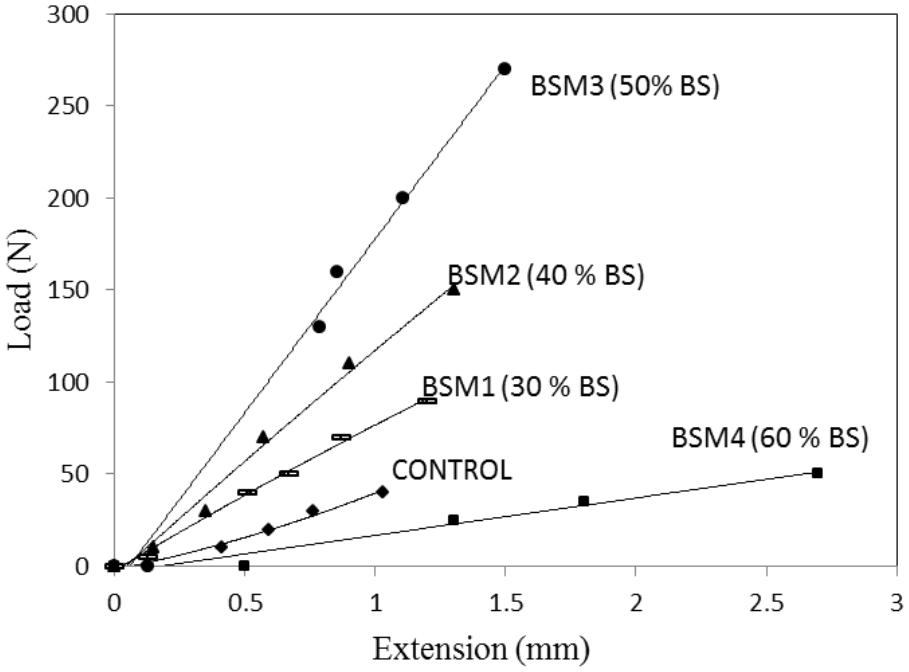

Figure 4.26: The effect of increasing BS concentration on flexural load

Figure 4.27 show the effect of increasing the concentration of BS on the flexural modulus. The flexural modulus increased with increasing concentrations of BS in the resin. When compared to the control resin, 30% BS showed 81% increase, 40% BS showed 93% increase, 50% BS showed 190% increase and 60% BS showed 43% increase in flexural modulus. However 60% BS showed lower modulus than the other concentrations of BS.

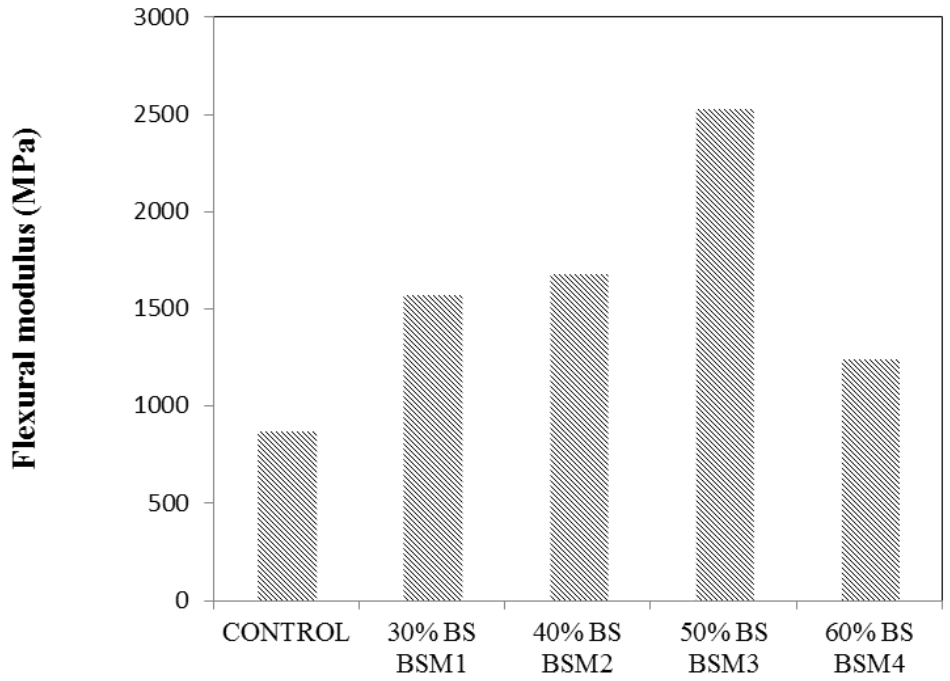

Figure 4.27: Effect of increasing BS on flexural modulus compared to the control resin

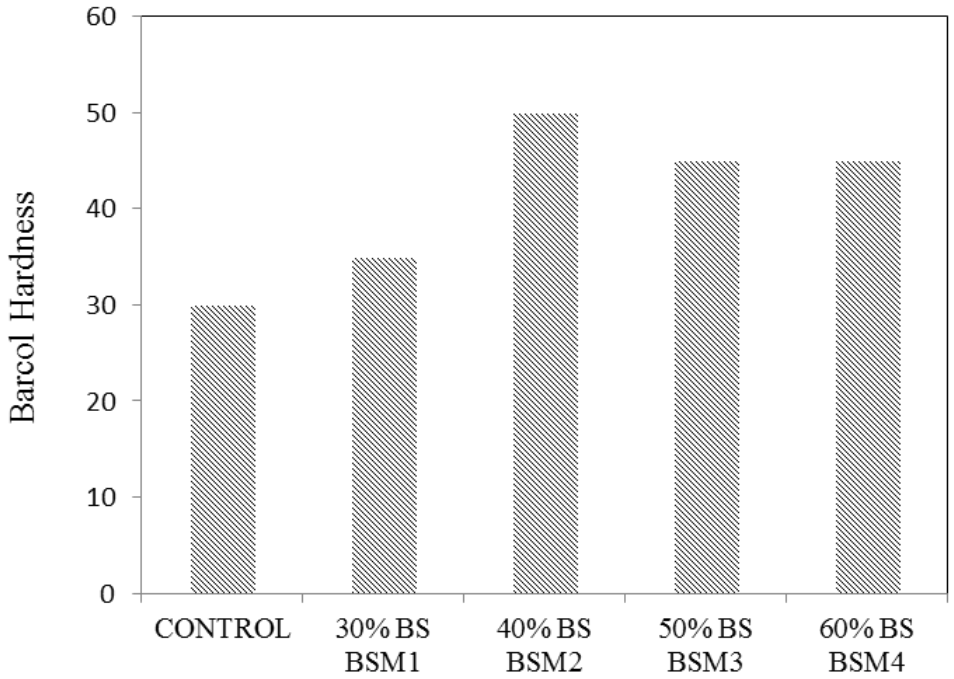

Figure 4.28 Effect of increasing concentration of BS on hardness compared to control sample

Measurement of the hardness of a resin or polymeric material is related to the strength and elastic characteristics of the biopolymer. The Barcol hardness value (measured on a scale of 0-100) was obtained by measuring the resistance to penetration of a sharp steel point under a spring load. The hardness value is used to measure the degree of cure of the plastic. The reaction with 40% BS produced a resin with the highest value of hardness of 50 units as shown in Figure 4.28.

It has thus been observed that the addition of BS to the resin mixture contributed positively to mechanical properties of the bio-resin. The mechanical results showed that BSM1 to 3 were stronger than but not as tough as the control sample. BSM 4 showed lower strength and toughness. The mechanical properties showed that BSM2 (40% BS) and BSM 3 (50% BS) gave optimum results. It was therefore decided to use 50% BS in the formulation of the resin.

4.4 Summary

The physical testing of BS gave the TDS, pH, conductivity and density of the *musa cavendish* species. The ICP-AES analysis showed the elements present in BS with potassium and magnesium being the most abundant. Qualitative analysis proved the presence of carbohydrates by a positive Molisch test. This was further verified by HPLC analysis that quantified the sucrose, fructose and glucose present in the sap. GC-MS results showed that BS is a complex matrix with esters, phenolic compounds, aromatic compounds to mention a few. Predictions were made for the possible reaction of fructose and glucose on the maleate polymer backbone. There was an increase in molecular weight when BS was added to the resin formulation. Gel times and cure times were improved with BSM compared to control resin. FTIR analysis showed that the ketone peak from BS and strong carbon-carbon double bonds making a positive contribution to the resin formation. The addition of BS increases the molecular weight of the BSM bio-resin and consequently improves the thermal degradation and mechanical properties. The optimum concentration of BS to be added to the resin was 50% producing optimum tensile and flexural properties.

CHAPTER 5 –RESULTS AND DISCUSSION: SYNTHESIS AND ANALYSIS OF BIOCOMPOSITE

Introduction

Biocomposites produced from natural fibres have been successfully used in various resins, however there is still a need to research and develop new plant based biocomposites [166] such as those based on BS and banana fibres. The first part of this chapter focuses on the analysis of the banana fibre and the second part deals with the synthesis and analysis of a biocomposite[8] compared to the control sample.

The last part of Chapter 5 focuses on the fortification of the bio-resin and biocomposite with nanoclay.

5.1 Banana fibres

This section outlines the chemical composition of the banana fibre and also addresses the problem of the hydrophilic nature of the fibre by chemical treatment.

5.1.2 Chemical analysis of banana fibres

The banana fibres obtained from a local garden in Durban, South Africa was extracted as discussed in section 3.2.1. A chemical assay of the fibres was obtained.

Table 5.1 shows that banana fibres consist of 58.92% cellulose, 16.11% hemicellulose and 7.31% lignin. These results are consistent with results obtained by others [39], where 63% cellulose, 19% hemicellulose and 5% lignin in banana fibres was reported.

[8] Extracts from Chapter 5 have been published as "Mechanical, thermal and morphological properties of a bio-based composite derived from banana plant source", Composites Part A 68, (2015), 90-100

Table 5.1: Chemical assay of banana fibres[9]

Av dry matter (%)	93.89
Ash (%)	3.28
Crude protein (%)	1.62
Cellulose (%)	58.92
Hemicellulose (%)	16.11
Lignin (%)	7.31
Starch (%)	11.72
Crude fat (%)	1.06
Gross energy (%)	40.36
Arabinose (%)	2.93
Galactose (%)	1.26
Glucose (%)	53.65
Xylose (%)	8.82
Mannose (%)	1.01

5.1.3 Chemical treatment of banana fibre

Chemical modification was used to enhance the compatibility of the resin with the banana fibre. The procedure for the chemical modification is outlined in section 3.2.4. SEM images at magnification between 500-2000 X were obtained for treated and untreated fibres. Figure 5.1A shows the SEM image of untreated fibre. A smooth surface containing lignin, pectin, cellulose and hemicellulose (Table 5.1) was observed. The treatment of banana fibre with 2% NaOH resulted in a rough surface where the hemicellulose and pectin where removed and the hydrogen bonds were broken (Figure 5.1B).

[9] Results obtained in accordance to ASTM conducted at the Animal Sciences department at North Dakota State University

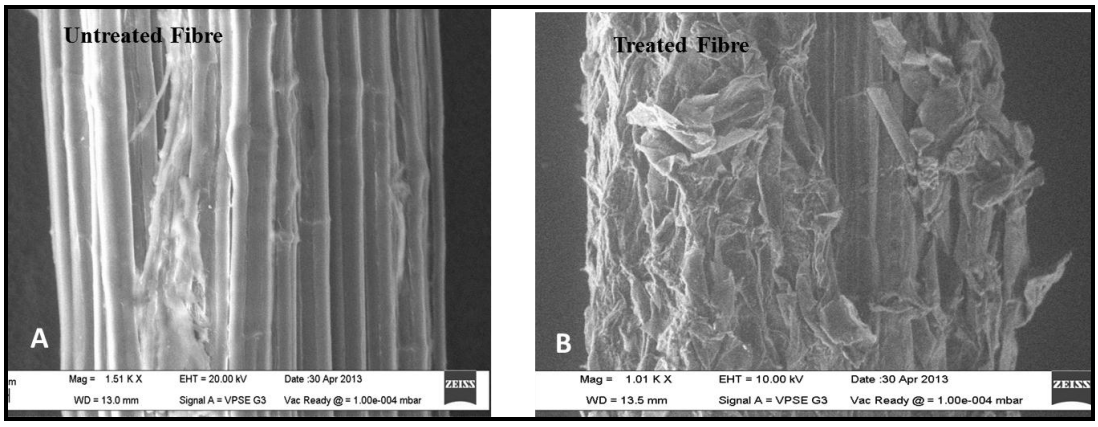

Figure 5.1: SEM images of banana fibres:

(A) untreated and (B) treated with 2% NaOH

5.1.4 FT-IR analysis of untreated and treated fibre

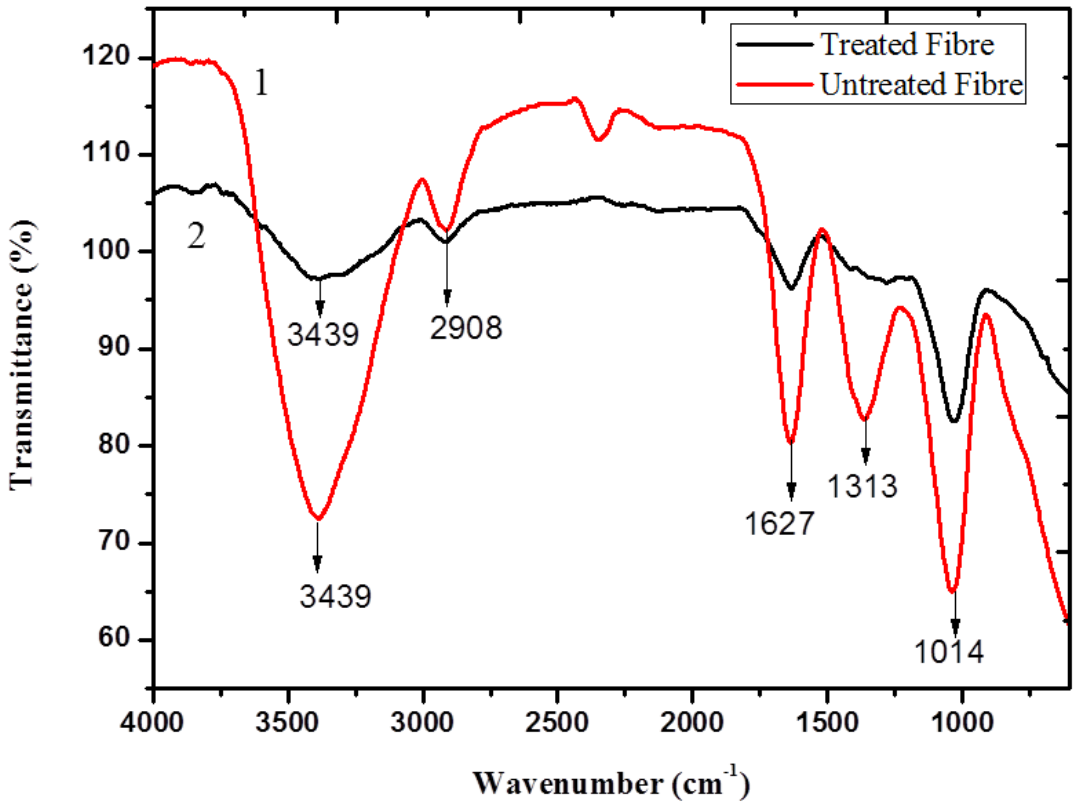

Figure 5.2: A comparison of FTIR spectra of (1) untreated and (2) treated with 2 % NaOH

Figure 5.2 show the functional groups of the untreated and treated fibres. For the untreated fibre, the broad band observed at 3439 cm^{-1} is related to the stretching vibration of the OH groups from the cellulose (carbon 2, 3 and 6 of the glucose) [175, 176]. After the alkali treatment the intensity of this band was reduced due to the hydrogen bonding caused by OH group. The peak at 2908 cm^{-1} assigned to the C-H aliphatic stretching band of fibre was reduced after the alkali treatment due to the removal of the hemicellulose [177]. In the untreated BF the peak at 1627 cm^{-1} corresponded to the C=O stretching of hemicellulose. After alkali (NaOH) treatment, a major reduction in peak intensity was observed, possibly indicative of the removal of hemicellulose and lignin from the fibre surface; a result analogous to the alkali treatment of kenaf fibres reported by El-Shekeil *et al*. [178]. The reduction in intensity of the absorption band at 1627 cm^{-1} may be attributed to a decrease of lignin and consequently a reduction of the C=O functionality. A similar observation was made by Barreto *et al.* with alkali treatement of sisal fibres [179]. The sharp peak observed at 1313 cm^{-1} was assigned to C-H asymmetric deformation and disappeared after alkylation thus indicating crosslinking. The prominent peak at 1014 cm^{-1} was due to the vibration of the –C–O–C–. The intensity of this peak increased after alkali treatment possibly due to the relaxation of crosslinking that increased the intensity and resolution [64]. From the FTIR analysis, it was evident the alkali treatment removed the lignin and hemicellulose from the surface of the fibre. The NaOH breaks the intermolecular H- bonding of the fibre and formed –ONa bonds on the fibre surface which in turn reduced the hydrophilic behaviour of the fibre as shown in the following reaction [180]:

$$\text{Fibre} - OH + NaOH \longrightarrow \text{Fibre} - O^{-} Na^{+} + H_2O$$

This resulted in the surface becoming less crystalline, which was further suggested by the less resolute FT-IR peaks, thereby allowing improved fibre/matrix adhesion. In comparison, the untreated fibre was more crystalline or more orderly structured as seen by the high resolute peaks.

An important consequence of fibre treatment is the matrix –fibre interface that will be discussed under fibre pull-out test in section 5.2.8.

5.2 Analysis of biocomposite

5.2.1 Chemical resistivity tests

Chemicals can affect the strength, flexibility, surface appearance, colour, dimensions or weight of plastics [97]. Chemical attack on the polymer chain results in the reduction of chemical properties such as oxidation, reaction of functional groups and depolymerization. Furthermore, physical changes take place such as adsorption of solvent resulting in the softening and swelling of the polymer, permeation of the solvent through the polymer and dissolution in the solvent. Table 5.2 shows the chemical resistivity of the control and BSM composites when exposed to various solvents for a period of one week. The differences in sample weights were calculated before and after immersion into the solvent. It was observed that the control composite generally had adsorbed more solvent than the BSM specimen. Since stronger bonds exist within the BSM biocomposite less solvent was adsorbed onto the surface. Polar solvents such as water and ethanol were absorbed to a greater extent than the non-polar solvent such as petrol. This observation of chemical similarity in absorption of the solvents can be stated in traditional chemistry as "like dissolves like", which implies that polar solvents strongly affect polar polymers and non-polar solvents have a strong interaction with polar polymers [97]. From this observation, it is suggested that BSM bio-resin was more polar than the control bio-resin.

The samples were observed and classified as: high resistance with no attack or limited resistance with a slight attack by absorption or swelling and no resistance where the material decomposed or dissolved. For instance, the reactivity of the specimens with water were classified as high resistance since there was no chemical attack on the surface but with slight swelling as indicated by the percentage absorption. In another instance, the reactivity with NaOH showed no resistance since they started to decompose after one week.

Although the biocomposite produced in this study favoured minimum solvent reaction because of its application in non-functional motor vehicle components, Strong has drawn attention to the advantages of chemical exposure of polymers [97]. For instance, the softening of polyvinyl chloride with certain chemicals renders it

soft and pliable for usage. Another example is the reaction of cellulose with nitric acid to form cellulose nitrate or the reaction of cellulose with acetic acid to form cellophane.

Table 5.2: Chemical resistivity test on control and BSM biocomposite

	BSM biocomposite		**Control biocomposite**	
	% absorption	Resistance	% absorption	Resistance
Water	9.07	1	11.42	1
Ethanol	9.50	1	12.97	1
Benzene	8.81	1	8.50	1
Acetone	9.40	2	13.57	2
Chloroform	16.58	2	17.06	2
Petrol	3.83	2	4.60	2
10 % H_2SO_4	6.70	2	7.76	2
10 % HCl	6.15	1	9.06	1
10 % HNO_3	9.39	1	8.99	1
10 % NaOH	13.36	3	17.25	3

1- high resistance **2- limited resistance** **3- no resistance**

5.2.2 Water absorption behaviour

One of the main concerns of natural fibre reinforced composites is their susceptibility to moisture absorption and the effect on physical, mechanical and thermal properties [181].

Figure 5.3 shows the water uptake curves of the BSM and control composite materials. The water uptake continuously increased over a period of 96 hours for both samples and saturation was achieved from approximately 72 hours. However, the control composite absorbed 1.12 % more moisture than the BSM composite at 72 hours. Similar results were discussed in section 5.2.1.

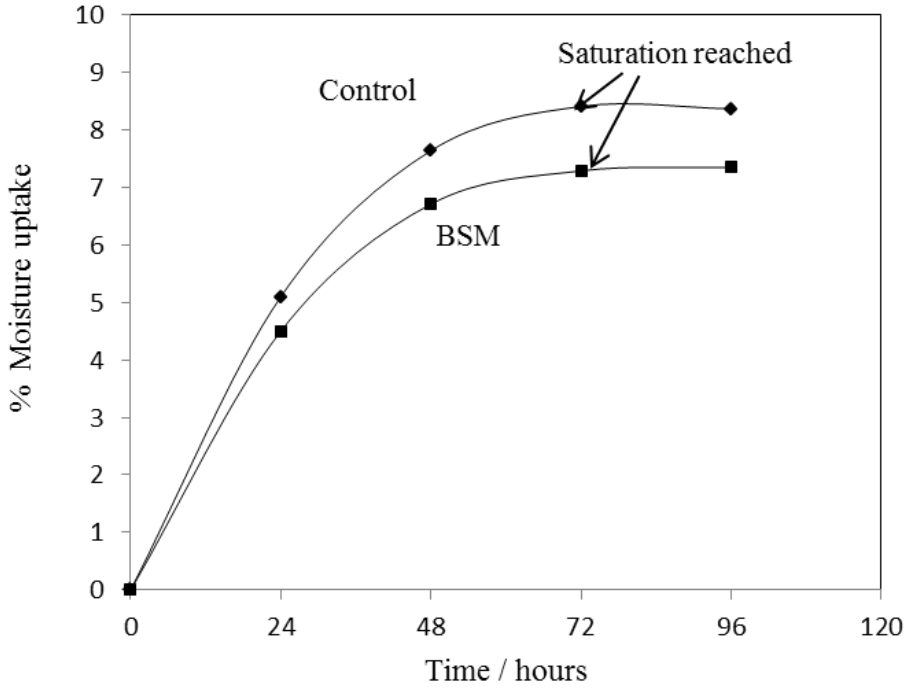

Figure 5.3: Moisture absorption at 24, 48, 72 and 96 hours of BSM and control biocomposites

The diffusion of water in the composite material was studied using Fick's steady state flow equation. Table 5.3 shows that the BSM composite had a lower water uptake, however the diffusion, sorption and permeability coefficients were similar. The permeability coefficient indicated the amount of moisture permeated through uniform area of the composite per second. The permeability coefficient was be considered as the total effect of diffusion and sorption as referred to work done by Indira *et al.* [180].

Table 5.3: Water uptake characteristics of control and BSM composite samples buried in nutrient rich soil

Sample	Water uptake at infinite time M∞ (%)	Diffusion coefficient *D* (mm^2/s)	Sorption coefficient *S*	Permeability coefficient *P* (mm^2/s)
Control Composite	8.37	1.34E-05	1.641	2.19E-05
BSM Composite	7.39	1.35 E-05	1.642	2.21E-05

Giridhar and Rao found that the compactness of the fibre accounted for the absorption level of moisture in the composite [182]. Espert also explained that moisture diffusion in polymeric composites took place in three different ways [183]. Firstly diffusion of molecules occurred inside the micro voids in the polymer chains, thereafter water flowed through capillary action into the voids at the interfaces between fibre and the matrix and finally the transport of micro cracks in the matrix occurred from the swelling of the natural fibre particularly in natural fibre composites [184]. SEM of the cross section of a banana fibre is given in Figure 5.4. When the biocomposite was exposed to moisture, the cross section of the hydrophilic banana fibre swelled; consequently inducing micro cracks in the resin. The high cellulose content of the fibre further contributed to more water being adsorbed [185]. On a micro level, these cracks increased in dimension, water molecules reacted with the interface, hence loosening the fibre and the matrix and consequently decreasing the tensile and flexural behaviour.

It has been concluded that the determination of the water absorption of biocomposites is an important aspect to study since the research deals with natural fibres.

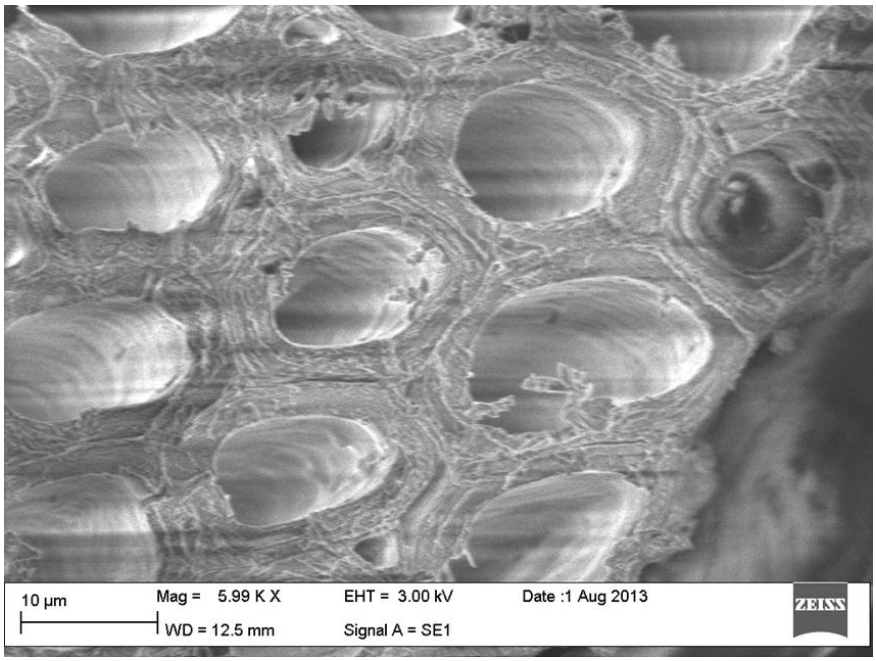

Figure 5.4: Scanning electron micrograph of the cross section of banana fibre showing the bundles into which moisture can be absorbed

Further to studying the absorption behaviour of the biocomposites with water, the swelling test of the neat BSM and control resins with toluene was studied.

5.2.3 Swelling index and cross-link density determination

When a cross-linked polymer is placed in a solvent such as toluene, it will absorb the solvent. Consequently, it will swell rather than dissolving in it. The steady state swelling ratio is a direct function of the extent of cross-linking of the sample, hence a swelling test is a simple, low-cost technique to characterize the polymer network [186]. In this study, the swelling test was conducted on the BSM and control resins to give an indication of the swelling index and cross-link density. These resins were used in the manufacture of the biocomposite. The swelling index measured the swelling resistance of the BSM and control bio-resins in toluene and is given in Table 5.4. The BSM resin was found to have a higher swelling resistance to toluene. A probable explanation for this could be due to an improved polymer network structure as shown in Figure 3.10 where amorphous and crystalline morphologies exist. Furthermore, Table 4.9 showed that BSM had a marginal increase in

crystallinity value. BSM with a higher crystallinity value implied that there was a neater packing of the polymer molecules. The control resin with a lower crystallinity value has spaghetti like polymer chains which allowed for easier diffusion of the toluene. This was compared to the BSM resin which had neatly packed polymer chains of a more crystalline structure, where it was found that the toluene a took longer to be diffused.

The cross-link density is an important property affecting the major characteristics of a cross-linked system. The swelling of the cross-linked polymer prevented the molecule from becoming completely surrounded by the fluid but had caused swelling [187].

Table 5.4: Swelling index values of resin samples

Sample	Swelling index values (%)
Control resin	0.44
BSM resin	0.83

Table 5.5: Apparent cross-link density values (1/Q) of resin

Sample	Apparent cross-link density values
Control resin	5.56
BSM resin	8.80

Apparent cross-link densities of the BSM and control resins is given by the reciprocal of Q (amount of solvent absorbed) shown in Table 5.4. According to Strong lower cross-link density means that the material is less strong, less stiff and more sensitive to solvent attack and has a lower decomposition temperature [97]. Therefore the control resin with a lower molecular weight (2114 $g.mol^{-1}$) and consequently lower cross-link density (5.56) would have the following characteristics: 1) be more susceptible to solvent attack 2) have lower decomposition temperature and 3) reduced strength. These findings were consistent with the

chemical resistance test discussed in section 5.2.1; thermal properties in section 5.2.5 and mechanical properties in section 5.2.10 of the BSM and control biocomposites.

5.2.4 Heat distortion temperature (HDT)

As elevated temperature performance of structural composites is an important consideration, HDT of the biocomposite was determined. HDT is temperature at which a polymer deforms under a specific load. Figure 5.5 show the HDT values of BSM and control composite material at 108.50 °C and 104.68 °C respectively. The higher HDT value of the BSM biocomposite denotes the deflection temperature under load at which the specimen may be used as a rigid material. Moreover, the HDT value of a material depends on the compactness (stiffness) and the glass transition temperature. Strong suggests that HDT should not be considered a fundamental property of plastics as are the thermal transitions properties such as glass transition and melting point [97] which will be discussed in the next two sections.

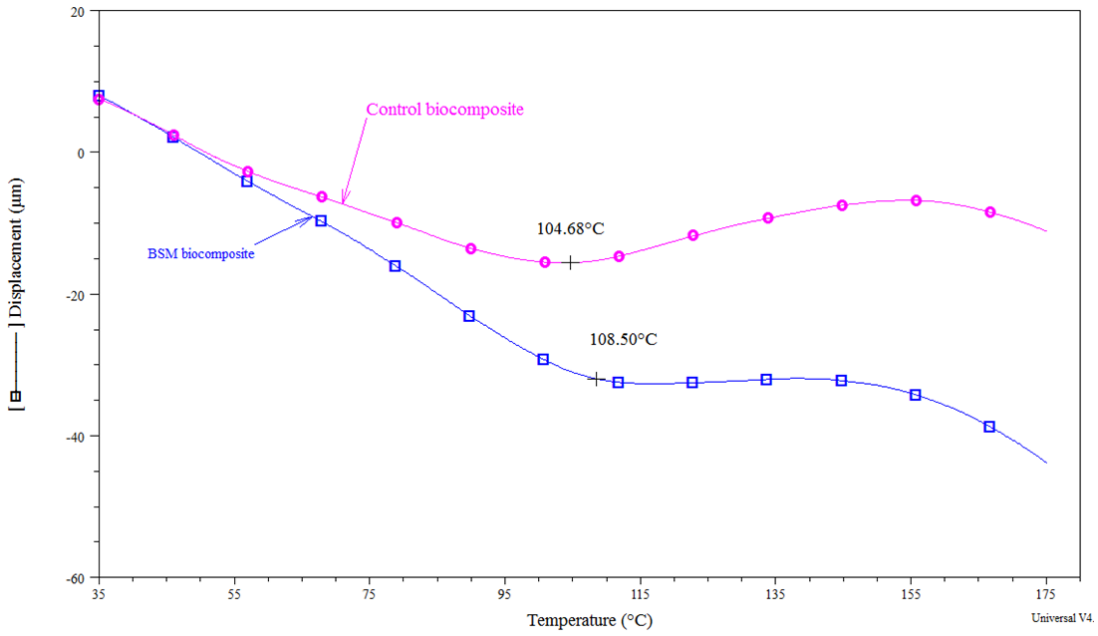

Figure 5.5: HDT curves showing the deflection temperature of BSM and control biocomposites

5.2.5 Thermal analysis

Thermal stability of biocomposite material is of significant importance especially for its application in non-functional components in motor vehicles since exposure to temperature is inevitable.

The thermogravimetric curves of the BSM and control composites are given in Figures 5.6. The degradation temperature of the BSM and control composites occurred at 377 °C and 363 °C respectively. It is suggested that the higher degradation temperature of the BSM composite could be attributed to the presence of organics such as esters and phenolic compounds in the BS [164] which resulted in increased thermal stability.

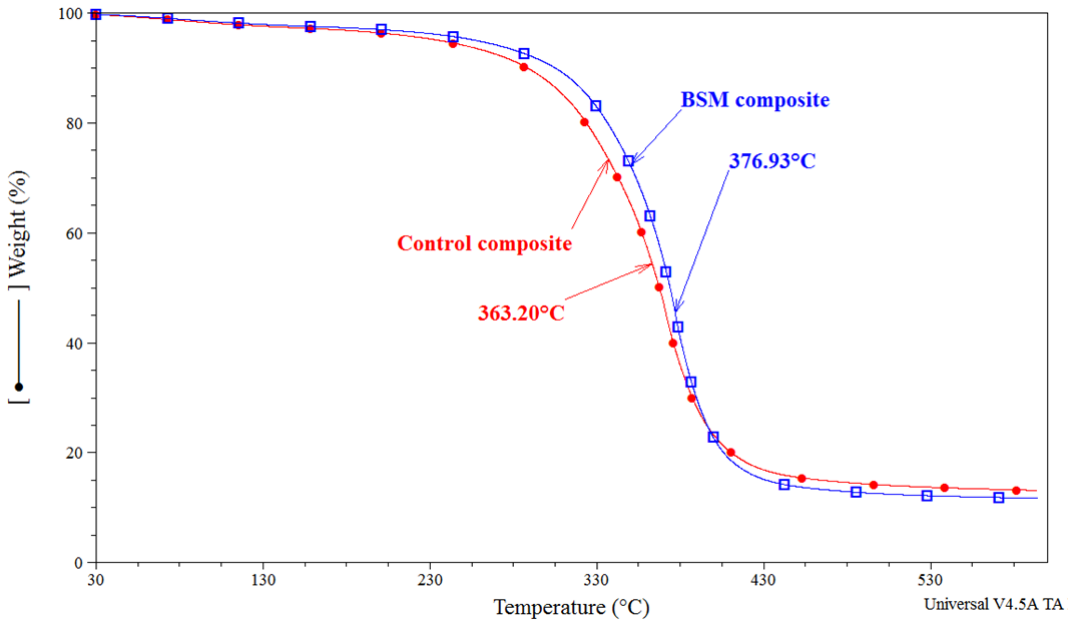

Figure 5.6: The mass loss of BSM and control biocomposites from 200-500 °C

The DSC curves of BSM and control composites are given in Figure 5.7. The melting point temperatures (T_m) of the control and BSM composites were 369 °C and 385 °C, respectively. The crystallization temperature of the control and BSM composite were 317 °C and 343 °C respectively. The broad peaks observed were due to the impurities in the biocomposite material, which in this case is the banana fibre.

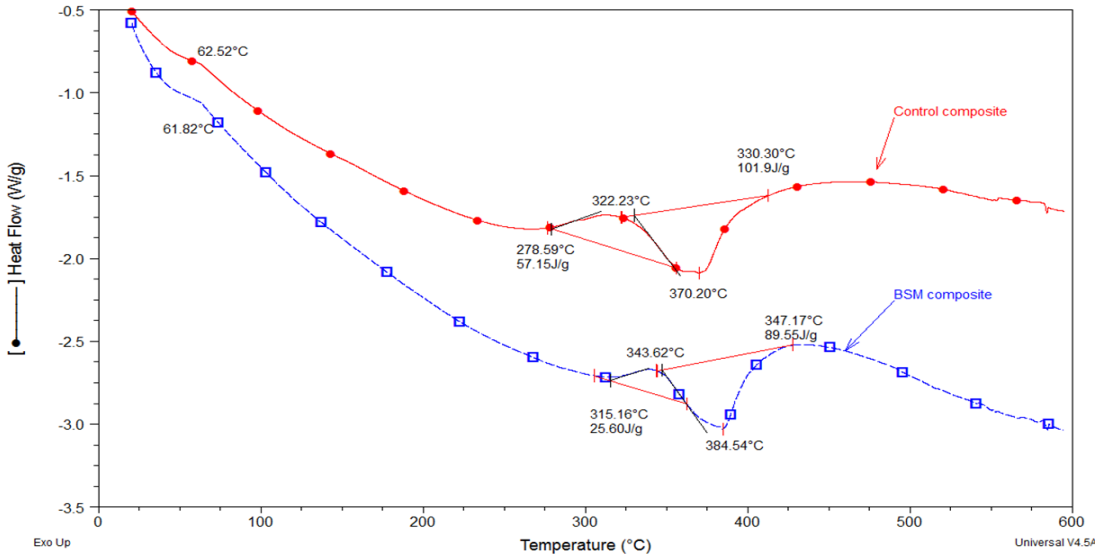

Figure 5.7: DSC curves of BSM and control biocomposites showing the T_m and crystallization temperatures

The degree of crystallinity was determined from the crystallization exotherm on heating (see Figure 5.7) using the Equation 5.1 below:

$$\text{Degree of crystallinity} = \frac{\Delta H_f - \Delta H_c}{\Delta H_{f100\%}} 100\% \qquad (5.1)$$

where ΔH_f is the enthalpy of melting, ΔH_c is the enthalpy of crystallization, and $\Delta H_{f100\%}$ is the enthalpy of melting for a fully crystalline polymer (140 J/g) [173]. Table 5.6 show that the BSM composite had 45% degree of crystallinity indicating that there was a more orderly polymer network arrangement than the control composite. Crystallinity is an indication of the amount of the crystalline region in the polymer with respect to amorphous content thereby rendering the BSM biocomposites as amorphous and crystalline since a purely crystalline material would be 100%. Crystallinity affects many of the polymer properties such as hardness, modulus, tensile, stiffness and melting point [165, 188].

Table 5.6: Comparison of the degree of crystallinity of BSM and control biocomposites

Sample	Melt enthalpy (J/g)	Crystallization enthalpy (J/g)	Degree of Crystallinity (%)
Control Composite	101.7	57.15	31.72
BSM Composite	89.55	25.66	45.64

5.2.6 Dynamic Mechanical Analysis (DMA)

5.2.6.1 Storage Modulus (*E'*)

The storage modulus as a function of temperature of the BSM and control composites is shown in Figure 5.8. With increasing temperature the storage modulus of the biocomposites decreased as the matrix softened. From Figure 5.8 it was noted that the change in storage modulus at approximately 150 °C of the BSM and control composites occurred between 2600-2300 MPa. The results were compared to the change in modulus of the pristine BSM resin at a value of 1640 at 150 °C as shown in Figure 4.22. The increase in modulus of the biocomposite was associated with restriction imposed by the banana fibres on molecular motion in the matrix at higher temperature. Similar findings were reported by Manikandan *et al.* and Joseph *et al.* [189, 190]. However, the decrease of matrix modulus in composites was partially compensated by the stiffness of the fibre. Furthermore, Pothan and co-workers reported that neat polyester resin had a higher dynamic modulus than the fibre filled system and the lowering of the modulus was due to the dilution of the polymer [3]. This study showed that the BSM biocomposite had a larger modulus than the BSM resin. The increase in storage modulus suggests enhanced adhesion between the banana fibre and the BSM matrix leading to better stress transfer from matrix to fibre.

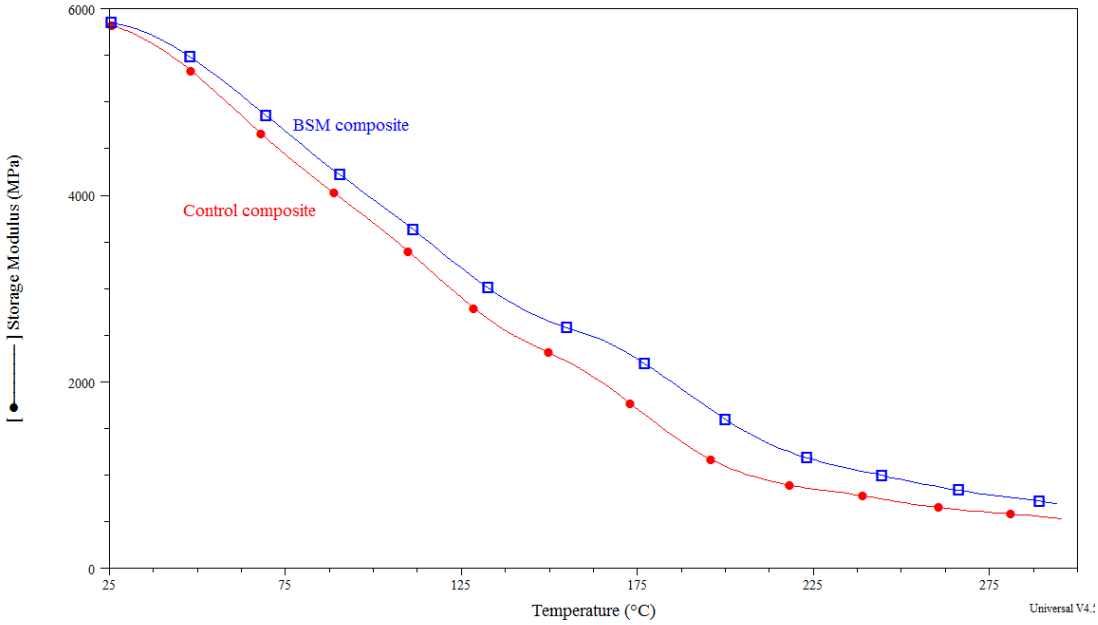

Figure 5.8: Temperature dependence of storage modulus (*E′*) of BSM and control biocomposites at 10 Hz

5.2.6.2 Loss Modulus (*E″*)

The effect of temperature on the loss modulus of the BSM and control composite is shown in Figure 5.9. It was observed that from ambient to approximately 166 °C, the BSM composite had a higher loss modulus than the control composite. Thereafter, there was a crossover of the loss modulus values with BSM biocomposite having a lower modulus. Since loss modulus is often associated with "internal friction" and can be affected by various molecular motions, transitions and morphology [191], the behaviour of the BSM biocomposite can be explained in similar light. It is possible that the bonding between the BSM resin and banana fibres is stronger than the control composite resulting in less internal friction till 166 °C. It appears that thereafter the control biocomposite dissipated more energy than the BSM composite.

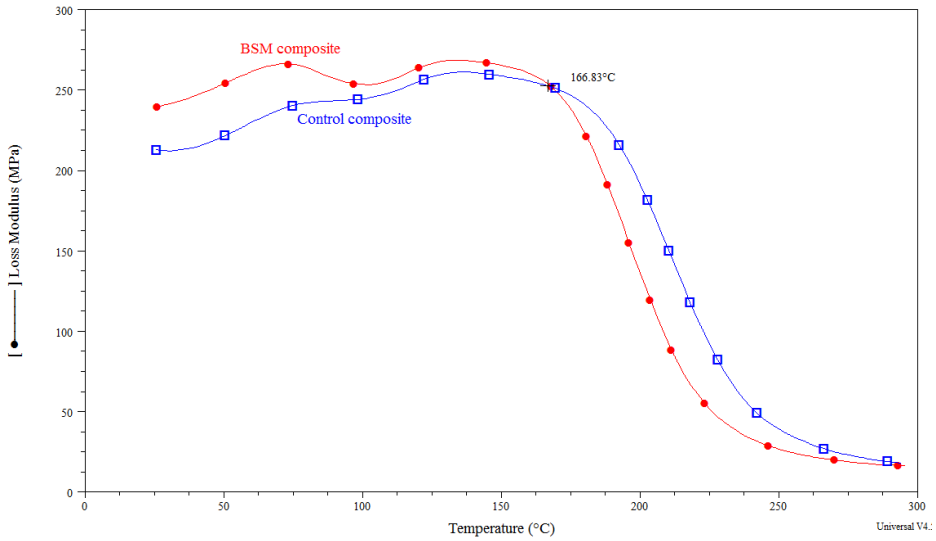

Figure 5.9: Temperature dependence of Loss Modulus for BSM and control biocomposites at 10 Hz

5.2.6.3 Damping Factor (Tan Delta)

The ratio of E' and E'' gives the tangent of the phase angle δ and tan δ is known as the damping that gives the energy dissipation. Figure 5.10 showed that damping of BSM resin and control resin occurred at 184 °C and 196 °C respectively with the BSM biocomposite taking place at a higher amplitude. Martinez-Hernandez *et al.* reported that a weak fibre matrix adhesion will result in higher values of tan δ [192]. When the fibre is strongly bonded to the matrix, the mobility of the polymer chains is lessened thus reducing the damping [193]. Figure 5.10 show that the control and BSM biocomposites had a lower tan δ when compared to the neat BSM resin in Figure 4.24. It was also noted that the BSM composite showed a lower tan δ value than the control composite inferring that BSM resin had better bonding properties than the control resin used in the composite preparation.

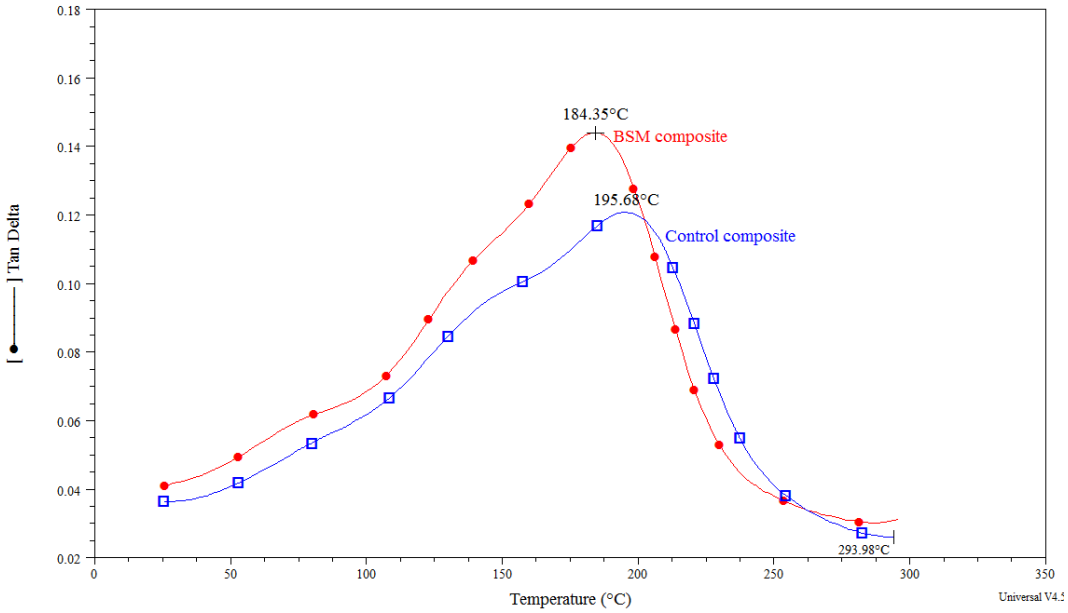

Figure 5. 10: Comparison of tan delta as a function of temperature of BSM and control biocomposite at 10 Hz

5.2.7 Scanning Electron Microscopy (SEM)

Scanning electron microscopy images of the fractured surfaces of the tensile test were taken to study the fracture mechanism of (A) BSM and (B) control specimens shown in Figure 5.11. Figure 5.11A shows that fibre breakage and to a lesser degree fibre pull-out took place with the BSM specimen. However Figure 5.11B showed that the fracture caused the fibres to be pulled out and more holes in the control specimen was observed. Since the matrix and reinforcement were from the same banana plant source greater compatibility was expected. It appears that the BSM bio-resin and fibre were well bonded compared to the control specimen. When the adhesion is poor and load was applied, the fibres were easily pulled out. Figure 5.11B showed that in the control composite, fibre/matrix debonding was evident because the fibre was not well-bonded to the control resin. It is suggested that to improve the fibre/matrix bonding, the fibre should be chemically treated. To study the fibre/matrix interface, fibre pull-out test was necessary.

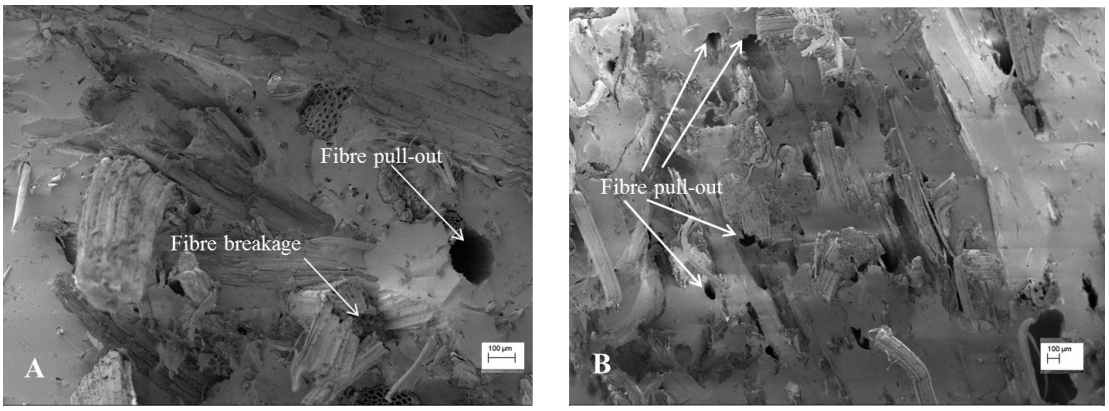

Figure 5.11: SEM images of tensile fracture surface of (A) BSM biocomposite and (B) control biocomposite (200 X magnification)

5.2.8 Fibre pull-out tests

The interface between the fibre and the matrix often significantly influences the composite performance in all types of composites [194]. Furthermore the interfacial properties play an important role in fracture mechanism and toughness of the composite [194]. Fibre pull-out test was done to quantify the interface strength between the fibre and the matrix. In this test the fibres which were embedded in the resin were pulled in the tensile mode. Fibre breakage is indicative of good fibre/matrix adhesion. Figure 5.12 show a positive correlation between load and extension. The loading of the treated fibres was greater than the untreated fibres. The treated fibres had a stronger bond to the resin than the untreated fibres as shown from the fibre pullout test where the treated fibre snapped at a load of 6.9 N (Figure 5.12) whereas the untreated fibre broke off at 5.6 N. The rough surface improved the adhesion of the fibre to the resin. The single fibre pull-out test has shown that greater interface strength existed between the treated banana fibre and the BSM bio-resin.

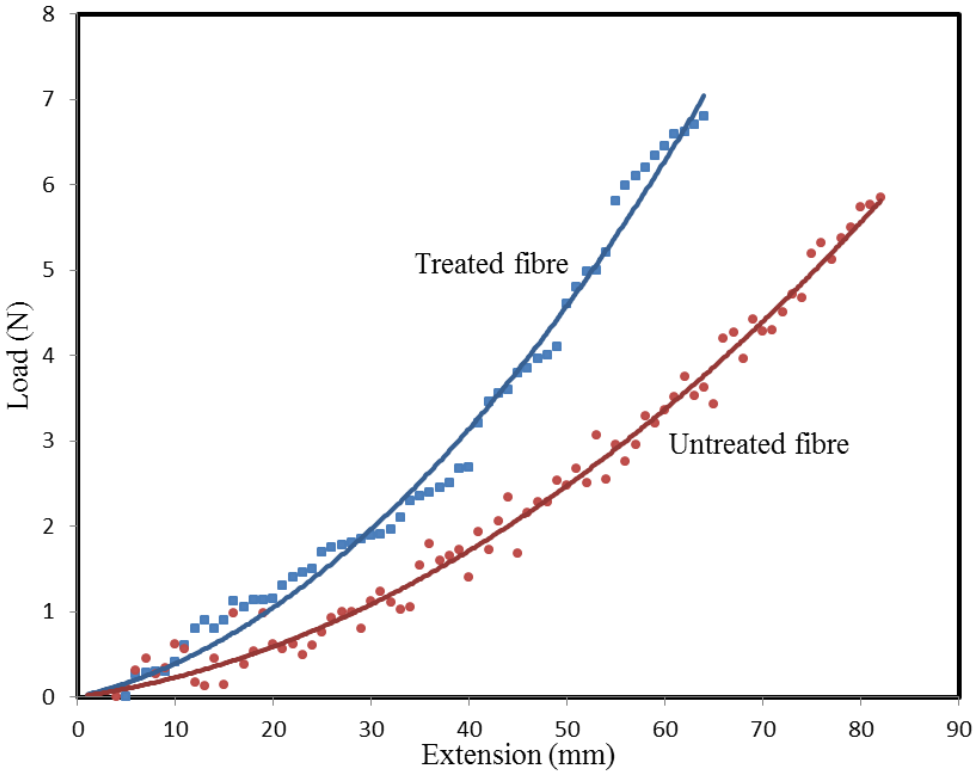

Figure 5.12: Fibre pullout test of treated and untreated fibres

5.2.9 X-Ray Diffraction analysis

Figure 5.13 show the XRD patterns of BSM resin and BSM composite material. Broad XRD peaks indicative of semi- crystalline polymers occurred from 5 to 30°. Thermal analysis confirmed the amorphous/semi crystalline nature of the bio-resin and biocomposite as shown in Tables 4.9 and 5.6. In addition, BSM resin and composite exhibited strong reflections at 22° that is characteristic of 110 plane of face centered cubic (FCC). The BSM composite exhibited a minor reflection at 52° that is characteristic of 320 plane.

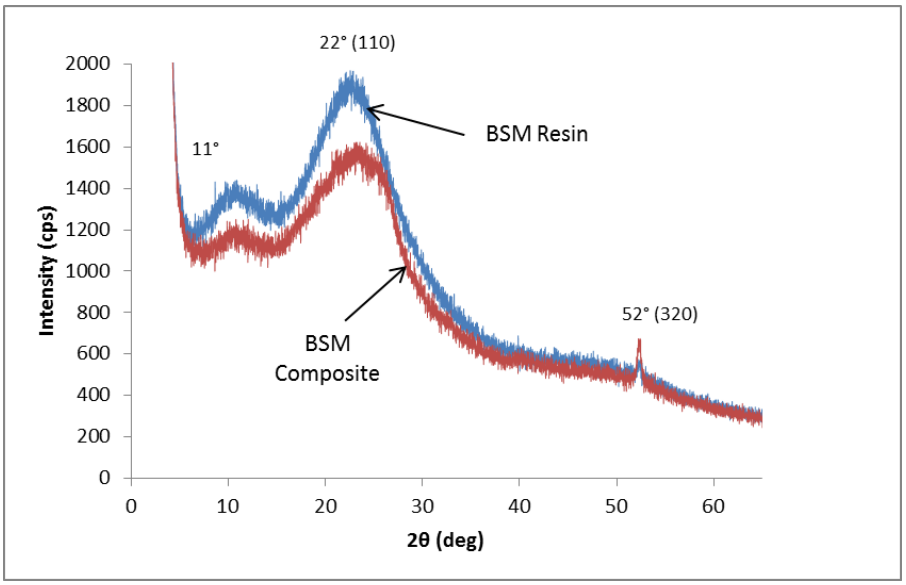

Figure 5.13: X-ray diffraction pattern of BSM resin and BSM composite

The d-spacing of the neat BSM resin and BSM composite calculated from equation 3.1 (Chapter 3) is listed in Table 5.7. The peaks appearing at 3.48 ° corresponded to the neat BSM resin with d_{001} = 29.48. In BSM composite sample, the peak shifted to a lower angle (2θ = 3.16, d_{001} = 32.45) suggesting the formation of an intercalated morphology [195]. This intercalation stemmed from the insertion of the banana fibres within the resin.

Table 5.7: Interlayer spacing in the neat BSM and BSM composite

Sample	2θ (°)	*d*-spacing (nm)
Neat BSM	3.48	29.48
BSM composite	3.16	32.45

5.2.10 Mechanical properties of biocomposite

Mechanical properties are an important indicator of a polymeric or composite material's behaviour under loading. In this work, tensile, flexural, impact, creep and fracture behaviour were conducted for BSM and control biocomposites.

Figure 5.14 illustrates the tensile stress-strain curves of the BSM and control biocomposites. The addition of BS to the matrix resulted in an increase in the tensile stress when compared to the control resin. The BSM composite failed at a mean stress value of 26.1± 1.14 MPa while the control specimen failed at 22.2 ± 0.82 MPa. This represents an 18% increase in tensile stress. From Table 5.8A, the value of P=0.04 indicated a significant difference between the BSM and control composite. Furthermore, the mean tensile moduli of the BSM and control composites were 2968 ± 148.3 MPa and 2609 ± 218.2 MPa, respectively, indicating a significant difference between the BSM and control composites. The only difference between these two composite materials is the presence of BS in BSM composite. In a previous paper [164], phenolic compounds were detected in BS that form strong hydrogen bonds [196] and it was proposed that these phenolic compounds attach themselves to the polymer backbone that could contribute to the strength of the material.

The flexural test result is presented in Figure 5.15. The BSM composite has a mean flexural stress value of 32.3 MPa and the control sample at 30.4 MPa resulting in a 6% increase in flexural strength. Statistical analysis showed no significant difference between the two samples (P=0.24). Sapuan and co-workers produced a banana fibre reinforced epoxy biocomposite for household utilities and they reported tensile stress value of 14 MPa and flexural stress of 26 MPa [74]. However the values for flexural strength in this study were higher than those reported by Sapuan. The BS used in the manufacture of the BSM bio-resin imparted improved mechanical properties. This may be due to the strong chemical bond between the fibre and BSM matrix as confirmed with SEM analysis.

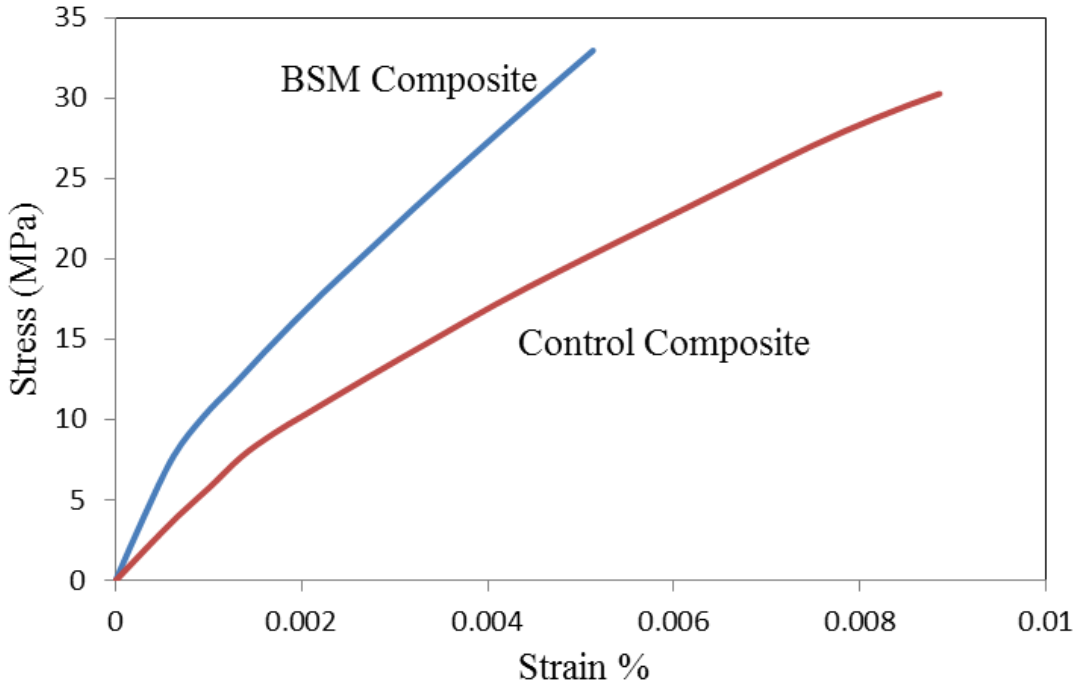

Figure 5.14: Variation of tensile stress as a function of % strain of BSM and control biocomposite

Table 5.8A: Mechanical properties of BSM and control biocomposites at ambient temperature

Mechanical property	**BSM biocomposite** (mean values with SD)	**Control biocomposite** (mean values with SD)	**P** α=0.05
Tensile Strength (MPa)	26.1± 1.14	22.0 ± 0.82	0.04*
Flexural Strength (MPa)	32.3 ± 2.32	30.4 ± 3.5	0.24
Tensile Modulus (MPa)	2968 ± 148.3	2609 ± 218.2	0.04*
Flexural Modulus (MPa)	1994 ± 122	1492 ± 45.2	0.001*

*Denotes significant difference with α=0.05

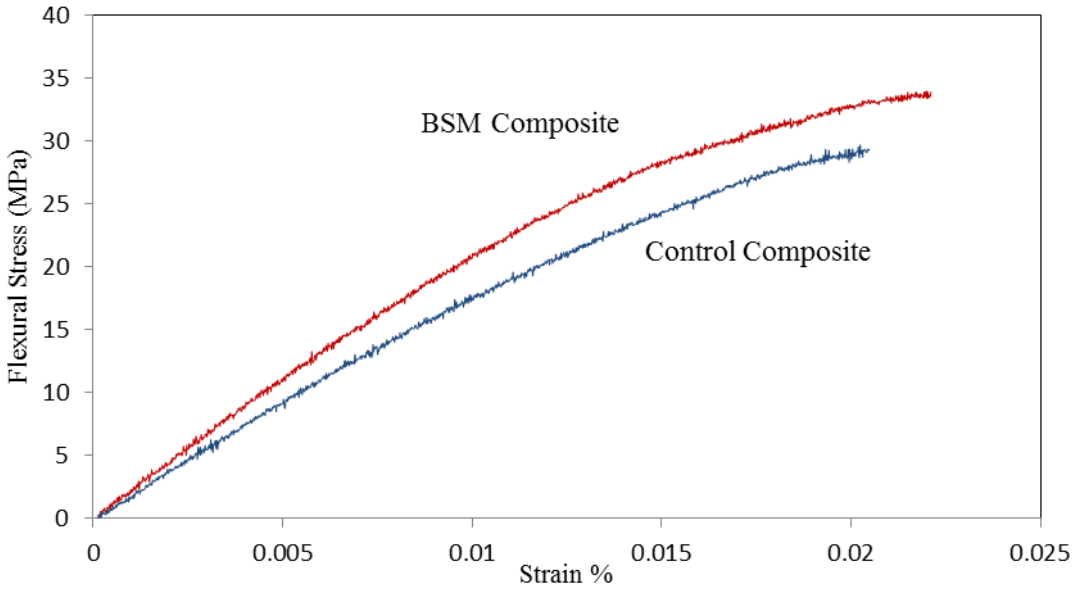

Figure 5.15: Variation of flexural stress as a function of strain of control and BSM biocomposite

5.2.11 Tensile and flexural tests at ambient and elevated temperatures

Table 5.8B shows the mean and standard deviation values of the tensile and flexural properties of the BSM biocomposite at ambient and elevated temperatures. At a 95% confidence interval, the mean and standard deviation of the flexural modulus of BSM composite at ambient temperature was 1994 ± 122 MPa. At 55 ± 5 °C the flexural modulus of the BSM composite decreased to 1557 ± 150 MPa. Similarly, the mean and standard deviation value of the tensile modulus of BSM composite at ambient temperature was 2968 ± 148 MPa. At 55 ± 5 °C, the tensile modulus of the BSM composite decreased to 2413 ± 328 MPa. The P values in Table 5.8B showed the significance difference in the mechanical properties between the BSM composite at ambient and elevated temperatures with $P \leq 0.05$.

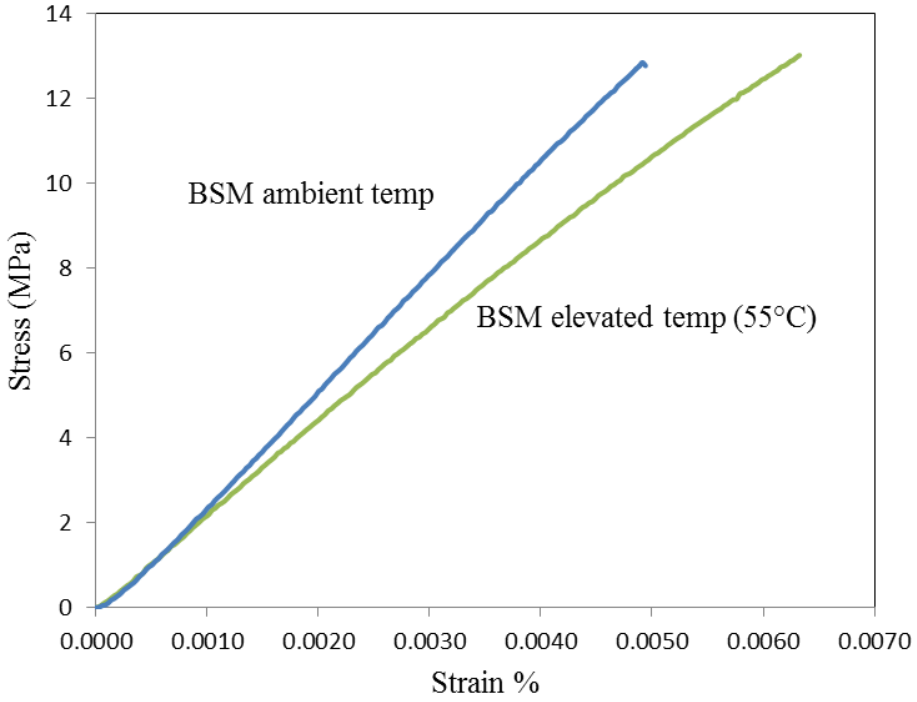

Figure 5.16: Comparison of tensile strength of BSM biocomposite at ambient and elevated temperatures

Table 5.8B: Mechanical properties of BSM composite at ambient and elevated temperature

Mechanical property	**BSM composite** (mean values with SD)	**BSM composite** (mean values with SD)	**P** $\alpha = 0.05$
	Ambient Temp	Elevated Temp (55 ±5 ° C)	
Tensile Strength (MPa)	26.1± 1.14	18.20 ± 1.68 (30% ↓)	0.0005*
Flexural Strength (MPa)	32.3 ± 2.32	22.8 ± 2.42 (29% ↓)	0.006*
Tensile Modulus (MPa)	2968 ± 148.3	2413 ± 328 (19% ↓)	0.02*
Flexural Modulus (MPa)	1994 ± 122	1557.6 ± 150 (22%↓)	0.009*

*Denotes significant difference with α=0.05

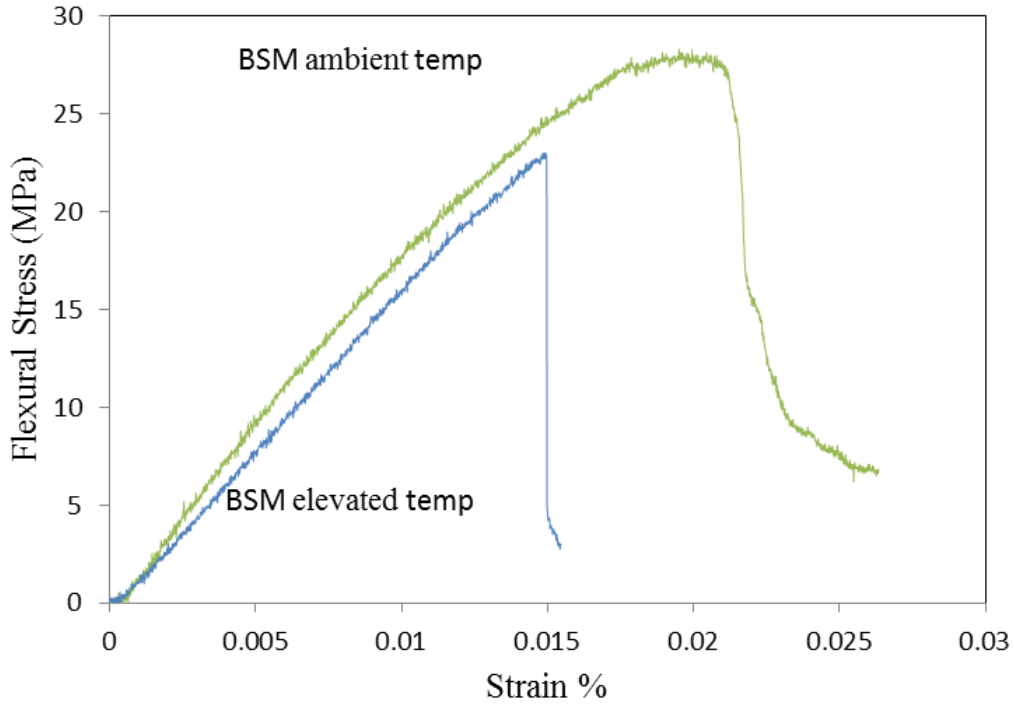

Figure 5.17: Comparison of flexural strength of BSM biocomposite at ambient and elevated temperatures

Figures 5.16 and 5.17 illustrates flexural and tensile properties of the BSM composite material at ambient and elevated temperatures (55 ± 5 °C). The tensile strength decreased from 26.1± 1.14 MPa to 18.20 ± 1.68 MPa. The flexural strength decreased from 32.3 ± 2.32 MPa to 22.8 ± 2.42 MPa. From Table 5.8B significant difference was noted for the tensile and flexural test between the control and BSM composite. Factors such as adhesion at interface between the fibre and the resin, the mechanical properties of the fibre and resin can affect the strength and performance of composite material [197].

5.2.12 Impact tests

Table 5.9 show the energy absorbed by impact of the resins and biocomposite materials. The BSM and control resins shattered on impact and were classed as brittle. As expected the neat resins absorbed lesser energy than the biocomposite specimens since the fibres in the biocomposites were the adsorbents to absorb the impact. On impact 2.37 $J.m^3$ of energy from the drop-weight was transferred to the control biocomposite whereas 2.18 $J.m^3$ was transferred to the BSM biocomposite. Since BSM biocomposite absorbed 9% less energy than the control biocomposite, it was reckoned that the ability of BSM bio-resin to dissipate energy by crack propagation was lower than the control resin. According to the drop-weight impact test, BSM biocomposite had a higher resistance to crack formation (discussed further in section 5.2.13). It was therefore concluded that the interface between the BSM bio-resin and fibre was greater than the control resin and fibre. Impact toughness is significantly affected by molecular weight [101] and is generally increased by higher molecular weights of the polymer. The molecular weights of the BSM and control resins were 2179 and 2114 units respectively suggesting that the polymer network of BSM with a higher molecular weight did not have as much movement thereby concentrating the energy in one area. There was a decreased ability to transfer the energy between the chains hence the impact energy was lower. Stronger bonds impart greater stiffness, hence decreasing the energy required for impact. Figure 5.18 compares the impact indent images of the control and BSM composites.

Table 5.9: Impact energy values of test samples

Sample	Impact ($J.m^3$)
Control Resin	0.75-0.95
BSM Resin	0.71
Control biocomposite	2.37
BSM biocomposite	2.18

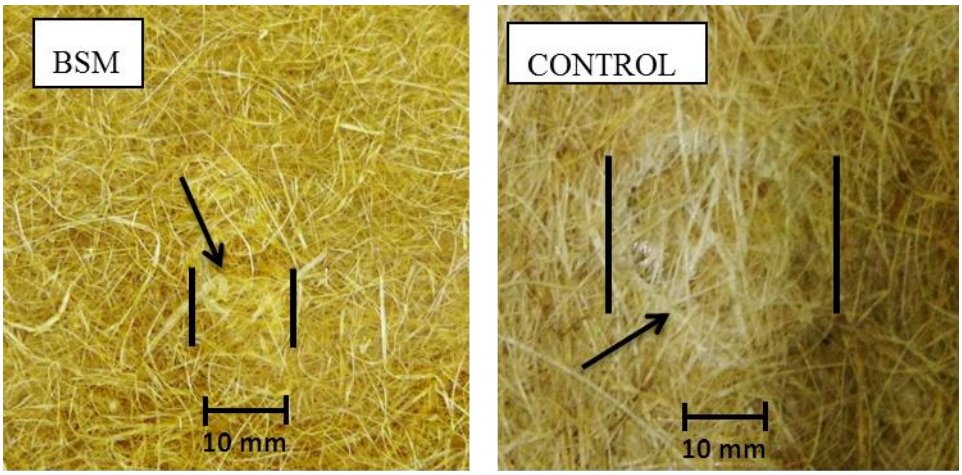

Figure 5.18: Images of impact damage observed for biocomposites impacted by drop weight

5.2.13 Fracture toughness of biocomposite material

5.2.13.1 Single edge notch beam test

Four layers of banana fibres were used for the infusions of the control resin and the BSM resins. Samples were cut according to ASTM D 5045[10] specifications [198]. The samples were marked for measurement of the crack length. The crack length measured as a function of time was video recorded to capture the crack growth. Figure 5.19 shows the image of the crack length initiated by crack growth beneath the loading of 1kN. The crack initiated directly beneath the loading point, which was typical of Mode 1 crack.

[10] ASTM D5045 test method for Fracture Toughness and Strain Energy Release Rate of Plastic Materials

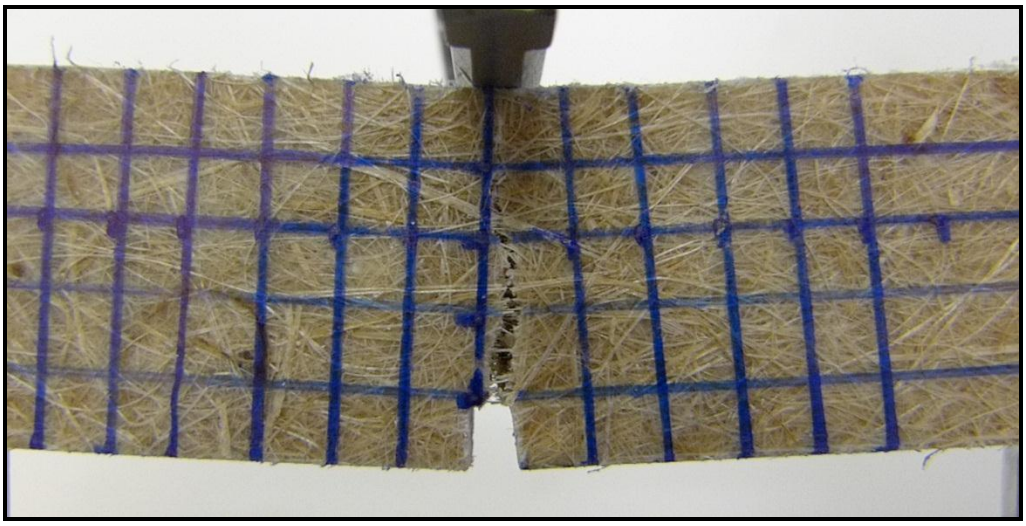

Figure 5. 19: Image of BSM biocomposite showing crack growth

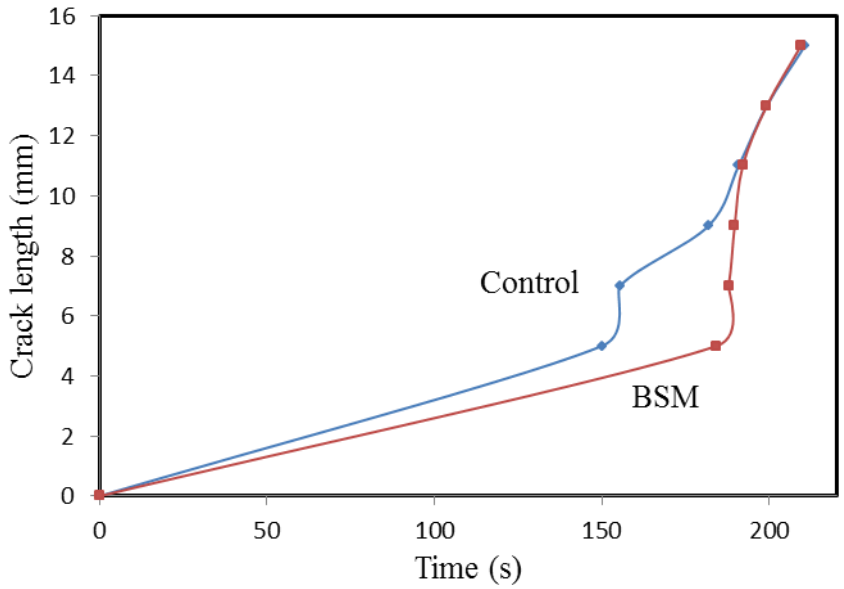

Figure 5.20: Time dependence on crack length of control and BSM biocomposites

Figure 5.20 shows the crack length formation as a function of time. Crack initiation of the BSM biocomposite commenced at 184 seconds compared to 150 seconds for the control composite. This delay in time was accounted for by a stronger bond between the BSM bio-resin/ fibre interface than the control resin/fibre. It was also shown in the impact studies in section 5.2.13 that the ability of BSM bio-resin to

dissipate energy by crack propagation was lower than the control resin. BSM showed a linear increase of crack length with time. However, at around 150 s the crack length of the control biocomposite was constant. There could have been bundles of fibres attached to the resin that took a longer time for the crack to grow. It was also important to note that these were random fibres and the propagation of the crack had least resistance. Likewise, the addition of banana fibre content increased the possibility of fibre agglomeration, which created regions of stress concentration that required less energy to elongate the crack propagation [199].

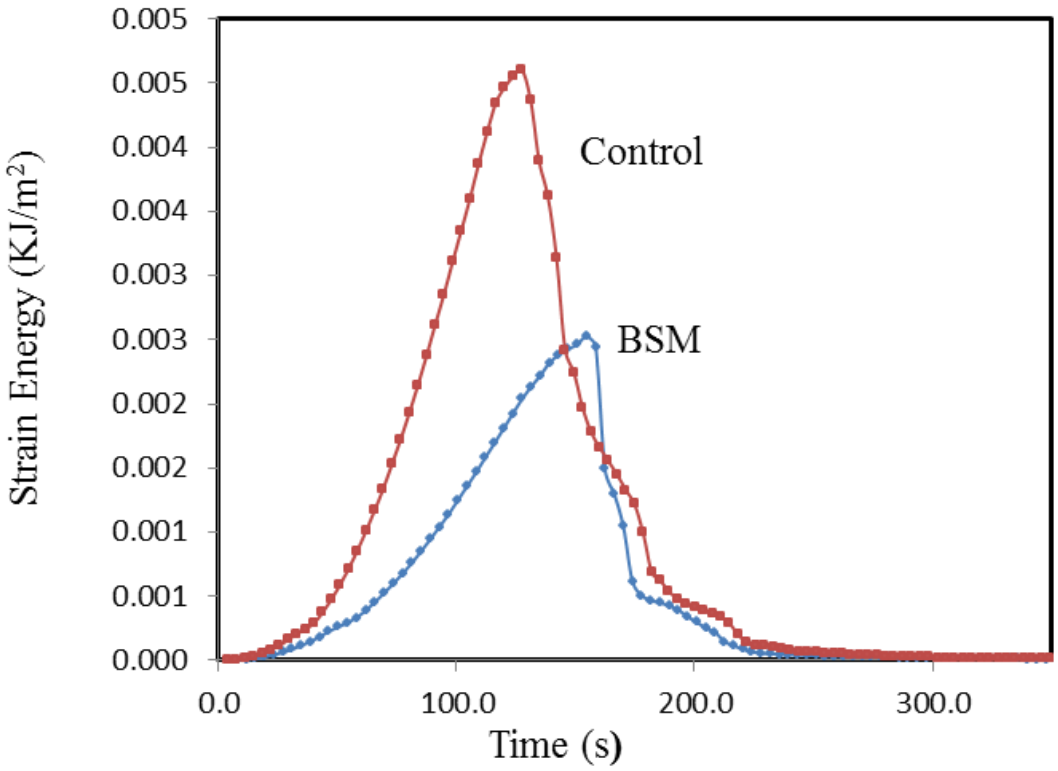

Figure 5.21: Strain energy versus time of Control and BSM biocomposite

Figure 5.21 compares the strain energy of the BSM and control composites calculated using equation 3.5. An increase in the strength and the modulus resulted in a decrease in the fracture toughness of the BSM composite. As the modulus increased, the strain energy decreased which was related to fracture toughness.

5.2.14 Creep tests

Creep behaviour of polymer matrix composites is a critical issue for many modern engineering applications such as aerospace, civil engineering and automotive components [200]. DMA was a useful apparatus used to predict the creep behaviour of the composites under accelerated conditions. Although DMA predictions were conducted at low stress levels, some qualitative creep level predictions were deduced from this method. Since it was not practical to conduct creep tests for entire lifetime of the material, the creep predictions were attempted by accelerated testing. The procedure used for the tensile creep test was a revised version of the testing procedure used by Goertzen and Kessler [201]. Figure 5.22 compares the creep compliance of BSM and control biocomposites as a function of time. These analyses were conducted over a period of 22 hours and the results were analysed using the TA Universal software. It was noted that the creep compliance of BSM biocomposite gradually increased from approximately 11 hours.

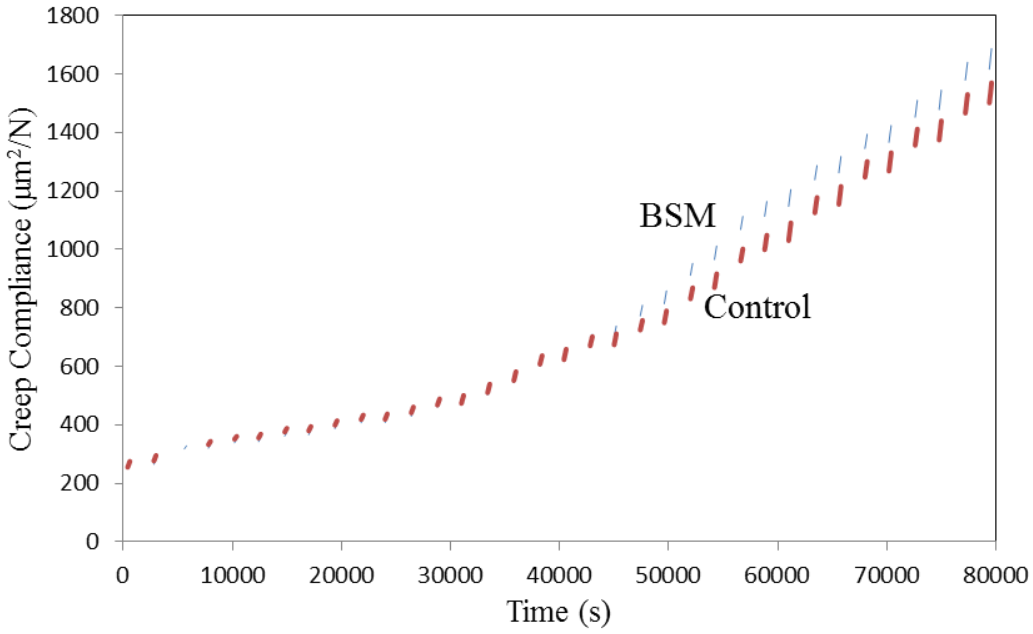

Figure 5.22: Creep compliance of BSM and control biocomposite as a function of time

When the specimens were heated under applied, BSM showed a higher creep than the control biocomposite from 12 hours. Strong explained that transitional

movements occur when atoms move from one place to another in space within the polymer and these movements allow the polymer chain to slowly disentangle and move apart [97]. Similarly, when the biocomposite was subjected to an applied load, the solid polymer slowly began to creep. Molecular weight of the bio-resin can affect the creep resistance of the biocomposite. In this study the molecular weights of BSM bio-resin and the control resin were 2179 $g.mol^{-1}$ and 2114 $g.mol^{-1}$ respectively. Strong also stated that in general, a higher molecular weight increased properties such as creep [97].

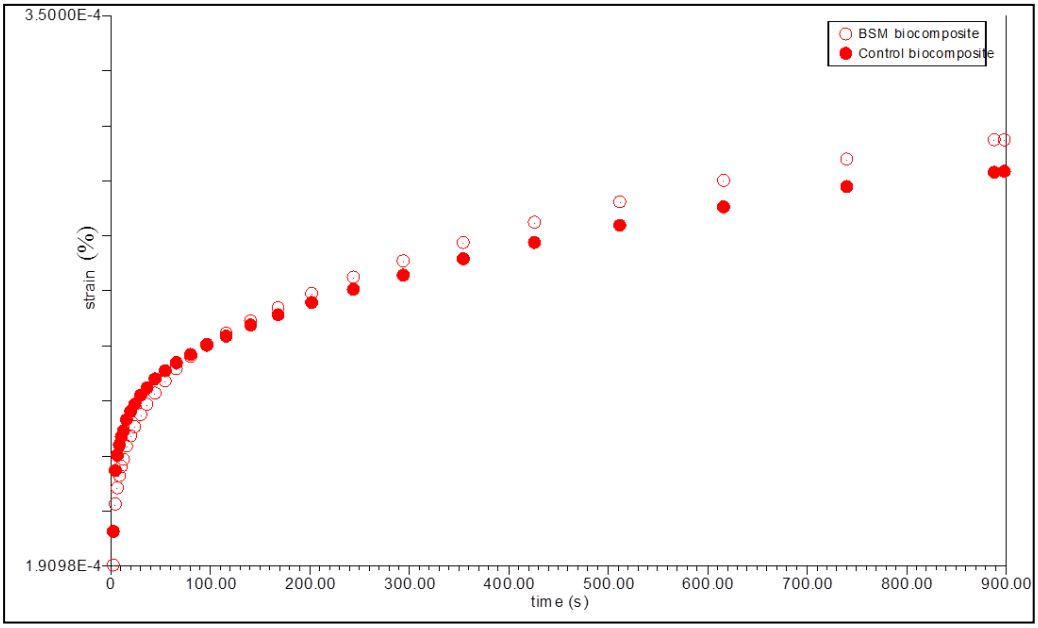

Figure 5. 23: Creep data of BSM and control biocomposites showing increasing creep (strain) as a function of time

Figure 5.23 shows the creep data of percentage strain as a function of time using the Rheology Advantage Data Analysis software where the x-axis showed the time limited to 900 seconds. With an increase in time BSM had a higher creep than the control corresponding to a higher molecular movement within the polymer. Initially the control composite showed better creep resistance; however from 125 °C onwards the BSM composite showed improved creep resistance at higher temperatures. This phenomenon was explained by the limited movement of the molecular chains of the polymer matrix due to the chemical reaction between the BS and maleate resin.

5.3 Nanoclay infusion in resin and biocomposite

Since the biocomposites were not of required strength, it was decided to fortify the resin with nanoclay to improve the strength.

5.3.1 Mechanical analysis

5.3.1.1 Tensile tests

Figure 5.24 show the effect of increasing concentrations of Cloisite 30B on the tensile strength of virgin BSM and the nano-infused BSM specimens.

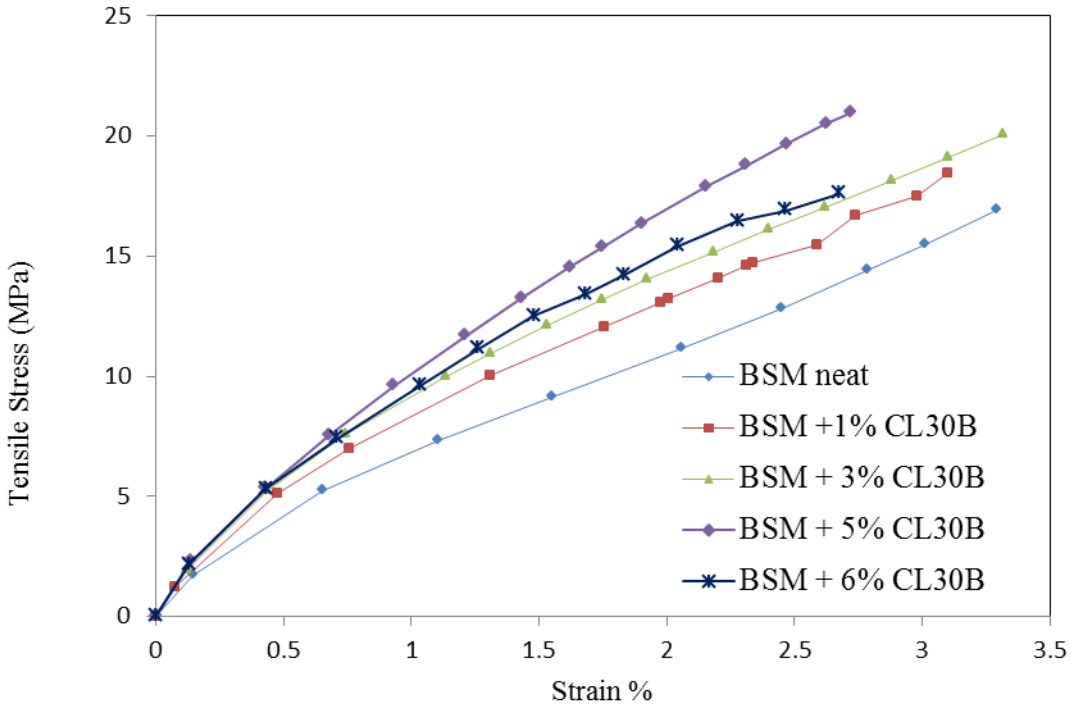

Figure 5.24: Tensile strength of neat BSM resin and BSM nanocomposites infused with different nanoclay weight

An increase in nanoclay concentration in the bio-resin resulted in an increase in stiffness. When 1% clay was added into the resin, the tensile strength increased to 9.2% (18.45 MPa) compared to the neat BSM resin (16.90 MPa). Similarly there was 18.7% and 24.0% increase for 3% and 5% nanoclay infusion, respectively. Incorporation of nanoclays into the polymer led to improved stiffness. Similar

conclusions of nanoclay inclusion leading to improved stiffness-toughness balance were presented by Miyagawa and co-workers [202].

However, as shown in Figure 5.24, further increase in clay content to 6% decreased the tensile strength as the excess clay formed agglomeration sites. Similar findings were reported by Agag *et al.* [203].

5.3.1.2 Flexural tests

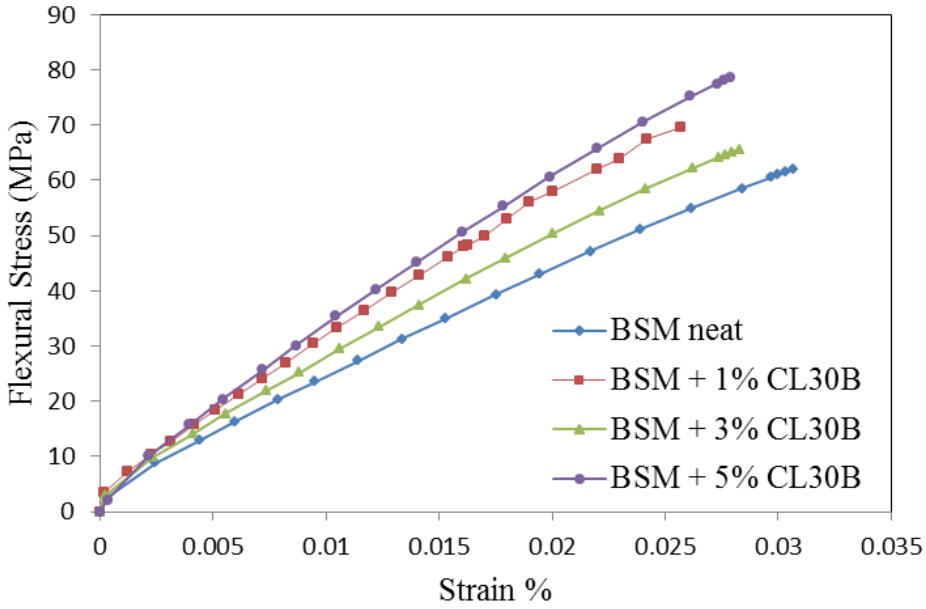

Figure 5. 25: Effect of increasing nanoclay concentration on flexural strength of neat BSM and BSM nanocomposites

Figure 5.25 shows that the flexural properties of the BSM increased with increasing nanoclay concentration. When compared to the neat resin there was a 7% increase in flexural strength with 3% nanoclay, and 28% increase with the 5% nanoclay. Although there was 18% decrease in the flexural strength with the 1% nanoclay, the modulus for all the clay infused samples increased.

5.3.2 Thermal analysis

The thermal behaviour of the bio-resin improved when fortified with increasing amounts of nanoclay. Figure 5.26 show the TGA curves of the onset temperatures of the neat BSM and the nanoclay infused BSM. Tables 5.5 show the increase in degradation temperatures and melt temperatures when increasing amounts of nanoclay were added.

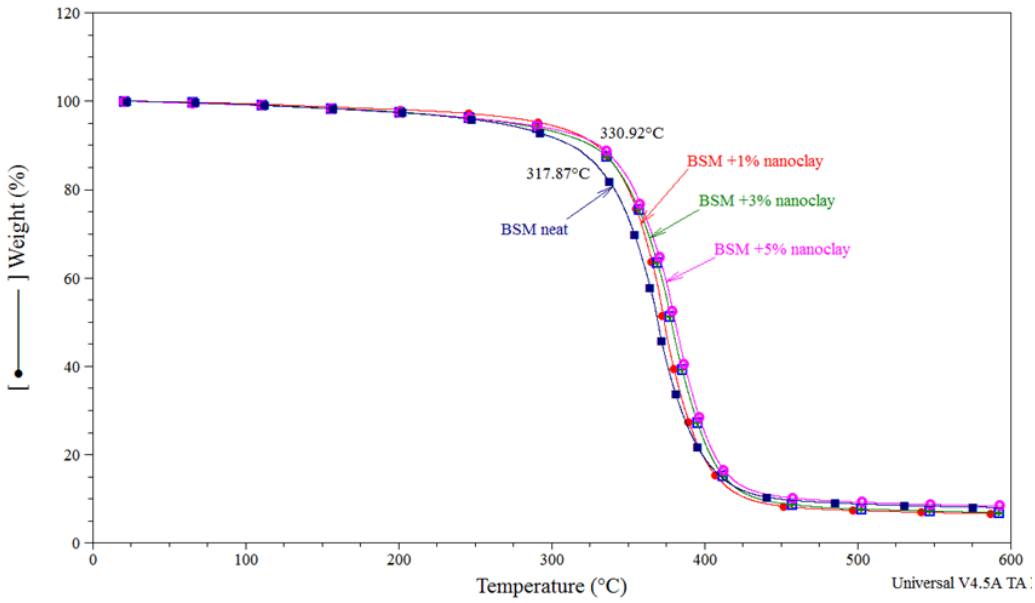

Figure 5.26: The effect of increasing nanoclay concentration on the onset temperature of TGA

Table 5.10: Effect of nanoclay concentration on onset and degradation temperatures

Sample	Onset temp (°C)	T_m (°C)
BSM Neat	318	371
BSM + 1% nanoclay	331	374
BSM + 3% nanoclay	334	380
BSM + 5% nanoclay	336	382

The onset temperature obtained from TGA indicated that decomposition of the bio-resin increased with increasing clay loading when compared to the neat resin. The dispersed clay created a barrier that delayed the release of thermal degradation products when compared to the neat resin as shown by Agag *et al.* [204]. DSC curves (Figure 5.27) provided the degradation temperatures of the blended nanocomposites and the neat resin. An increase in clay content resulted in an increase in degradation temperature.

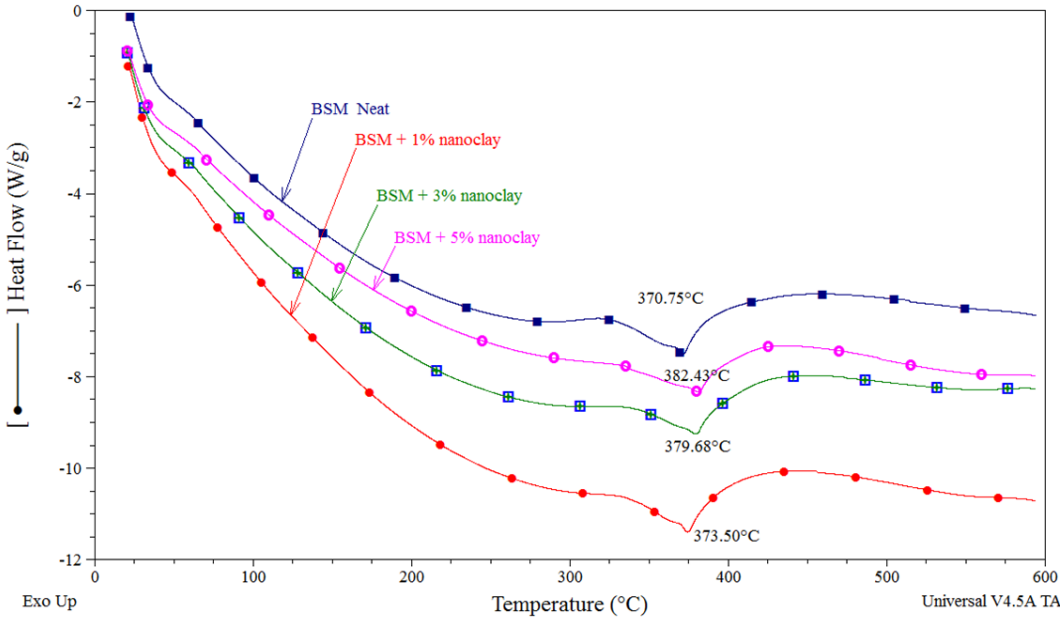

Figure 5.27: The effect of increasing nanoclay concentration on the degradation temperature of the DSC thermograph

5.3.3 Dynamic Mechanical Analysis

A parametric study was done to investigate the effect of adding increasing amounts of nanoclay on the viscoelastic properties of the bio-resin. This section discusses the storage modulus, loss modulus and damping of the BSM bio-resin with nanoclay.

The effect of adding increasing amount of nanoclays on the storage modulus as a function of temperature is shown in Figure 5.28. It is well established that fillers or nanoclays as in this instance, increases the storage modulus [205]. There was an incremental increase in storage moduli from 7320 MPa (neat resin), 7552 MPa (1% clay), 7851 MPa (3% MPa) and 8173 MPa (5% clay). A 12% increase in storage

modulus was noted between the neat BSM and BSM +5% nanoclay. The first change in modulus was related to the relaxation of the amorphous phase (α-phase relaxation). In this state, the glassy state of the amorphous phase goes through its glass transition temperature and there was a sharp drop in modulus [206].

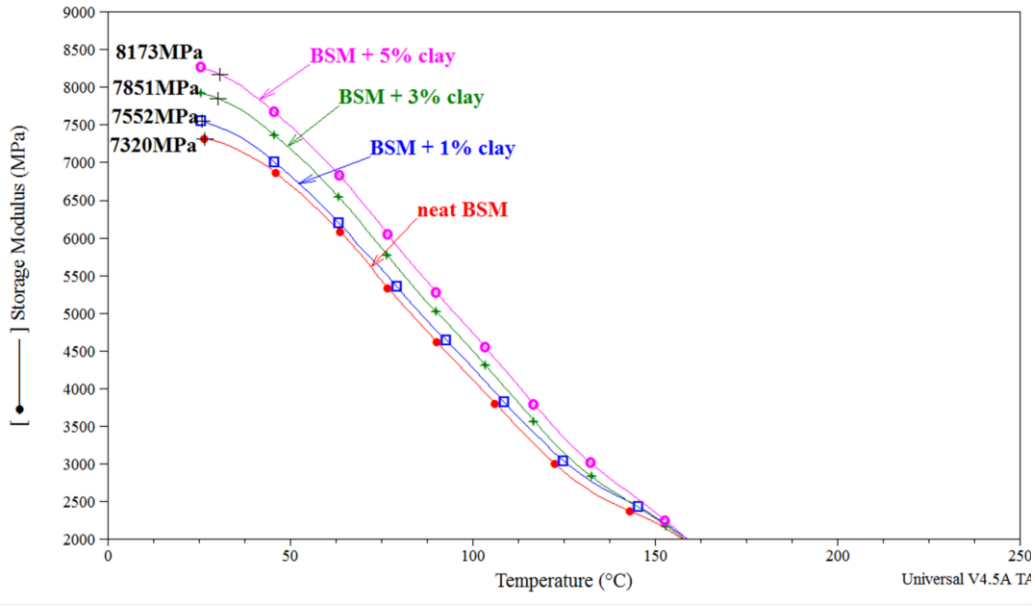

Figure 5.28: The effect of increasing amounts of nanoclay on storage modulus of BSM resin

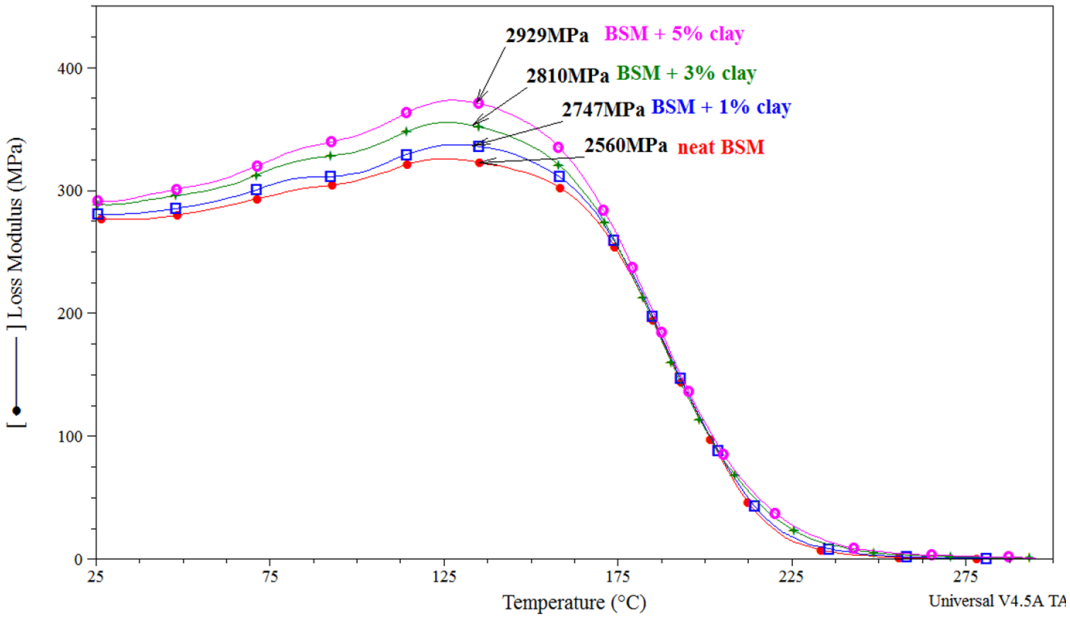

Figure 5. 29: The effect of increasing amounts of nanoclay on loss modulus of BSM bio-resin and nanoclays

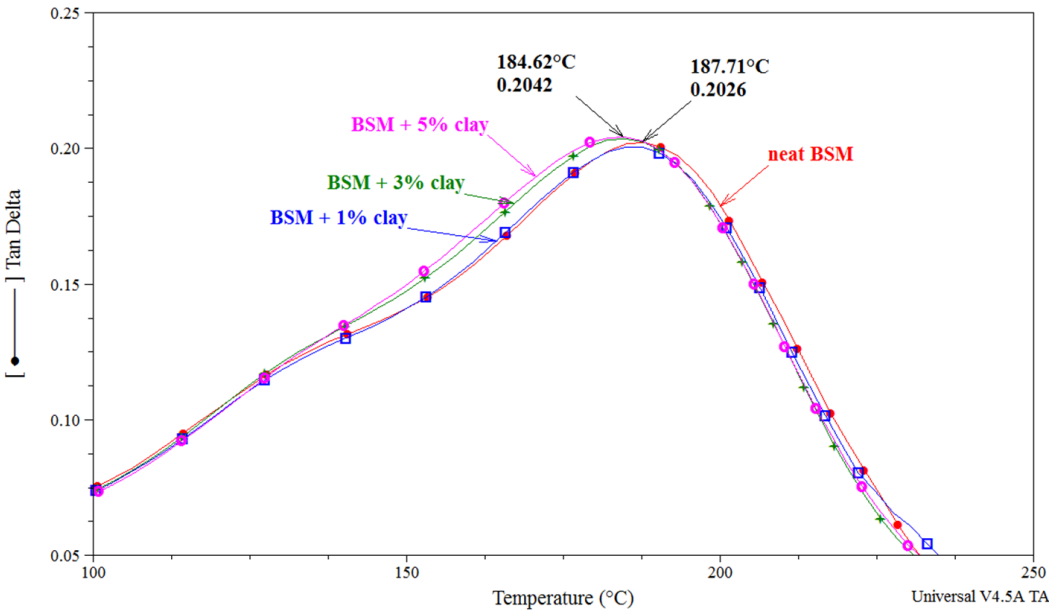

Figure 5.30: The effect of increasing amounts of nanoclay on damping of BSM resin

Figure 5.30 shows the tan delta values of the BSM and BSM with nanoclays and not much variation in results are observed. The T_g temperature was between 184 °C to 187°C with the tan delta maximum between 0.2042 and 0.2026.

5.4 Summary

A new plant based biocomposite was produced using banana fibre and banana sap based bio-resin. Mechanical, chemical, physical and morphological properties of this material were determined. It was shown that the tensile and flexural properties improved by 18% and 6% respectively when compared to a control biocomposite. The fractured surfaces are inspected using the SEM and it was found that in some instances poor adhesion between the fibre and matrix existed evident by the presence of voids or holes. To overcome the fibre pullout from the matrix, it was deemed necessary to chemically treat the fibres for improved adhesion. Consequently the treated fibres showed greater interfacial strength. Stronger bonds between the fibre and resin impart greater stiffness, hence decreasing the energy required for impact.

The lower impact performance of BSM composite could depend on the nature of the constituent and the fibre/matrix interface.

There was an improvement in thermal properties of the BSM biocomposite compared to the control biocomposite. DMA showed the viscoelastic properties of the composite. The increase in storage modulus of the BSM composite indicated enhanced adhesion between the banana fibre and the BSM matrix leading to better stress transfer from matrix to fibre.

In order to improve the strength of the composites, Cloisite 30B nanoclay was added to the resin. Tensile, flexural and thermal degradation properties also improved when the nanoclay was added.

It was suggested that the BSM could be used for non-functional components in the automotive industry but the industry requires that the material degrade after its end of life. The next chapter discusses the biodegradability of the biocomposites and bio-resin.

CHAPTER 6 –RESULTS AND DISCUSSION: BIODEGRADATION STUDIES OF BSM BIO-RESIN AND BIOCOMPOSITE

Introduction

This chapter discusses the biodegradation studies of the BSM bio-resin and biocomposites using soil burial, microbial growth and respirometric testing techniques[11]. The soil burial and microbial growth tests give an indication of the physical and chemical degradation, whereas the respirometric testing quantifies the evolution of CO_2 during biodegradation.

6.1 Results

6.1.1 Soil burial tests

Biodegradability of biocomposites was measured using the soil burial test method as described by Kumar [112]. Table 6.1 shows the percentage mass loss of the control and BSM biocomposite over a 120 day period due to the disintegration that took place in the soil. The mass loss of the control and BSM biocomposites increased with increasing time. Although BSM biocomposite had a higher final mass loss, a lag period was observed between days 30 to 60 for the BSM sample. This could be due to the resin and fibre taking a longer time to disintegrate. The higher weight loss could be attributed to the absorbance of moisture making it more prone to attack by mirco-organisms such as fungi. The average mass loss for the control composite after 120 days was 7.15% ± 0.53 and the BSM composite had a mass loss of 7.12% ± 1.24. At 95 % confidence interval, there was no significant difference ($P = 0.975 > 0.05$) in the mean values.

[11] Extracts from Chapter 6 have been published as "Mechanical, thermal and morphological properties of a bio-based composite derived from banana plant source", Composites Part A 68, (2015), 90-100

Table 6.1: Mass loss of control and BSM biocomposite samples buried in nutrient rich soil

Day	Control biocomposite (% mass loss)	BSM biocomposite (% mass loss)
30	6.1	6.1
60	6.6	6.1
90	6.8	7.1
120	7.5	8.6
Mean	**7.15**	**7.12**
SD	**0.53**	**1.23**

6.1.1.1 Microscopic evaluation of biodegraded samples

Optical light microscopic images were taken to observe the microbial growth of the control and BSM biocomposite samples before and after soil burial as shown in Figure 6.1. From Figure 6.1 it was observed that no fungal growth was visible in the control composite material at day 0 and after 120 days. Although Table 6.1 shows a mass loss for the control sample, no fungal growth was visible. This is suggestive that there was no interaction between the nutrients and microbes in the soil and the control resin.

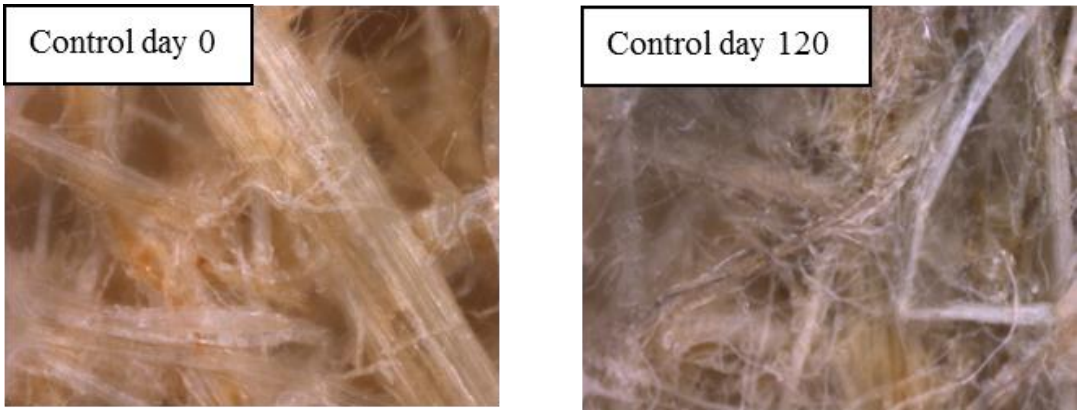

Figure 6.1 : Optical Microscope images of control composite samples on days 0 and 120 with 20 x magnification

Figure 6.2 shows fungal growth of the fibres in the BSM biocomposite at day 30, 60, 90 and 120 indicated by the black growth on the fibres. The one difference between Figure 6.1 and 6.2 is the use of the BSM resin in the latter. It is therefore possible that the micro-organisms attached themselves on the BSM bio-resin and facilitated fungal growth on the fibres. Arutchelvi *et al.* made similar observations suggesting that micro-organisms can attach to the surface of the polymer surface [207].

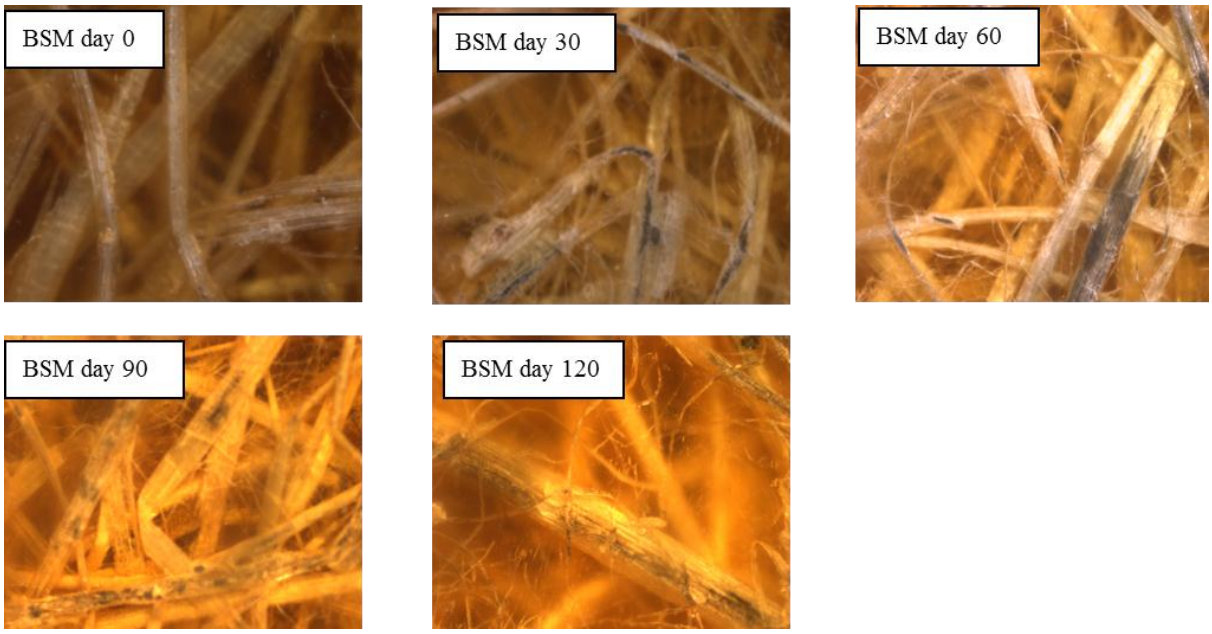

Figure 6.2 : Optical microscope images of BSM biocomposite sample from day 0 to day 120 with 20 x magnification

Burying the BSM composite in soil or placing it in any other natural environment such as lakes or rivers may represent the ideal practical environmental conditions; however there are several shortcomings associated with these types of test. Firstly, environmental conditions such as temperature, pH, or humidity cannot be well controlled; moreover, the analytical opportunities to monitor the degradation process are limited. To address this shortcoming, alternate test methods such as fungal growth test were conducted.

6.1.2 Fungal growth test

The fungal growth test as described in section 3.8.2 was performed in a controlled environment where temperature and humidity were controlled in an incubator.

Observation of the optical images shown in Figure 6.3(A) and (B), the microbial growths of fungal species (*Aspergillus niger*) had been identified on the both control biocomposite and BSM biocomposite. Although both biocomposites supported growth, the BSM biocomposite showed a more concentrated growth than the control sample as seen in Figures 6.3 (A) and (B). Once the organism attached itself to the surface of the composite, it began to grow by using the polymer and the cellulosic fibres as the carbon source as also shown by Arutchelvi *et al.* [207].

However, the fungal species cannot be easily quantified by microbial observation as compared to bacterial species due to the fungal mycelium thickness. Figure 6.3 (A) shows that the BSM biocomposite had a denser fungal growth than the control composite**.** However, attempts were made to measure the growth by dilution plating and measurement of optical density of the suspension culture. Figures 6.4 (A) and (B) showed that the BSM composite had a zone diameter of 14 mm and the Control composite had a zone diameter of 11mm after 72 hours of incubation.

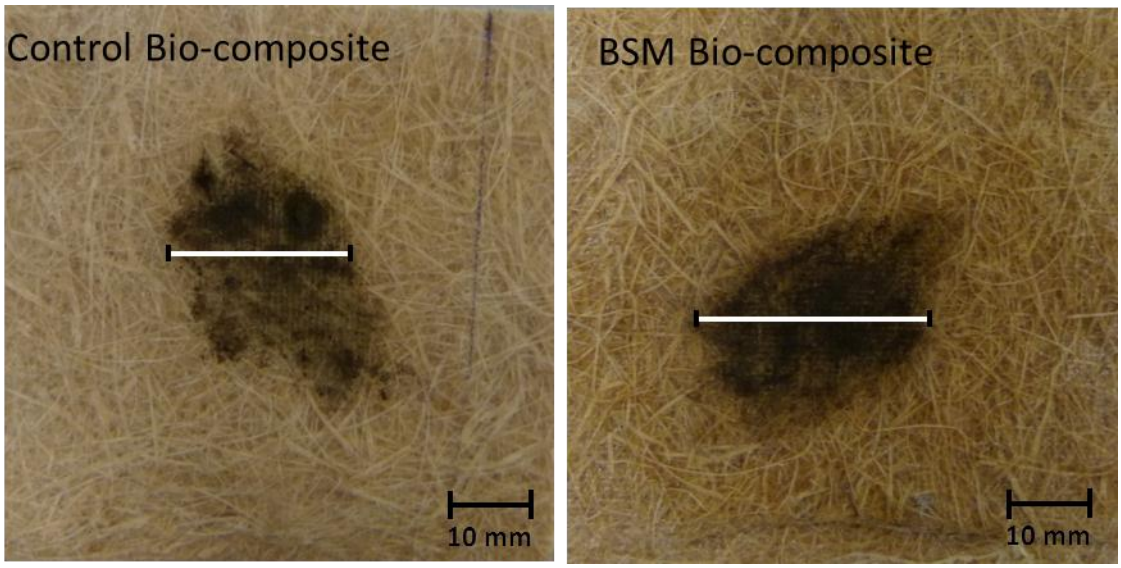

Figure 6.3: Image of *Aspergillus niger* growth on (A) control biocomposite and (B) BSM biocomposite sample

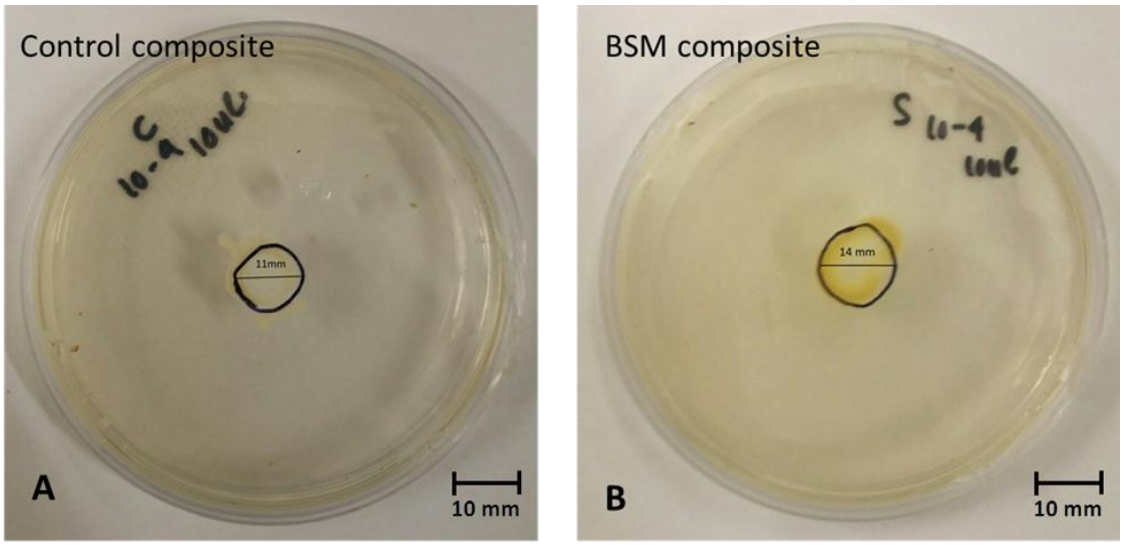

Figure 6.4: Image of zone diameter of growth measurement of dilution plating of fungal growth on control composite and BSM composite

Optical density measurements by UV/visible spectroscopy of the diluted culture suspensions of the BSM composite showed an absorbance value of 1.51 absorbance units whereas the control sample had an absorbance value of 1.29.

From the zone diameter measurements of the microbial growth and the optical density measurements, BSM composite supported more microbial growth than the control sample.

6.1.3 Respirometric tests

The respirometric test was conducted according to ASTM D5338 to determine the cumulative measurement of CO_2 emission by acid-base titration. Aerobic biodegradation of the BSM composite materials was carried out for a 55 day incubation period under composting conditions. The amount of CO_2 emitted (average of three samples) was plotted against incubation time as shown in Figure 6.5.

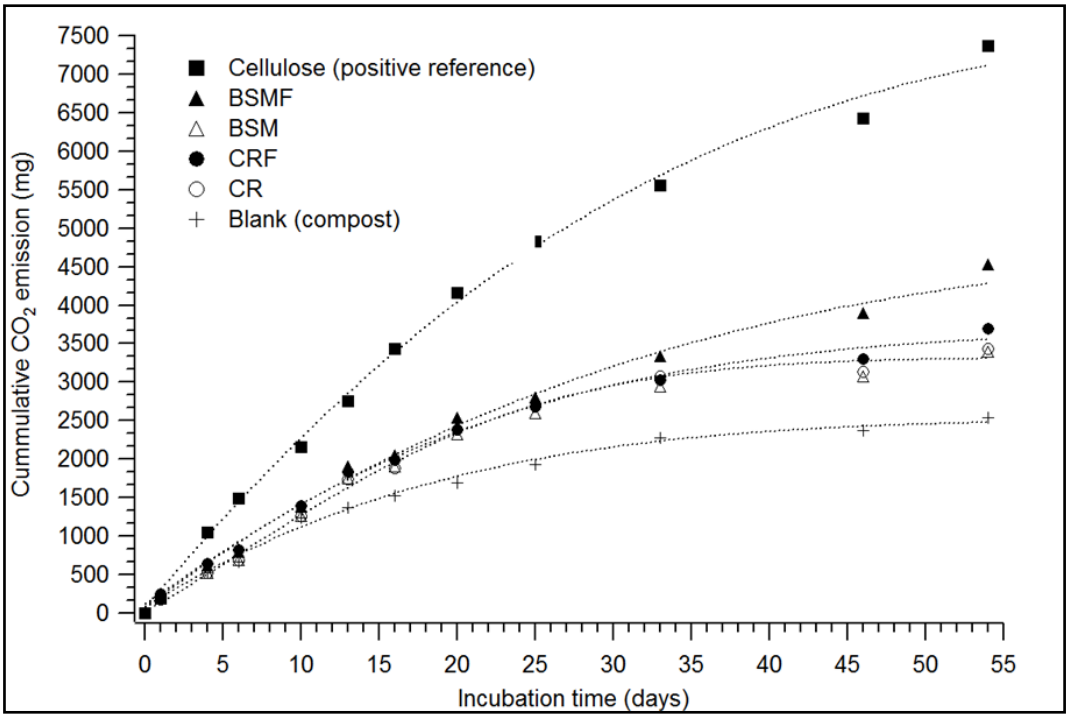

Figure 6.5: CO_2 emission of BSM composite and control resin samples

Figure 6.5 illustrated that all the samples as described in Table 3.7 had a lower rate of biodegradability compared to cellulose, used as a positive reference material described in section 3.8.3. BSMF biocomposite showed an increase of biodegradability compared to BSM, CR and CRF. A further illustration was made in Figure 6.6 to show the comparison of the CO_2 emission between the BSMF and CRF. The BSMF and CRF emitted CO_2 during the biodegradation process. However, it was noticed that from day 13, more CO_2 was emitted from the BSMF than CRF. Furthermore, from day 33 a significant difference in CO_2 emission was noticed. A two-tailed test revealed a P value of 0.0462. P values < 0.05 are deemed significant therefore, BSMF was significantly different from CRF. It is obvious that the banana fibres will degrade to a greater extent, however it can be further explained that the fructose and glucose from the BS cross-linked with the polymer backbone as shown in Figure 4.4 and 4.5 contributed to the increased biodegradation of the biocomposite. Similarly, Singh and co-workers concluded that by attaching sugars to non-degradable hydrocarbon polymers encouraged biodegradation by bacteria and fungi [41].

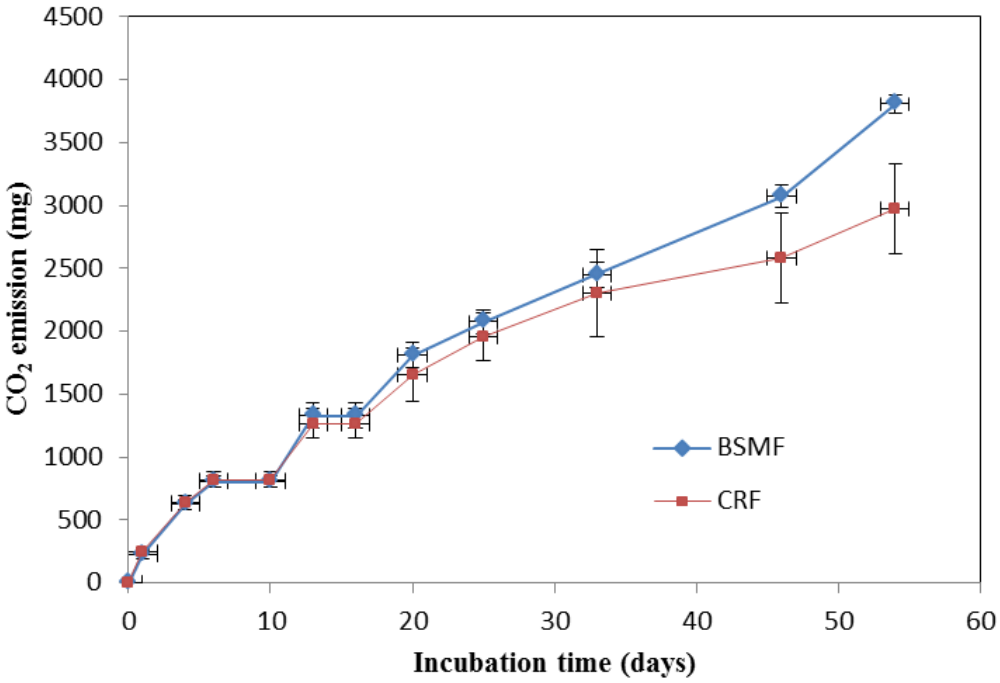

Figure 6.6: CO_2 emission of the BSMF compared to CRF after 13 days of incubation

Generally, compost is a heterogeneous substance with various carbon sources and the degradation of polymeric intermediate products cannot be determined with sufficient accuracy. As a consequence, carbon mass balance can be only guaranteed to assess the ultimate biodegradation, namely plastic carbon to carbon dioxide is measured (CO_2 = C plastic). The percentage of biodegradation can be calculated from the difference to the initial carbon and as per Equation 3.16 in Chapter 3.

Table 6.2 shows the percentage biodegradation of BSM biocomposite and test samples described in Table 3.7 in Chapter 3 that were studied in the compost medium.

Table 6.2: Biodegradability of composites and test materials

Sample	Carbon (% m/m)	Carbon (mg)	$ThCO_2$ (mg)	Biodegradation (%)
Cellulose	42.30	2117.1	7762.7	62.2
BSMF	61.32	3084.6	11310.2	17.6
BSM	65.49	3285.2	12045.7	7.1
CRF	60.17	3015.1	11055.4	8.1
CR	66.16	3311.1	12140.8	7.3

BSMF, BSM, CRF and CR showed 17.6%, 7.1%, 8.1% and 7.3% biodegradation respectively. Moreover cellulose, which was used a reference, showed 62.2% biodegradation suggesting that the conditions such as temperature and humidity of the compost inoculum were suitable to test biodegradation of plastic materials. On the other hand, the slow degradation that occurred for BSM biocomposite could be due to the biocomposite structure, the lack of chemical interaction and cross-linked nature of BSM materials, where it was difficult for the microorganism to breakdown the polymeric chains. Particularly, BSMF showed an exponential increase, which suggested that the BSM matrix degraded more effectively and at a faster rate compared to CRF that did not have banana sap in the formulation.

After 55 days of incubation a known amount of sample was recovered from respective test flasks to measure the structural and thermal properties of test materials. The recovered samples were further washed with deionized water and dried in oven at 40°C for 4 hours and analyzed using TGA, DSC, FTIR and SEM techniques.

6.1.3.1 Thermal analysis

Figure 6.7 shows the thermal degradation of the BSMF before and after composting at 55 days. The TGA showed that the biodegradation of BSMF showed a decrease in the thermal stability. The onset temperature and percentage mass loss decreased.

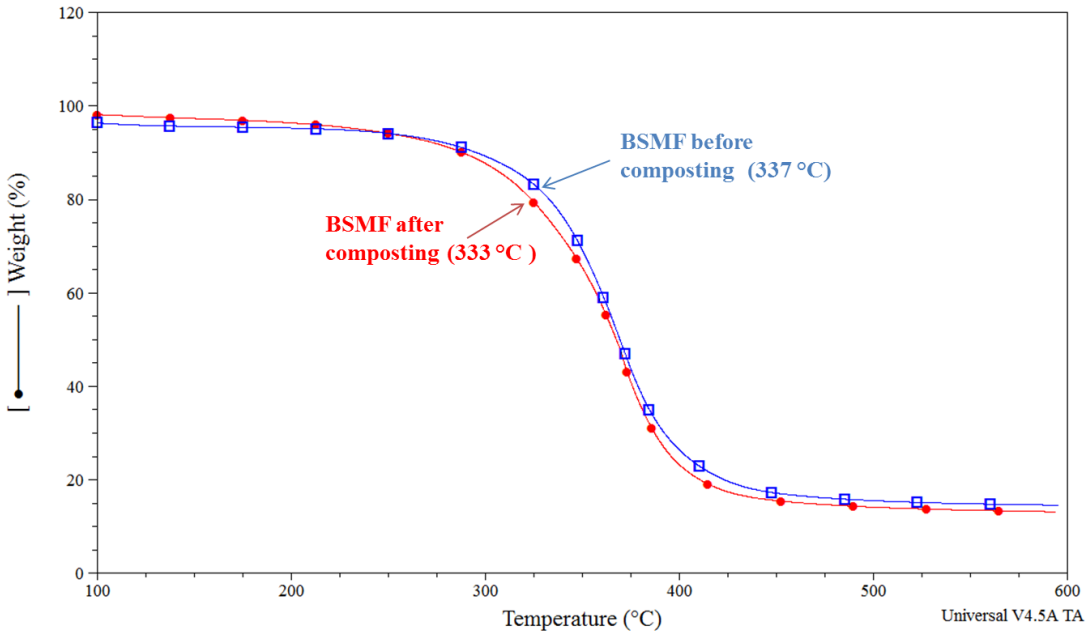

Figure 6.7: A comparison of the mass loss observed between the BSMF before and after composting showing the onset degradation temperatures

Table 6.3: T_m, enthalpy, crystallinity, onset temperature and percentage residue of the samples at day 0 and day 55

Thermal Properties	BSM	BSMF	CR	CRF
T_m (°C)[a]	371	373	379	378
T_m (°C)[b]	363	371	378	365
Enthalpy (ΔH) (J/g) [a]	208	134	152	98
Enthalpy (ΔH) (J/g) [b]	204	81	137	53
Crystallinity (%)[a]	53	58	45	44
Crystallinity (%)[b]	52	39	40	40
T onset (°C) [a]	345	337	352	346
T onset (°C) [b]	343	333	358	330
(%) Residue at 600°C [a]	11	16	6	14
(%) Residue at 600°C [b]	16	17	13	16

[a] day 0 [b] day 55

The melting temperatures (T_m), enthalpy (ΔH), corresponding crystallinity, onset degradation temperature and percentage residue observed in the TG and DSC scans for the resin and biocomposites at the initial and final composting times are presented in Table 6.3. The T_m and ΔH for all the samples decreased with composting time. The percent crystallinity was calculated based on 140 J/g for a 100 % crystalline polymer (polyethylene terephthalate). After 55 days of composting, crystallinity for BSM decreased from 53% to 52%, for BSMF decreased from 58% to 39%, for CR decreased from 45% to 40% and CRF from 44% to 40%. The decrease in crystallinity could be explained by the microbial attack on the amorphous region of the polymer. Generally a crystalline structure is less susceptible to chemical attack due to the ordered packing which makes penetration of the polymers extremely difficult. An amorphous arrangement is easier to penetrate, due to the disorder in the structure of the compound. In essence if the microbial attack is oxidation then the amorphous region is more susceptible to attack than a crystalline region for the reasons cited above.Similar conclusions were made by Manzur and co-workers where they suggested that microorganisms first attack the amorphous phase and then the crystalline phase [208]. They found that with biodegradation, the onset temperature, melting temperature and crystallinity of LDPE samples decreased.

6.1.3.2 FTIR analysis

Figure 6.8 illustrates the FTIR spectrum of BSMF before and after composting. The initial stage of biodegradation consists of water diffusion into the amorphous region of the polymer followed by hydrolytic scission of the ester bond [209]. Absorption of moisture into the polymer surface was confirmed by the OH peak at 3435 cm^{-1}. The peak at 2950 cm^{-1} which represents the C=C stretch was reduced in intensity after composting as there was degradation of the polymer chain. The C=O ester bond at 1736 cm^{-1} was also reduced in intensity due to the breaking up of the ester bond.

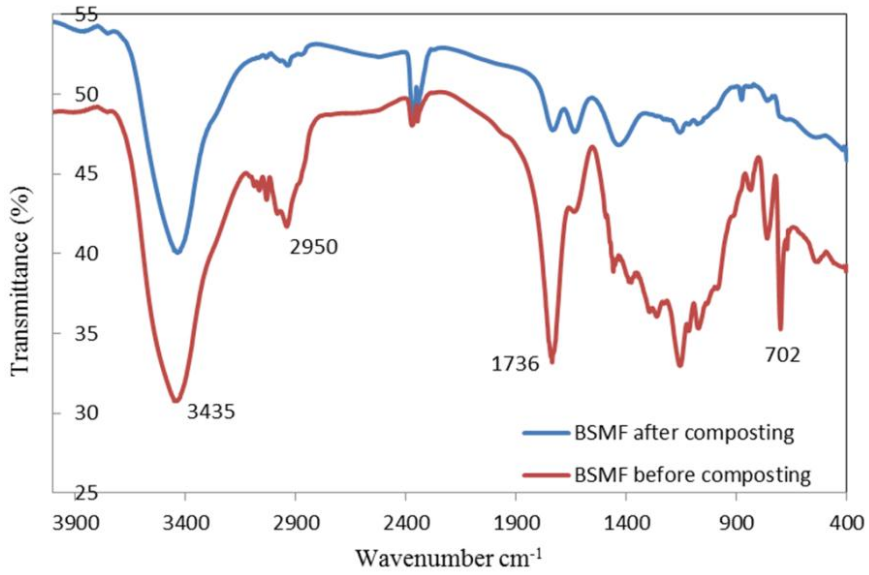

Figure 6.8: FTIR overlay scan showing BSMF before (bottom scan) and after (top scan) composting for 55 days

A possible reaction scheme for the removal of C=O peaks and the formation of CO_2 is shown in Figure 6.9. The reduction in intensity of carbonyl peak at 1735 cm^{-1} was confirmed by FTIR shown in Figure 6.8. The mechanism showed that during biodegradation the removal of the carbonyl functional group and the formation of CO_2 took place. The ester bonds (-O-C=O) are susceptible to attack by the moisture and microbes from the soil. During biodegradation, these bonds break with the release of CO_2.

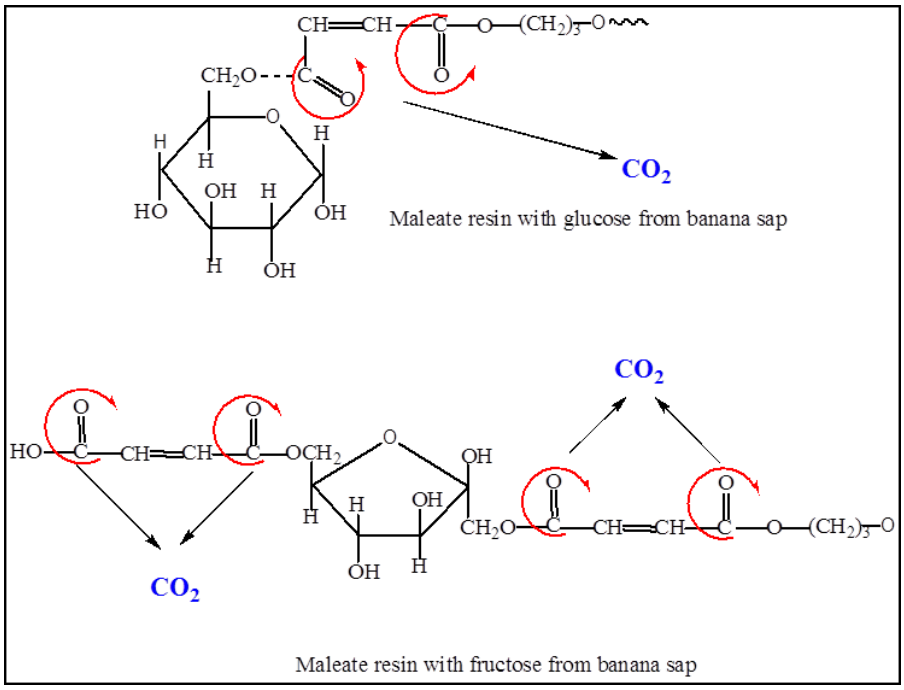

Figure 6.9: Possible reaction scheme for removal of -C=O peaks from the BSM resin and the formation of CO_2

6.1.3.3 SEM analysis

SEM micrographs of the surface characteristics of CR and BSM before and after composting are shown in Figure 6.10. SEM micrographs of CR and BSM before composting referred to as initial in the figure showed smooth surfaces. However, after 55 days of composting, CR showed erosion of the resin surface. The surface of the BSM showed microvoids, cracks and erosion. The surfaces appeared rough and embrittled as the microbes in the soil interacted with the resin and CO_2 was emitted. After biodegradation, the surface became irregular and a large number of pits and roughness appeared.

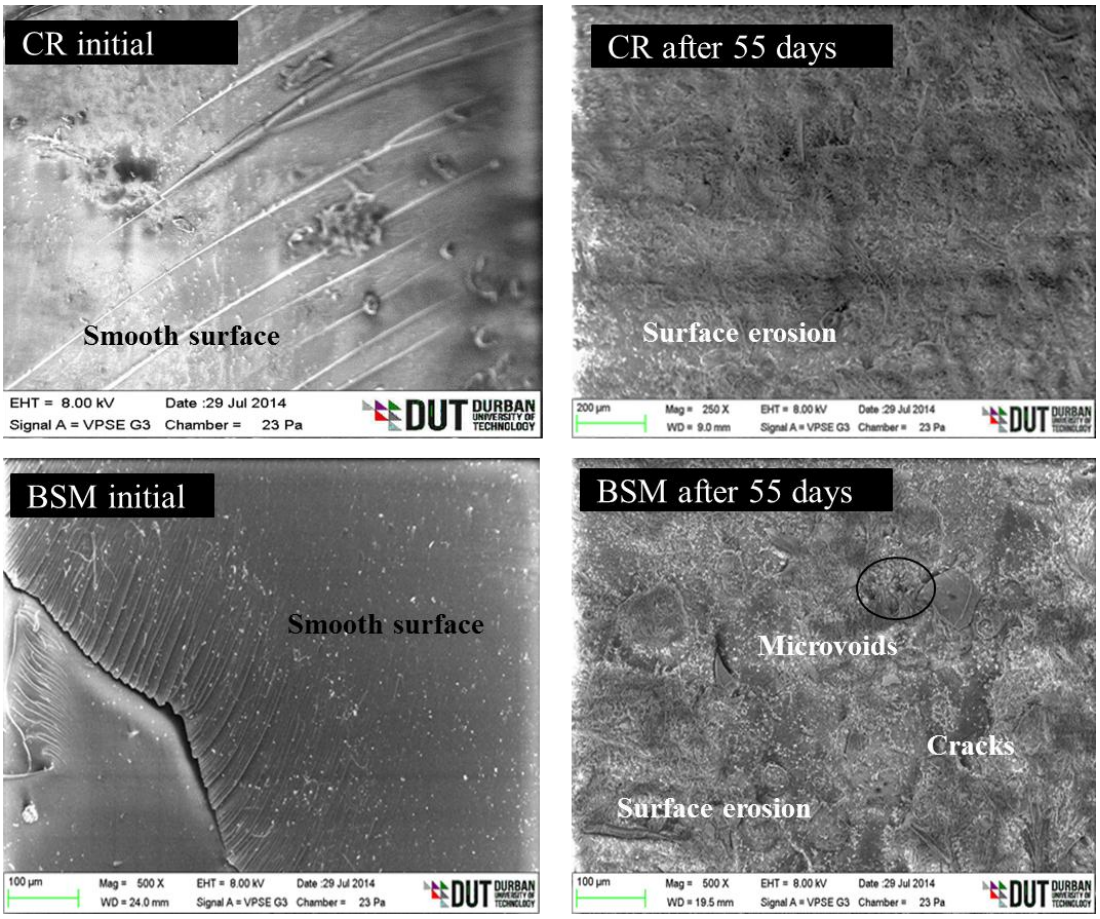

Figure 6.10: SEM images of CR and BSM before and after biodegradation

Figure 6.11 shows the surface morphology of the decomposted BSMF and CRF samples in comparison to the samples before composing. BSMF and CRF showed smooth surfaces at the initial stage. After 55 days of composting, the surface of BSMF and CRF showed erosion as fibres were exposed and the resin was breaking apart. The fibres appeared more exposed due to the microbial attack of resin. The SEM results confirmed that under composting conditions, microorganisms attack the surface of the neat resins and the composites, by illustration of the changes in morphology of the specimens.

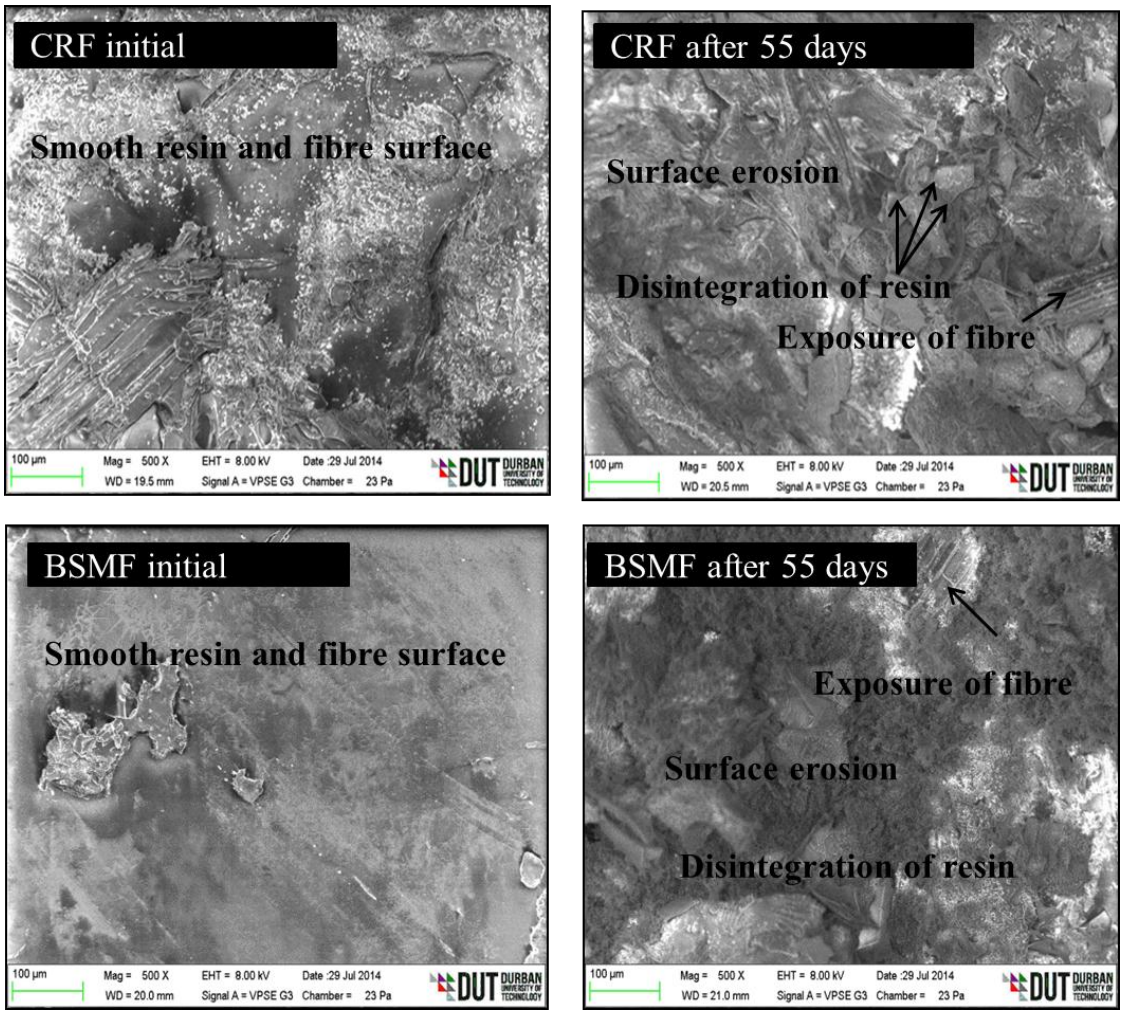

Figure 6.11: SEM images of CRF and BSMF before and after biodegradation

6.2 Summary

Biodegradation assessment of the control resin and biocomposite and the BSM bio-resin and biocomposite was done by three methods namely soil burial, microbial growth measurement and respirometric measurement of CO_2 emission. All three tests were indicative of degradation of the specimens.

Soil burial showed that the moisture from the soil made the conditions favourable for nutrients to be absorbed onto the fibres initiating the degradation of the biocomposite. The mass loss of the BSM biocomposite was 11% more than control sample after 120 days with soil burial.

The fungal species could not be easily quantified due to the fungal mycelium thickness supported by filamentous growth. However the growth was measured by dilution plating and measurement of optical density of the suspension culture. The zone diameters of the BSM and control biocomposites were 14 mm and 11 mm respectively after 72 hours of incubation. The optical densities of the BSM and control biocomposites were 1.51 and 1.29 absorbance units respectively.

The respirometric test method gave a quantification of the CO_2 emitted during the biodegradation period of 55 days. Results indicated that compost microbial systems and conditions provided a very suitable environment for the biodegradation of the BSM biocomposites. A 17.6% biodegradation was noted for BSMF which was 54% more than the CRF indicating that the extent of conversion of organic carbon to CO_2 of the two biocomposites. This conversion resulted in the bio-assimilation of the composite material. The eroded surface morphologies were confirmed by SEM images. The disintegration of the material resulted in a decrease in onset degradation temperatures, melt temperatures and crystallinity confirmed by TGA and DSC results. FTIR confirmed disintegration of the biocomposites by indication of the reduction of intensity of the main functional groups.

Biodegradation of the biocomposites was favoured under suitable conditions such as temperature, humidity, nutrients and micro-organisms in the soil.

CHAPTER 7 - CONCLUSIONS AND RECOMMENDATIONS

Summary

The conclusion of the presented doctoral thesis is summarized in the following items.

A novel bio-resin using banana sap as a precursor, reinforced with banana fibres to produce a biocomposite was successfully synthesized and characterized. In an attempt to address the dire environmental issues, this beneficial product was made from agricultural waste.

The banana sap was used as a precursor to synthesize the hybrid resin, called BSM, which was further characterized for viscosity, acid value, molecular weight, density, gel times, thermal, mechanical and chemical properties. It was concluded that the sugars, particularly fructose and glucose, and organics from the BS may have served as cross-linkers increasing the molecular chain length in the bio-resin formulation, which imparted improved strength to the resin. Furthermore, it was found that improved adhesion between fibre and resin took place when the fibres were chemically treated with alkaline solution.

The biocomposite was characterized for mechanical, thermal, morphological and biodegradation properties. Since this application was for the automotive sector, mechanical tests were conducted at ambient and elevated temperatures and it was found that tensile and flexural properties decreased at elevated temperatures. An increase in the strength and the modulus resulted in a decrease in the fracture toughness of the BSM composite. As the modulus increased, the strain energy decreased which is related to fracture toughness. The fructose and glucose in the banana sap increased the cross-link density impacting on the fracture toughness. Impact properties are considered as an important aspect for the automotive sector. Impact studies showed that the BSM biocomposite had a lower value due to the

stronger bonds within the BSM bio-resin that imparted greater stiffness, hence decreasing the energy required for impact.

On closer investigation of the BSM biocomposite, it was found that the mechanical and thermal properties improved when the bio-resin was fortified with Cloisite 30B nanoclay.

Regarding biodegradability, the biocomposites showed evidence of biodegradation at the end of their lifespan. Soil burial, microbial growth and respirometric testing of CO_2 emission proved that over time degradation of the BSM biocomposite was underway. However, the short-coming of predicting the exact time frame for complete disintegration was still evident.

This work has shown that BS can be effectively used as a precursor in the bio-resin formulation which can be used as a matrix for the synthesis of the bio-composite.

7.1 Recommendations for future work

The accomplishment of this research has brought to fore certain limitations, challenges and consequently opportunities for future research directions. It is expected that by addressing these keys areas, it will help future researchers to realize the goal of producing 100% bio-based bio-composites to be used as functional components in the automotive sector. The following section outlines the recommendations for future research.

7.1.1 Renewable precursors for bio-resin formulation

This research has utilized non-renewable acid and alcohol to form the polyester based bio-resin. To improve the sustainability of the bio-resins, aliphatic polyesters need to replace the aromatic polyesters in the synthetic formulation. Polyesters can

be produced from the poly-condensation of 1,4 butanediol and succinic acid to form poly butyl succinate (PBS) and the banana sap can be incorporated into the poly-condensation reaction. Since very little research has been done in this respect with banana sap, theoretically positive results are expected. Researchers have developed systems to reduce or replace styrene monomers in acrylated biopolymers [210]. However, bio-based monomers for BS based resins also need to be investigated and developed so that styrene emission can be reduced.

7.1.2 Consistent quality of biocomposite/ speed of production

An important concern is the possible variation in quality of the biocomposite due to deficiency of standardized banana fibres. Climatic and geographic conditions have a huge impact on the quality and properties of the fibres. This is a major drawback if the biocomposites are to be used as functional components in the motor vehicle. It is therefore recommended that the fibres of consistent properties of strength and diameter (within 10% standard deviation) be used for the biocomposite.

To use the biocomposite for functional components that are invariably larger in size, the speed of production is a major setback. Vacuum infusion is suitable for smaller components, however for larger parts where high mechanical strength is needed, an alternative method such as sheet moulding compounds (SMC) is recommended.

7.1.3 Fibre-matrix interfacial adhesion of BSM bio-resin and banana fibres

In this research, the fibres were chemically treated with alkaline solution. However, the effect of different fibre treatments should be studied to investigate the improvement of mechanical and chemical properties compared to untreated fibres. The fibre/matrix interface needs to be further investigated to understand the bonding taking place at a molecular level.

7.1.4 Fibre loading in the biocomposite

Since varying the fibre loading was not within the scope of the work it is recommended that various fibre loading be investigated. Varying the distribution of the fibres in the bio-composite production will maximize the databank of mechanical properties and it would give good insight into optimizing loading properties.

7.1.5 Effect of nanoclay in the bio-resin

This work involved the use of Cloisite 30B only. It would be of great interest to obtain a databank of mechanical and chemical properties of the bio-resin with an array of nanoclays.

7.1.6 Biodegradability predictions

Although this study focused on the biodegradability of the bio-composite, it is of greater importance to predict the exact time of disintegration into CO_2, H_2O and cell biomass. Furthermore, a life cycle analysis (LCA) should be conducted to ascertain life-cycle cost, production and transportation of the banana sap and fibres and the end-of-life recyclability. Presently this work is nonexistent for banana sap based polymers and bio-composites, and is a fundamental requirement for commercialization.

REFERENCES

1. Mohanty, A., Misra, M., Drzal, L., Selke, S.E., B.R., H., and Hinrichsen, G., Natural Fibres, Biopolymers and Biocomposites: An Introduction, in Natural Fibers, Biopolymers, and Biocomposites, M.M. Mohanty A, Drzal L, Editor. 2005, Taylor Francis: USA. p. 1-36.
2. Qiu, K., Biobased and biodegradable polymer nanocomposites. 2012, Cornell University.
3. Pothan, L.A., Oommen, Z., and Thomas, S., Dynamic mechanical analysis of banana fiber reinforced polyester composites. Composites Science and Technology, 2003. **63**(2): p. 283-293.
4. Yu, L., Dean, K., and Li, L., Polymer blends and composites from renewable resources. Progress in Polymer Science, 2006. **31**(6): p. 576-602.
5. Alves, C., Ferrão, P., Silva, A., Reis, L., Freitas, M., Rodrigues, L., and Alves, D., Ecodesign of automotive components making use of natural jute fiber composites. Journal of Cleaner Production, 2010. **18**(4): p. 313-327.
6. Holbery, J. and Houston, D., Natural-fiber-reinforced polymer composites in automotive applications. Journal of Minerals & Materials Characterization & Engineering, 2006. **58**(11): p. 80-86.
7. Japan Automobile Recycling Promotion Centre. The authorized automotive recycling coordinator. [online] 2010 [cited 2014.]; Available from: http://www.jarc.or.jp/en/recycling/.
8. Anstey, A., Muniyasamy, S., Reddy, M.M., Misra, M., and Mohanty, A., Processability and Biodegradability Evaluation of Composites from Poly (butylene succinate)(PBS) Bioplastic and Biofuel Co-products from Ontario. Journal of Polymers and the Environment: p. 1-10.
9. Bismarck, A., Baltazar-Y-Jimenez, A., and Sarikakis, K., Green composites as panacea? Socio-economic aspects of green materials. Environment, Development and Sustainability, 2006. **8**(3): p. 445-463.
10. Casado, U., Marcovich, N., Aranguren, M., and Mosiewicki, M., High-strength composites based on tung oil polyurethane and wood flour: Effect of the filler concentration on the mechanical properties. Polymer Engineering & Science, 2009. **49**(4): p. 713-721.
11. Nava, H., Brooks, S., and Skrobacki, T., Soybean based hybrid unsaturated polyester resin system. Technical Paper at Composites, 2010.
12. Guimarães, J.L., Wypych, F., Saul, C.K., Ramos, L.P., and Satyanarayana, K.G., Studies of the processing and characterization of corn starch and its composites with banana and sugarcane fibers from Brazil. Carbohydrate Polymers, 2010. **80**(1): p. 130-138.
13. Miyagawa, H., Mohanty, A.K., Burgueño, R., Drzal, L.T., and Misra, M., Novel biobased resins from blends of functionalized soybean oil and unsaturated polyester resin. Journal of Polymer Science Part B: Polymer Physics, 2007. **45**(6): p. 698-704.

14. Wambua, P., Ivens, J., and Verpoest, I., Natural fibres: can they replace glass in fibre reinforced plastics? Composites Science and Technology, 2003. **63**(9): p. 1259-1264.
15. O'Donnell, A., Dweib, M., and Wool, R., Natural fiber composites with plant oil-based resin. Composites Science and Technology, 2004. **64**(9): p. 1135-1145.
16. Annie Paul, S., Boudenne, A., Ibos, L., Candau, Y., Joseph, K., and Thomas, S., Effect of fiber loading and chemical treatments on thermophysical properties of banana fiber/polypropylene commingled composite materials. Composites Part A Applied Science and Manufacturing, 2008. **39**(9): p. 1582-1588.
17. Bledzki, A.K. and Gassan, J., Composites reinforced with cellulose based fibres. Progress in polymer science, 1999. **24**(2): p. 221-274.
18. Ellison, G., McNaught, R., and Eddleston, E., The use of natural fibres in nonwoven structures for applications as automotive component substrates. Ministry of Agriculture Fisheries and Food., 2000. **26**(04).
19. Gironès, J., Lopez, J.P., Vilaseca, F., Bayer R, J., Herrera-Franco, P.J., and Mutjé, P., Biocomposites from Musa textilis and polypropylene: Evaluation of flexural properties and impact strength. Composites Science and Technology, 2011. **71**(2): p. 122-128.
20. Nayak, S.K., Degradation and flammability behavior of PP/banana and glass fiber-based hybrid composites. International Journal of Plastics Technology, 2009. **13**(1): p. 47-67.
21. Ray, D., Nayak, L., Ammayappan, L., and Nag, D., Energy conservation drives for efficient extraction and utilization of banana fibre. International Journal of Emerging Technology and Advanced Engineering, 2013. **3**(8): p. 296-310.
22. Satyanarayana, K., Sukumaran, K., Kulkarni, A., Pillai, S., and Rohatgi, P., Performance of banana fabric-polyester resin composites, in Composite Structures 2. 1983, Springer. p. 535-548.
23. Pervaiz, M. and Sain, M.M., Carbon storage potential in natural fiber composites. Resources, conservation and Recycling, 2003. **39**(4): p. 325-340.
24. Henton, D.E., Gruber, P., Lunt, J., and Randall, J., Polylactic acid technology, in Natural fibers, biopolymers, and biocomposites, M.M. Mohanty A, Drzal L, Editor. 2005, CRC Press: USA. p. 527-616.
25. Brouwer, W.D. Natural fibre composites in structural components: alternative applications for sisal? [online] 2001 [cited 2013.]; Available from: http://www.fao.org/docrep/004/Y1873E/y1873e0a.htm.
26. Palucka, T. and Bensaude-Vincent, B. Origins of Composites. [online] 2002 [cited July 2014.]; Available from: http://authors.library.caltech.edu/5456/1/hrst.mit.edu/hrs/materials/public/composites/Composites_Overview.htm.
27. Matthews, F. and Rawlings, R., Composite materials: Engineering and science. Vol. 1. 1999, Abington, England: Woodhead Publishing.
28. Karbhari, V.M., Materials considerations in FRP rehabilitation of concrete structures. Journal of materials in civil engineering, 2001. **13**(2): p. 90-97.

29. Mazumdar, S., Composites manufacturing: Materials, Product and Process Engineering. Vol. 1. 2001, Florida, USA: CRC Press.
30. Chung, D., Composite materials for electrical applications, in Composite Materials: Science and Applications. 2003, Springer: London. p. 73-89.
31. Plastic News. Fiber-reinforced plastics use. [online] 2002 [cited August 2014.]; Available from: http://www.plasticsnews.com/article/20020826/FYI/308269999/fiber-reinforced-plastics-use-2002.
32. Thomas, S. and Pothan, L.A., Natural Fibre Reinforced Polymer Composites from Macro to Nanoscale. 2009, USA: Old City Publishers.
33. Plastic News. Plastics demand increasing, but supply outlook still plentiful. [online] 2012 [cited August 2014.]; Available from: http://www.plasticsnews.com/article/20120830/NEWS/308309985/plastics-demand-increasing-but-supply-outlook-still-plentiful.
34. Glenn, G., Holtman, K., Ludvik, C., Chiou, B., Iman, S., Orts, W., and Wood, D., Green composites derived from natural fibres, in Natural Fibre Reinforced Polymer Composites from Macro to Nanscale, S. Thomas and L.A. Pothan, Editors. 2009, Old City Publishing, Inc.: Philadelphia, USA. p. 113-139.
35. Meier, M.A., Metzger, J.O., and Schubert, U.S., Plant oil renewable resources as green alternatives in polymer science. Chemical Society Reviews, 2007. **36**(11): p. 1788-1802.
36. Puglia, D., Biagiotti, J., and Kenny, J., A Review on Natural Fibre-Based Composites—Part II. Journal of Natural Fibers, 2005. **1**(3): p. 23-65.
37. John, M.J. and Thomas, S., Biofibres and biocomposites. Carbohydrate Polymers, 2008. **71**(3): p. 343-364.
38. Indira, K., Parameswaranpillai, J., and Thomas, S., Mechanical Properties and Failure Topography of Banana Fiber PF Macrocomposites Fabricated by RTM and CM Techniques. ISRN Polymer Science, 2013. **2013**.
39. Joseph, S., Sreekala, M.S., Oommen, Z., Koshy, P., and Thomas, S., A comparison of the mechanical properties of phenol formaldehyde composites reinforced with banana fibres and glass fibres. Composites Science and Technology, 2002. **62**(14): p. 1857-1868.
40. Liu, H., Wu, Q., and Zhang, Q., Preparation and properties of banana fiber-reinforced composites based on high density polyethylene (HDPE)/Nylon-6 blends. Bioresource Technology, 2009. **100**(23): p. 6088-6097.
41. Singh, R., Gupta, R., Adsul, M.G., Kuhad, R.C., Gokhale, D.V., and Varma, A.J., Biodegradation of Styrene-Butadiene-Styrene Coploymer via Sugars Attached to the Polymer Chain. Advances in Materials Physics and Chemistry, 2013. **3**: p. 112.
42. Pothan, L.A., Thomas, S., and Neelakantan, N., Short banana fiber reinforced polyester composites: mechanical, failure and aging characteristics. Journal of Reinforced Plastics and Composites, 1997. **16**(8): p. 744-765.
43. Savastano Jr, H., Warden, P., and Coutts, R., Brazilian waste fibres as reinforcement for cement-based composites. Cement and Concrete Composites, 2000. **22**(5): p. 379-384.
44. Majhi, S.K., Nayak, S.K., Mohanty, S., and Unnikrishnan, L., Mechanical and fracture behavior of banana fiber reinforced Polylactic acid

biocomposites. International Journal of Plastics Technology, 2010. **14**: p. 57-75.
45. Doan, T.T.L. and Loan, T., Investigation on jute fibres and their composites based on polypropylene and epoxy matrices. 2006, Disertasi. Vietnam: Fakultat Maschinenwesen der Technischen Universität Dresden. p. 1-126.
46. Peijs, T. Composites turn green. Department of Materials, Queen Mary, University of London [online] 2002 [cited 2014.]; Available from: http://www.e-polymers.org/.
47. Westman, M.P., Fifield, L.S., Simmons, K.L., Laddha, S., and Kafentzis, T.A., Natural Fiber Composites: A Review. 2010: Pacific Northwest National Laboratory.
48. Leao, A.L., Rowell, R., and Tavares, N., Applications of natural fibers in automotive industry in Brazil—thermoforming process, in Science and technology of polymers and advanced materials. 1998, Springer. p. 755-761.
49. Luz, S.M., Caldeira-Pires, A., and Ferrao, P., Environmental benefits of substituting talc by sugarcane bagasse fibers as reinforcement in polypropylene composites: Ecodesign and LCA as strategy for automotive components. Resources, Conservation and Recycling, 2010. **54**(12): p. 1135-1144.
50. Shih, Y.-F. and Huang, C.-C., Polylactic acid (PLA)/banana fiber (BF) biodegradable green composites. Journal of Polymer Research, 2011. **18**(6): p. 2335-2340.
51. El-Meligy, M.G., El-Zawawy, W.K., and Ibrahim, M.M., Lignocellulosic composite. Polymers for advanced technologies, 2004. **15**(12): p. 738-745.
52. Schuh, T.G., Renewable materials for automotive applications. Daimler-Chrysler AG, Stuttgart, 1999.
53. Environment and Plastics Industry Council, Biodegradable polymers: a review. 2000, EPIC.
54. Müller, R.J., Biodegradability of polymers: regulations and methods for testing. Biopolymers Online, 2005.
55. Puechner, P., Mueller, W.-R., and Bardtke, D., Assessing the biodegradation potential of polymers in screening-and long-term test systems. Journal of Environmental Polymer Degradation, 1995. **3**(3): p. 133-143.
56. Hoffmann, J., Řezníčèková, I., Vaňòková, S., and Kupec, J., Manometric determination of biological degradability of substances poorly soluble in aqueous environments. International Biodeterioration & Biodegradation, 1997. **39**(4): p. 327-332.
57. Smith, R., Biodegradable polymers for industrial applications. 2005: CRC Press
58. Gautam, S. Bio-degradable Plastics- Impact on Environment. [online] 2009 [cited September 2013.]; Available from: http://www.cpcb.nic.in/upload/NewItems/NewItem_150_PlasticsWaste.pdf.
59. Francesca Jourdan. The papyrus and its origins. [online] 1999 [cited 2012.]; Available from: http://www.ptahhotep.com/articles/Papyrus.html.
60. Bogoeva-Gaceva, G., Avella, M., Malinconico, M., Buzarovska, A., Grozdanov, A., Gentile, G., and Errico, M.E., Natural fiber eco-composites. Polymer composites, 2007. **28**(1): p. 98-107.

61. Saheb, D.N. and Jog, J., Natural fiber polymer composites: a review. Advances in Polymer Technology, 1999. **18**(4): p. 351-363.
62. Li, X., Tabil, L.G., and Panigrahi, S., Chemical treatments of natural fiber for use in natural fiber-reinforced composites: A review. Journal of Polymers and the Environment, 2007. **15**(1): p. 25-33.
63. Jayaraman, K., Manufacturing sisal–polypropylene composites with minimum fibre degradation. Composites Science and Technology, 2003. **63**(3): p. 367-374.
64. Elanthikkal, S., Gopalakrishnapanicker, U., Varghese, S., and Guthrie, J.T., Cellulose microfibres produced from banana plant wastes: Isolation and characterization. Carbohydrate Polymers, 2010. **80**(3): p. 852-859.
65. Jonas, R. and Farah, L.F., Production and application of microbial cellulose. Polymer Degradation and Stability, 1998. **59**(1): p. 101-106.
66. Heydarzadeh, H., Najafpour, G., and Nazari-Moghaddam, A., Catalyst-free conversion of alkali cellulose to fine carboxymethyl cellulose at mild conditions. World Applied Sciences Journal, 2009. **6**(4): p. 564-569.
67. Nevell, T.P. and Zeronian, S.H., Cellulose chemistry fundamentals, in Cellulose chemistry and its applications, T.P. Nevell and S.H. Zeronian, Editors. 1985, Ellis Horwood Ltd: England. p. 15-30.
68. Herrera, F.P.J. and Valadez-Gonzalez, A., Fibre-matrix adhesion in natural fiber composites, in Natural fibers, biopolymers and biocomposites, M.M. Mohanty A, Drzal L, Editor. 2005, CRC Press, Taylor Francis Group: USA. p. 177-230.
69. Chloe Van. Cellulose. [online] 2010 [cited 2014.]; Available from: https://myorganicchemistry.wikispaces.com/Cellulose.
70. Rong, M.Z., Zhang, M.Q., Liu, Y., Yang, G.C., and Zeng, H.M., The effect of fiber treatment on the mechanical properties of unidirectional sisal-reinforced epoxy composites. Composites Science and Technology, 2001. **61**(10): p. 1437-1447.
71. Joseph, K., Thomas, S., and Pavithran, C., Effect of chemical treatment on the tensile properties of short sisal fibre-reinforced polyethylene composites. Polymer, 1996. **37**(23): p. 5139-5149.
72. Daneel, M., Dillen, N., Husselman, J., De Jager, K., and De Waele, D., Results of a survey on nematodes and diseases of Musa in household gardens in South Africa and Swaziland. InfoMusa, 2003. **12**: p. 8-11.
73. Reddy, N. and Yang, Y., Biofibers from agricultural byproducts for industrial applications. Trends in Biotechnology, 2005. **23**(1): p. 22-27.
74. Sapuan, S., Leenie, A., Harimi, M., and Beng, Y.K., Mechanical properties of woven banana fibre reinforced epoxy composites. Materials and Design, 2006. **27**(8): p. 689-693.
75. Marcovich, N.E., Reboredo, M.M., and Aranguren, M.I., Dependence of the mechanical properties of woodflour–polymer composites on the moisture content. Journal of Applied Polymer Science, 1998. **68**(13): p. 2069-2076.
76. Stark, N., Influence of moisture absorption on mechanical properties of wood flour-polypropylene composites. Journal of Thermoplastic Composite Materials, 2001. **14**(5): p. 421-432.

77. Laine, L. and Rozite, L. Eco-efficient composite materials. [online] 2010 [cited August 2013.]; Available from: http://www.ketek.fi/anacompo/STATE%20OF%20THE%20ART.pdf.
78. George, J., Bhagawan, S., and Thomas, S., Effects of environment on the properties of low-density polyethylene composites reinforced with pineapple-leaf fibre. Composites Science and Technology, 1998. **58**(9): p. 1471-1485.
79. Wang, W., Sain, M., and Cooper, P.A., Study of moisture absorption in natural fiber plastic composites. Composites Science and Technology, 2006. **66**(3-4): p. 379-386.
80. Gassan, J. and Bledzki, A.K., Possibilities for improving the mechanical properties of jute/epoxy composites by alkali treatment of fibres. Composites Science and Technology, 1999. **59**(9): p. 1303-1309.
81. Pothan, L.A., Thomas, S., and Groeninckx, G., The role of fibre/matrix interactions on the dynamic mechanical properties of chemically modified banana fibre/polyester composites. Composites Part A: Applied Science and Manufacturing, 2006. **37**(9): p. 1260-1269.
82. Joshy, M., Isora Fibre Reinforced Polyester and Epoxy Composites, in Faculty of Technology. 2007, Cochin University of Science and Technology: India. p. 254.
83. Nassif, R.A., Effect of chemical treatment on the some electrical and thermal properties for unsaturated polyester composites using banana fibers. Matrix, 2010. **1**: p. 7.
84. Wang, C., Fracture mechanics of single-fibre pull-out test. Journal of Materials Science, 1997. **32**(2): p. 483-490.
85. Yue, C. and Cheung, W., Interfacial properties of fibrous composites. Journal of materials science, 1992. **27**(12): p. 3181-3191.
86. International Network for the Improvement of Banana and Plantain. Bananas. [online] 2000 [cited September 2013.]; Available from: http://www.bioversityinternational.org/fileadmin/bioversity/publications/pdfs/664_Networking_Banana_and_Plantain.pdf.
87. Aziz, N., Ho, L., Azahari, B., Bhat, R., Cheng, L., and Ibrahim, M., Chemical and functional properties of the native banana pseudo-stem and pseudo-stem tender core flours. Food Chemistry, 2011. **128**(3): p. 748-753.
88. Department of Agriculture. A profile on the South African banana market value chain. 2011 [cited August 2012.]; Available from: http://www.nda.agric.za/docs/AMCP/Bananamvcp2011-12.pdf.
89. Nation Master. Agriculture statistics- banana production (most recent) by country. 2000 [cited 14 July 2012.]; Available from: http://www.nationmaster.com/red/graph/agr_ban_pro-agriculture-banana-production&b_map=1.
90. Oliveira, L., Cordeiro, N., Evtuguin, D.V., Torres, I.C., and Silvestre, A.J.D., Chemical composition of different morphological parts from 'Dwarf Cavendish' banana plant and their potential as a non-wood renewable source of natural products. Industrial Crops and Products, 2007. **26**(2): p. 163-172.
91. Li, K., Fu, S., Zhan, H., Zhan, Y., and Lucia, L.A., Analysis of the chemical composition and morphological structure of a banana psuedo-stem. BioResources, 2010. **5**(2).

92. De Beer, Z. and Sigawa, A. Banana (Musa spp.) juice production in South Africa. 2008.
93. Wigglesworth. Uses of Abaca. 2007; Available from: http://www.wigglesworthfibres.com/products/abaca/usesofabaca.html.
94. NCS resins. Unsaturated polyester resins. [online] n.d [cited 2013.]; Available from: http://www.ncsresins.com/unsaturated-polyester-resin.
95. Aziz, S.H., Ansell, M.P., Clarke, S.J., and Panteny, S.R., Modified polyester resins for natural fibre composites. Composites Science and Technology, 2005. **65**(3): p. 525-535.
96. Andjelkovic, D., Culkin, D., and Loza, R. Unsaturated polyester resins derived from renewable resources. in Composites and Polycon. 2009. Tampa, Florida, USA.
97. Strong, B., Plastics Materials and Processing. 3 ed. Vol. 1. 2006, New Jersey: Pearson Prentice Hall.
98. Skrifvars, M., Synthetic Modification and Characterisation of Unsaturated Polyesters. 2000: M. Skrifvars.
99. Celluwood, Bio-resin systems. 2008(ID: ECO/10/277331): p. 40-48.
100. Composites Technology. Bio-Composites Update: Bio-Based Resins Begin to Grow. 2008 [cited 23 September 2014.]; Available from: http://www.compositesworld.com/articles/bio-composites-update-bio-based-resins-begin-to-grow.
101. Strong, B., Microstructures in polymers, in Plastics Materials and Processing, D. Yarnell, Editor. 2006, Pearson Prentice Hall: New Jersey. p. 73-117.
102. Kim, S. and Kim, H.-J., Curing behavior and viscoelastic properties of pine and wattle tannin-based adhesives studied by dynamic mechanical thermal analysis and FT-IR-ATR spectroscopy. Journal of adhesion science and technology, 2003. **17**(10): p. 1369-1383.
103. Kim, S. and Kim, H.-J., Evaluation of formaldehyde emission of pine and wattle tannin-based adhesives by gas chromatography. Holz als Roh-und Werkstoff, 2004. **62**(2): p. 101-106.
104. Kim, S., Lee, Y.-K., Kim, H.-J., and Lee, H.H., Physico-mechanical properties of particleboards bonded with pine and wattle tannin-based adhesives. Journal of adhesion science and technology, 2003. **17**(14): p. 1863-1875.
105. Clarinval, A. and Halleux, C., Classification of biodegradable polymers, in Biodegradable polymers for industrial applications, R. Smith, Editor. 2005, Woodhead Publishing: Cambridge, GBR. p. 3-29.
106. Lubi, M.C. and Thachil, E.T., Cashew nut shell liquid (CNSL)-a versatile monomer for polymer synthesis. Designed Monomers and polymers, 2000. **3**(2): p. 123-153.
107. Ikeda, R., Tanaka, H., Uyama, H., and Kobayashi, S., Synthesis and curing behaviors of a crosslinkable polymer from cashew nut shell liquid. Polymer, 2002. **43**(12): p. 3475-3481.
108. Mwaikambo, L. and Ansell, M., Hemp fibre reinforced cashew nut shell liquid composites. Composites science and technology, 2003. **63**(9): p. 1297-1305.

109. Harlin, A., Edelmann, K., Immonen, K., Mroueh, U.-M., Pingoud, K., and Wessman, H., Industrial biomaterial visions. VIT Research Notes, 2009. **2522**: p. 1-94.
110. Oprea, S. and Doroftei, F., Biodegradation of polyurethane acrylate with acrylated epoxidized soybean oil blend elastomers by Chaetomium globosum. International Biodeterioration & Biodegradation, 2011. **65**(3): p. 533-538.
111. Iovino, R., Zullo, R., Rao, M., Cassar, L., and Gianfreda, L., Biodegradation of poly (lactic acid)/starch/coir biocomposites under controlled composting conditions. Polymer Degradation and Stability, 2008. **93**(1): p. 147-157.
112. Kumar, R., Yakubu, M., and Anandjiwala, R., Biodegradation of flax fiber reinforced poly lactic acid. Express Polymer Letters, 2010. **4**(7): p. 423-430.
113. Narayanan, N., Roychoudhury, P.K., and Srivastava, A., L (+) lactic acid fermentation and its product polymerization. Electronic Journal of Biotechnology, 2004. **7**(2): p. 167-178.
114. Vert, M., Aliphatic polyesters: Great degradable polymers that cannot do everything. Biomacromolecules, 2005. **6**(2): p. 538-546.
115. Cordeiro, N., Belgacem, M.N., Torres, I.C., and Moura, J., Chemical composition and pulping of banana pseudo-stems. Industrial Crops and Products, 2004. **19**(2): p. 147-154.
116. Mukhopadhyay, S., Fangueiro, R., Arpaç, Y., and Şentürk, Ü., Banana Fibers–Variability and Fracture Behaviour. Cellulose, 2008. **31**: p. 3.61.
117. Hirose, S., Hatakeyama, T., and Hatakeyama, H. Synthesis and thermal properties of epoxy resins from ester-carboxylic acid derivative of alcoholysis lignin. in Macromolecular Symposia. 2003. Wiley Online Library.
118. Labcat. Simple sugars: fructose, glucose and sucrose. [online] 2009 [cited 20 September 2014.]; Available from: https://cdavies.wordpress.com/2009/01/27/simple-sugars-fructose-glucose-and-sucrose/.
119. Timothy R. Felthouse, Joseph C. Burnett, Ben Horrell, Michael J. Mummey, and Yeong-Jen Kuo. Maleic anhydride. [online] 2001 [cited 16 February 2013.]; Available from: http://jws-edck.interscience.wiley.com:8095/kirk_articles_fs.html.
120. Office of environmental health hazard assessment. Maleic anhydride. [online] 2001 [cited 16 February 2013.]; Available from: http://oehha.ca.gov/air/chronic_rels/pdf/maleic.pdf.
121. Coptis Formulation and Regulatory software For Cosmetic Laboratories. Propylene Glycol. 2012 [cited February 2014.]; Available from: http://www.drugs.com/inactive/propylene-glycol-270.html.
122. Property., M.M. Cloisite 30B nanoclay. 2011 [cited 2014; Available from: http://www.matweb.com/search/DataSheet.aspx?MatGUID=1213e923b3544011850ad51fa523571c.
123. Metter Toledo Petrochemicals News. Improved Water Analysis of Oils, Combining Two Techniques. [online] 2012 [cited 2013.]; Available from: http://us.mt.com/dam/LabDiv/SegNews/downloads/Petrochemicals_News_14_en.pdf.

124. Harper college. The Molisch Test. [online] n.d. [cited 15 February 2013.]; Available from: http://www.harpercollege.edu/tm-ps/chm/100/dgodambe/thedisk/carbo/molisch/molisch.htm.
125. Singleton, V. and Rossi Jr, J.A., Colorimetry of total phenolics with phosphomolybdic-phosphotungstic acid reagents. American journal of Enology and Viticulture, 1965. **16**(3): p. 144-158.
126. Goering, H. and Van Soest, P., Forage fiber analysis. ARS, USDA. Agr. Handbook, 1970. **379**.
127. Herrera-Saldana, R. and Huber, J., Influence of varying protein and starch degradabilities on performance of lactating cows. Journal of Dairy Science, 1989. **72**(6): p. 1477-1483.
128. Parkyn, B., Commercial polyester resins, in Polyesters, unsaturated polyesters and polyester plasticisers, B. Parkyn, F. Lamb, and B.V. Clifton, Editors. 1967, London Iliffe Books Ltd: London
129. Keener, T.J., Stuart, R.K., and Brown, T.K., Maleated coupling agents for natural fibre composites. Composites Part A Applied Science and Manufacturing, 2004. **35**(3): p. 357-362.
130. Joseph, P., Rabello, M.S., Mattoso, L., Joseph, K., and Thomas, S., Environmental effects on the degradation behaviour of sisal fibre reinforced polypropylene composites. Composites Science and Technology, 2002. **62**(10-11): p. 1357-1372.
131. Ramsaroop, A., Fracture properties of fibre and nano reinforced composite structures, in Department of Mechanical Engineering. 2007, Durban University of Technolgy: Durban.
132. Kissinger, H.E., Reaction kinetics in differential thermal analysis. Analytical chemistry, 1957. **29**(11): p. 1702-1706.
133. Flynn, J.H. and Wall, L.A., A quick, direct method for the determination of activation energy from thermogravimetric data. Journal of Polymer Science Part B: Polymer Letters, 1966. **4**(5): p. 323-328.
134. Elmer., P., Dynamic Mechanical Analysis Basics: Part 2 Thermoplastic Transitions and Properties. 2007.
135. Encyclopædia Britannica Online. Amorphous polymer: amorphous and semicrystalline polymer morphologies. [online] 2014 [cited 12 September 2014.]; Available from: http://www.britannica.com/EBchecked/media/268/Amorphous-and-semicrystalline-polymer-morphologies.
136. Dhakal, H., Zhang, Z., Richardson, M., and Errajhi, O., The low velocity impact response of non-woven hemp fibre reinforced unsaturated polyester composites. Composite structures, 2007. **81**(4): p. 559-567.
137. Moodley, V., The synthesis, structure and properties of polypropylene nanocomposites, in Mechanical Engineering. 2007, Durban University of Technology: South Africa.
138. Prasad, M.S., Venkatesha, C., and Jayaraju, T., Experimental Methods of Determining Fracture Toughness of Fiber Reinforced Polymer Composites under Various Loading Conditions. Journal of Minerals & Materials Characterization & Engineering, 2011. **10**(13): p. 1263-1275.

139. Thostenson, E.T., Ren, Z., and Chou, T.-W., Advances in the science and technology of carbon nanotubes and their composites: a review. Composites science and technology, 2001. **61**(13): p. 1899-1912.
140. Sinha Ray, S. and Okamoto, M., Polymer/layered silicate nanocomposites: a review from preparation to processing. Progress in polymer science, 2003. **28**(11): p. 1539-1641.
141. Zhao, F., Wan, C., Bao, X., and Kandasubramanian, B., Modification of montmorillonite with aminopropylisooctyl polyhedral oligomeric silsequioxane. Journal of Colloid and Interface Science, 2009. **333**(1): p. 164-170.
142. Girish, G., Synthesis-Structure-Processing-property relationships in polymer nanocomposites, in Chemical Engineering Department. 2003, Pune: India.
143. Utracki, L., Sepehr, M., and Boccaleri, E., Synthetic, layered nano-particles for polymeric nanocomposites (PNC's). Polymers for advanced technologies, 2007. **18**(1): p. 1-37.
144. Laoutid, F., Bonnaud, L., Alexandre, M., Lopez-Cuesta, J.-M., and Dubois, P., New prospects in flame retardant polymer materials: from fundamentals to nanocomposites. Materials Science and Engineering: R: Reports, 2009. **63**(3): p. 100-125.
145. Praveen, S., Chattopadhyay, P.K., Jayendran, S., Chakraborty, B.C., and Chattopadhyay, S., Effect of nanoclay on the mechanical and damping properties of aramid short fibre filled styrene butadiene rubber composites. Polymer International, 2010. **59**(2): p. 187-197.
146. Chiellini, E., Corti, A., and Swift, G., Biodegradation of thermally-oxidized, fragmented low-density polyethylenes. Polymer Degradation and Stability, 2003. **81**(2): p. 341-351.
147. D6400, A., Standard Specification for Labeling of Plastics Designed to be Aerobically Composted in Municipal or Industrial Facilities, in ASTM International,. 2012: West Conshohocken, PA.
148. Chiellini, E. and Solaro, R., Biodegradable polymers and plastic. 2003, New York, USA: Kluwer Academic/Plenum Publishers,.
149. D5338-03, A., Standard Test Method for Determining the Aerobic Biodegradation of Plastic Materials Under Controlled Composting Conditions. 2004: West Conshohocken, PA.
150. Transport Information Service. Bananas. [online] 2013 [cited 2014.]; Available from: http://www.tis-gdv.de/tis_e/ware/obst/banane/banane.htm.
151. Kumar, K., Bhowmik, D., Duraivel, S., and Umadevi, M., Traditional and Medicinal Uses of Banana. Journal of Pharmacognosy and Phytochemistry, 2012.
152. Feriotti, D. and Iguti, A. Proposal for Use of Pseudostem from Banana Tree (Musa cavendish). in International Congress of Engineering and Food. 2012.
153. Reusch, W. Carbohydrates. [online] 2013 [cited 2014.]; Available from: https://www2.chemistry.msu.edu/faculty/reusch/virttxtjml/carbhyd.htm.
154. Ashok, R. Coloured reactions of carbohydrates. [online] 2013 [cited 2014.]; Available from: http://www.authorstream.com/Presentation/raniashok-1429879-coloured-reactions-of-carbohydrates/.

155. Narain, R., Jhurry, D., and Wulff, G., Synthesis and characterization of polymers containing linear sugar moieties as side groups. European Polymer Journal, 2002. **38**(2): p. 273-280.
156. Jhurry, D. and Deffieux, A., Sucrose-based polymers: Polyurethanes with sucrose in the main chain. European Polymer Journal, 1997. **33**(10): p. 1577-1582.
157. Tillet, G., Boutevin, B., and Ameduri, B., Chemical reactions of polymer crosslinking and post-crosslinking at room and medium temperature. Progress in Polymer Science, 2011. **36**(2): p. 191-217.
158. Lamaming, J., Sulaiman, O., Sugimoto, T., Hashim, R., Said, N., and Sato, M., Influence of chemical components of oil palm on properties of binderless particleboard. BioResources, 2013. **8**(3): p. 3358-3371.
159. Rice-Evans, C., Miller, N., and Paganga, G., Antioxidant properties of phenolic compounds. Trends in plant science, 1997. **2**(4): p. 152-159.
160. Arrieta-Baez, D., Cruz-Carrillo, M., Gómez-Patiño, M.B., and Zepeda-Vallejo, L.G., Derivatives of 10, 16-dihydroxyhexadecanoic acid isolated from tomato (Solanum lycopersicum) as potential material for aliphatic polyesters. Molecules, 2011. **16**(6): p. 4923-4936.
161. Stales, C.A., Peterson, D.R., Parkerton, T.F., and Adams, W.J., The environmental fate of phthalate esters: a literature review. Chemosphere, 1997. **35**(4): p. 667-749.
162. IFI Claims Patent Services. High-molecular weight unsaturated polyester resin. [online] 2012 [cited 6 January 2015.]; Available from: http://www.google.com/patents/EP0503935B1?cl=en.
163. Albemarle. Ethanox 4703. [online] 2013 [cited 2013.]; Available from: http://albemarle.com/Products-and-Markets/Polymer-Solutions/Antioxidants/Lubricants-187.html.
164. Paul, V., Kanny, K., and Redhi, G., Formulation of a novel bio-resin from banana sap. Industrial Crops and Products, 2013. **43**: p. 496-505.
165. Raghavendra, Hegde, M., Kamath, G., and Atul Dahiya. Polymer crystallinity. [online] [cited 14 September 2014.]; Available from: http://web.utk.edu/Textiles/polymer20%Crystallinity.
166. Manthey, N., Development of hemp oil based bioresins for biocomposites, in Centre of Excellence in Engineered Fibre Composites, Faculty of Engineering and Surveying. 2013, University of Southern Queensland: Australia.
167. Pistor, V., Soares, S.S.d.S.d., Ornaghi Júnior, H.L., Fiorio, R., and Zattera, A.J., Influence of glass and sisal fibers on the cure kinetics of unsaturated polyester resin. Materials Research, 2012. **15**(4): p. 650-656.
168. Rantuch, P., Kačíková, D., and Nagypál, B., Investigation of activation energy of polypropylene composite thermooxidation by model-free methods. European Journal of Environmental and Safety Sciences, 2014. **2**(1): p. 12-18.
169. Barral, L., Cano, J., López, J., López-Bueno, I., Nogueira, P., Abad, M., and Ramirez, C., Kinetic studies of the effect of ABS on the curing of an epoxy/cycloaliphatic amine resin. Journal of Polymer Science Part B: Polymer Physics, 2000. **38**(3): p. 351-361.

170. Islam, M.S., Pickering, K.L., and Foreman, N.J., Curing kinetics and effects of fibre surface treatment and curing parameters on the interfacial and tensile properties of hemp/epoxy composites. Journal of Adhesion Science and Technology, 2009. **23**(16): p. 2085-2107.
171. Kosar, V. and Gomzi, Z., In-depth analysis of the mathematical model of polyester thermosets curing. European polymer journal, 2004. **40**(12): p. 2793-2802.
172. Bufa. Unsaturated Polyester Resins, Vinyl Ester Resins and Epoxy Systems. [online] 2013 [cited 15 August 2013.]; Available from: https://www.buefa.de/wps/wcm/connect/cf3beadf-b938-40ed-a7e5-e5141ebd4710/Komplettprogramm_2013_Englisch_UP_Harze.pdf?MOD=AJPERES&CACHEID=cf3beadf-b938-40ed-a7e5-e5141ebd4710.
173. Turi, E.A., Thermal Characterization of Polymeric Materials Vol. 1. 1981, London: Academic Press.
174. Sigma Aldrich. Plasticizers. [online] 2015 [cited 10 January 2015.]; Available from: http://www.sigmaaldrich.com/materials-science/material-science-products.html?TablePage=16371266.
175. Calado, V., Barreto, D., and d'Almeida, J., The effect of a chemical treatment on the structure and morphology of coir fibers. Journal of Materials Science Letters, 2000. **19**(23): p. 2151-2153.
176. Fan, M., Dai, D., and Huang, B., Fourier transform infrared Spectroscopy for natural Fibres. Fourier Transform–Materials Analysis. Intech, 2012.
177. Bessadok, A., Marais, S., Gouanvé, F., Colasse, L., Zimmerlin, I., Roudesli, S., and Métayer, M., Effect of chemical treatments of Alfa (Stipa tenacissima) fibres on water-sorption properties. Composites science and technology, 2007. **67**(3): p. 685-697.
178. El-Shekeil, Y., Sapuan, S., Abdan, K., and Zainudin, E., Influence of fiber content on the mechanical and thermal properties of Kenaf fiber reinforced thermoplastic polyurethane composites. Materials & Design, 2012. **40**: p. 299-303.
179. Barreto, A.C.H., Rosa, D.S., Fechine, P.B.A., and Mazzetto, S.E., Properties of sisal fibers treated by alkali solution and their application into cardanol-based biocomposites. Composites Part A Applied Science and Manufacturing, 2011. **42**(5): p. 492-500.
180. Indira.KN, Grohens.Y, Baley.C, Thomas.S, Joseph.K, and Pothen.LA, Adhesion and Wettability Characteristics of Chemically Modified Banana Fibre for Composite Manufacturing. Journal of Adhesion Science and Technology, 2011. **25**(13): p. 1515-153.
181. Thwe, M.M. and Liao, K., Effects of environmental aging on the mechanical properties of bamboo–glass fiber reinforced polymer matrix hybrid composites. Composites Part A: Applied Science and Manufacturing, 2002. **33**(1): p. 43-52.
182. Giridhar, J. and Rao, R., Moisture absorption characteristics of natural fibre composites. Journal of reinforced plastics and composites, 1986. **5**(2): p. 141-150.
183. Espert, A., Vilaplana, F., and Karlsson, S., Comparison of water absorption in natural cellulosic fibres from wood and one-year crops in polypropylene

composites and its influence on their mechanical properties. Composites Part A Applied Science and Manufacturing, 2004. **35**(11): p. 1267-1276.
184. Dhakal, H., Zhang, Z., and Richardson, M., Effect of water absorption on the mechanical properties of hemp fibre reinforced unsaturated polyester composites. Composites Science and Technology, 2007. **67**(7): p. 1674-1683.
185. Bismarck, A., Aranberri-Askargorta, I., Springer, J., Lampke, T., Wielage, B., Stamboulis, A., Shenderovich, I., and Limbach, H.H., Surface characterization of flax, hemp and cellulose fibers; Surface properties and the water uptake behavior. Polymer Composites, 2004. **23**(5): p. 872-894.
186. Cambridge Polymer Group. Swelling measurements of crosslinked polymers. [online] 2000 [cited 12 February 2014.]; Available from: http://www.campoly.com/files/3013/5216/6056/005.pdf.
187. Jose, J.P. and Thomas, S., Alumina–clay nanoscale hybrid filler assembling in cross-linked polyethylene based nanocomposites: mechanics and thermal properties. Physical Chemistry Chemical Physics, 2014. **16**(28): p. 14730-14740.
188. Hale, A. and Bair, H., Polymer blends in Thermal characterization of polymeric materials, E.A. Turi, Editor. 1997, Academic Press: New York. p. 745-886.
189. Manikandan Nair, K., Thomas, S., and Groeninckx, G., Thermal and dynamic mechanical analysis of polystyrene composites reinforced with short sisal fibres. Composites Science and Technology, 2001. **61**(16): p. 2519-2529.
190. Joseph, P., Joseph, K., Thomas, S., Pillai, C., Prasad, V., Groeninckx, G., and Sarkissova, M., The thermal and crystallisation studies of short sisal fibre reinforced polypropylene composites. Composites Part A Applied Science and Manufacturing, 2003. **34**(3): p. 253-266.
191. Kwan, K.S., The role of penetrant structure in the transport and mechanical properties of a thermoset adhesive. 1998, Virginia Polytechnic Institute and State University.
192. Martínez-Hernández, A., Velasco-Santos, C., De-Icaza, M., and Castaño, V.M., Dynamical–mechanical and thermal analysis of polymeric composites reinforced with keratin biofibers from chicken feathers. Composites Part B: Engineering, 2007. **38**(3): p. 405-410.
193. Shanmugam, D. and Thiruchitrambalam, M., Static and Dynamic Mechanical Properties of alkali treated unidirectional continuous Palmyra Palm Leaf Stalk Fiber/Jute fiber reinforced hybrid polyester composites. Materials and Design, 2013. **50**: p. 533-542.
194. Jia, Y., Yan, W., and HY, L. Numetrical study on carbon fibre pullout using a cohesive zone model in ICCM 18th International conference on composite materials. 21 - 26 August 2011. Korea.
195. Kord, B. and Kiakojouri, S.M.H., Effect of nanoclay dispersion on physical and mechanical properties of wood flour/polypropylene/glass fiber hybrid composites. BioResources, 2011. **6**(2): p. 1741-1751.
196. Surabhi Sinha. Phenols. [online] [cited 10 October 2014.]; Available from: http://www.britannica.com/EBchecked/topic/455507/phenol.
197. Mishra, S., Mohanty, A., Drzal, L., Misra, M., Parija, S., Nayak, S., and Tripathy, S., Studies on mechanical performance of biofibre/glass reinforced

polyester hybrid composites. Composites Science and Technology, 2003. **63**(10): p. 1377-1385.
198. D5045, A., Standard test method for plane strain fracture and strain energy release rate of plastic materials. 1996.
199. Huda, M., Drzal, L., D., R., A., M., and Mishra, M.K., Natural fibre composites in the automotive sector. 2008, Woodhead Publishing Limited.
200. Acha, B.A., Reboredo, M.M., and Marcovich, N.E., Creep and dynamic mechanical behavior of PP–jute composites: Effect of the interfacial adhesion. Composites Part A: Applied Science and Manufacturing, 2007. **38**(6): p. 1507-1516.
201. Goertzen, W. and Kessler, M., Creep behaviour of carbon fiber/epoxy matrix composites. Materials Science and Engineering A, 2006. **421**: p. 217-225.
202. Miyagawa, H., Mohanty, A.K., Burgueño, R., Drzal, L.T., and Misra, M., Characterization and thermophysical properties of unsaturated polyester-layered silicate nanocomposites. Journal of nanoscience and nanotechnology, 2006. **6**(2): p. 464-471.
203. Sathe, S.N., Srinivasa Rao, G., Rao, K., and Devi, S., The effect of composition on morphological, thermal, and mechanical properties of polypropylene/nylon-6/polypropylene-g-butyl acrylate blends. Polymer Engineering & Science, 1996. **36**(19): p. 2443-2450.
204. Agag, T., Koga, T., and Takeichi, T., Studies on thermal and mechanical properties of polyimide–clay nanocomposites. Polymer, 2001. **42**(8): p. 3399-3408.
205. Lee, B.L. and Nielsen, L.E., Temperature dependence of the dynamic mechanical properties of filled polymers. Journal of Polymer Science: Polymer Physics Edition, 1977. **15**(4): p. 683-692.
206. Lei, S., Hoa, S.V., and Ton-That, M.-T., Effect of clay types on the processing and properties of polypropylene nanocomposites. Composites Science and Technology, 2006. **66**(10): p. 1274-1279.
207. Arutchelvi, J., Sudhakar, M., Arkatkar, A., Doble, M., Bhaduri, S., and Uppara, P.V., Biodegradation of polyethylene and polypropylene. Indian Journal of Biotechnology, 2008. **7**(1): p. 9.
208. Manzur, A., Limón-González, M., and Favela-Torres, E., Biodegradation of physicochemically treated LDPE by a consortium of filamentous fungi. Journal of Applied Polymer Science, 2004. **92**(1): p. 265-271.
209. Pamuła, E., Błażewicz, M., Paluszkiewicz, C., and Dobrzyński, P., FTIR study of degradation products of aliphatic polyesters–carbon fibres composites. Journal of Molecular Structure, 2001. **596**(1): p. 69-75.
210. Campanella, A., La Scala, J.J., and Wool, R.P., The use of acrylated fatty acid methyl esters as styrene replacements in triglyceride-based thermosetting polymers. Polymer Engineering & Science, 2009. **49**(12): p. 2384-2392.

APPENDICES

Appendix A3.1

Processing of Banana Fibres

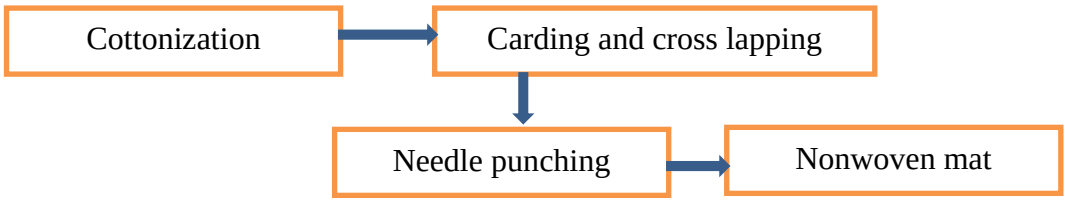

Banana fibre processed into a needle punched nonwoven mat in a two-step process. First step was the pre-processing which included cottonization and carding and cross lapping followed by needle punching.

Cottonization: It's a process where the long banana fibres were broken into short length fibres, and made finer. Furthermore, the fibre surfaces were free from any dust or sand particles attached to it by passing through the cottonization line. This line has a main rotating cylinder with spikes and knives which helps to break the long length fibres into short length fibres and simultaneously making it finer which is a requirement for the next line, carding. Cottonization process is a 2 lomy process with the following machine settings. 2 lomy means that the fibres passes through the cottonization line twice in order to make it shorter and finer, which is a standard practice.

Cottonization parameters:

	1st run (1 lomy)	**2nd run (2 lomy)**
Main cylinder speed	2840 rpm	1287 rpm
Knife 1 setting	0.2 mm	0.2 mm
Knife 2 setting	0.4 mm	0.4 mm
Air Pressure	4.6 bar	4.6 bar
Fibre feeding input weight	5 kg, Output: 2kg, Waste: 3 kg	3.6 kg,Output:2kg,waste: 1. 6 kg

Carding: Main function of the carding was to individualize the fibres, open them properly, and make them aligned to each other. It also used a main cylinder with barbed wires on it to open the fibres. Then, further fibre alignment is done with the

help of other rollers. Further alignment is achieved with the help of the cross lapper, which lays the carded web in to cross machine direction over one another so that there is uniform strength in the web in all directions (length and width wise).

Banana fibres after cottonization were subjected to a humidifier for 2 hours (95% humidity). Then, fibres were blended manually with the cotton fibres (carrier fibres) in a 90% / 10% mix. The mix was then fed into the carding machine. The first carding produced no usable web probably since the fibres had not been blended sufficiently. The mix was then fed into the card one more time, and the second time around a usable web was forming.

Carding machine and cross lapper parameters:

Fibre feeding speed: 0.9 m/min

Main cylinder speed: 200 rpm

Cross lapper speed: 0.9 m/min

Fibre mix: 90% banana, 10% cotton.

Note: It is not possible to process 100% banana fibres, because of the fibre are very weak and also very brittle. So it needs to mix with a carrier fibre for processing.

Needle punching: The carded cross-lapped web is subjected to the action of the barbed needles in a needle bed to produce nonwoven mat. By the mechanical action of the needles, fibres are bonded together. There are more than 2000 needles in the needle board. Each needle has a latch type of section at the tip of the needle. Initially the needles pass through a bulky fibre web and while doing so, it pushed down several fibres together. In the next step the same needle set, comes back to the original position. In this motion, it releases the fibres from the needle latch, thereby boning the fibres together by mechanical action.

Processing parameters:

Parameter	**Setting**
Fibres feeding	0.59 m/min
Needle depth	5 mm
Stroke Frequency	300 in

Appendix A3.2

Raw data for processing of resin

DATE	TIME	BATCH TEMP	S/H TEMP	ACID VALUE	MELT @ 120°C	DIST	COMMENTS
DAY 1	9.3	22.3	23				start batch
	10.25	65.6	26				batch clear
	10.45	165	100				start distillation
							178 exotherm
	11.45	158.8	100			65	
	13.5	192.4	96	124.5	0.9	255	
	14.5	190.3	75	105.4	1.1	290	
	15.5	189.6	71	100.8	1.3	295	
							heat off
DAY 2	7.3	26	21			296	heat on
	8.3	58	24				stirrer on
	9.3	195.8	80	92.7	1.9	300	
	10.25	189.4	39	99.2	1.9	305	
	11.45	205.1	94	96.7	2.1	315	
	12.45	208.7	94	89.6	2.8	325	added 35g PG
	3.3	208.1	93	80.7	3	335	
DAY 3	7.4	36.7	23			350	heat on
	8.55	147.5	25				stirrer on
	9.55	202.3	77	83.9	3.1	350	
	10.55	206.5	78	87.2	4	355	removed long column
	11.55	204.9	71	72.4	4.9	360	added 75g PG @1pm
	13.55	201.1	70	58.7	40	370	
	14.5	206.1	70	58.4	4.1		
	15.4						heat off

Appendix A3.3

Raw data for processing of resin

Date	Time	Batch temp	S/h temp	Acid value	Melt @ 120°c	Distillation	Comments
DAY 1	11.15	26	22				start batch
	11.45	103	99			200	
DAY 2	7.4					250	water distilled out
	4.3	104	98			800	heat off
DAY 3	8	73	21			1100	heat on
	11.45	183	101	147.05	0.1	1240	
	12.45	191	64	96.1	2.5	2120	
	1.4	190	82	86.7	2.8	2320	
	2.45	203	59	76.2	4	2500	
	3.4	200	59	67.7	4.9		
	3.5					heat off	
DAY 4	7.45					heat on	
	8					stirrer on	
	8.3	201	83	63.1	6.9		
	9.15	196	69	61.1	11		
	9.3	179	66				added 100g PG
	10	198	78	44.8	5		
	10.15			43	6	heat off	